Understanding the molecular basis of Rab-GEF activity and specificity of the mammalian TRAPP complexes

by

Noah James Harris
B.Sc. Biochemistry and Microbiology, University of Victoria, 2019

A Thesis Submitted in Partial Fulfillment
of the Requirements for the Degree of

MASTER OF SCIENCE

in the Department of Biochemistry and Microbiology

Supervisory Committee

Understanding the molecular basis of Rab-GEF activity and specificity of the mammalian TRAPP complexes

by

Noah James Harris
B.Sc. Biochemistry and Microbiology, University of Victoria, 2019

Supervisory Committee

Dr. John E Burke
Department of Biochemistry and Microbiology
Supervisor

Dr. Martin Boulanger
Department of Biochemistry and Microbiology
Departmental Member

Dr. Leigh Anne Swayne
Division of Medical Sciences
Outside Member

Abstract

Rab GTPases are among the most important families of proteins involved in regulating the trafficking and delivery of cellular cargo to their proper locations. The multi-subunit Transport Protein Particle complexes, TRAPPII and TRAPPIII, activate Rabs by catalyzing GDP/GTP nucleotide exchange. These two distinct complexes share seven subunits, yet they differ in their complex-specific subunits. Even though the TRAPP complexes are similar in subunit composition, they can activate different Rabs and therefore regulate distinct trafficking pathways. Intriguingly, the mechanism underlying the specificity of TRAPPII/III for different Rabs is poorly understood. This thesis is centered around understanding the molecular basis of TRAPP-Rab specificity in the mammalian TRAPPII/III complexes. To address this, we used a combination of different powerful techniques including biochemical nucleotide exchange assays, Hydrogen Deuterium eXchange Mass Spectrometry (HDX-MS), and electron microscopy to understand this specificity both in solution and on membranes. Biochemical assays against 20 different Rab GTPases revealed that TRAPPIII only has activity on Rab1 and Rab43. HDX-MS experiments comparing the TRAPPII and TRAPPIII complexes showed that there are extensive differences existing near the Rab binding site, thus highlighting the critical role that the complex specific subunits serve in modifying either complex's Rab binding interface. TRAPPII and TRAPPIII showed increased activity in the presence of lipid membranes and HDX-MS revealed large dynamic changes occurring in both TRAPP complexes in the presence of membranes. Altogether, the work summarized in this thesis provides novel insight into the unique functions of the two TRAPP complexes and it

reveals how the complex specific subunits can rearrange the Rab binding site which leads to a possible mechanism for Rab specificity.

Table of Contents

List of Tables

List of Figures

Acknowledgments

First, I would like to thank my supervisor, Dr. John Burke for giving me this opportunity and taking me on as a graduate student (with relatively little lab experience prior), and for your continual guidance and support during my short time in the lab. I am extremely grateful and lucky to have had you as a supervisor.

Secondly, I would like to thank my committee members, Dr. Leigh Anne Swayne and Dr. Martin Boulanger. Your feedback and input in our meetings have helped guide me in the right direction overall helping improve this thesis.

Thirdly, I'd like to thank our collaborators from the Calvin Yip lab in Vancouver. Specifically, Udit Dalwadi and Sung-Eun-Nam for your electron microscopy work on the TRAPPIII complex. This was a very nice and important addition to the article, and I am very grateful for your contributions.

Lastly, I'd like to thank everyone in the Burke lab, Manoj, Meredith, Kaelin, Harish, Brandon, Ed, and Matthew for your continual support and all the fun times we've shared along the way. Thank you, for an amazing and enjoyable working atmosphere that made coming into the lab and waiting for experiments not so dull. Special thanks to Manoj and Meredith for your training and mentoring. I feel like I rigorously harassed you both with questions and you were always there to answer them and help guide me; I could not have done this without you, and I am extremely grateful for your help. Of course, thanks to my family, friends, other graduate students whose constant encouragement and positivity helped make this all possible. I am extremely grateful to have had this opportunity and I could have not done it without you all and any others I may have missed.

List of Abbreviations

GEFs	Guanine nucleotide exchange factors
Rabs	Ras related in brain
GAPs	GTPase activating proteins
GDP	Guanosine diphosphate
GTP	Guanosine triphosphate
TRAPP	Transport protein particle
TBC	Tre-2 Bub2 Cdc16
HVT	Hypervariable tail
REP	Rab escort protein
GGTase	Geranylgeranyl transferase
GDI	GTP dissociation inhibitor
GDF	GDI displacement factor
LECA	Last eukaryotic common ancestor
Atg	Autophagy related gene
PAS	Phagophore assembly site
COPII	Coat protein complex II
PI3K	Phosphoinositide 3-kinase
TGN	Trans-Golgi network
Rab11-FIPs	Rab11 family interacting proteins
GPCR	G-protein coupled receptors
Ypt	Yeast protein transport
Trs	Trafficking subunit
Bet	Blocked early in transport
EM	Electron microscopy
SEDT	Spondyloepiphyseal dysplasia tarda
HDX-MS	Hydrogen deuterium exchange mass spectrometry
PBS	Phosphate buffered saline
BME	Beta mercaptoethanol
SEC	Size exclusion chromatography
CCD	Charged coupled device
CTF	Contrast transfer function
MS	Mass spectrometry
MS/MS	Tandem Mass spectrometry
2D	Two dimensional
Mant-GDP	3-(N-methyl-anthraniloyl)-2-deoxy-GDP
ITC	Isothermal titration calorimetry
PS	Phosphatidylserine
PI4P	L-α-phosphatidylinositol-4-phosphate
PC	phosphatidylcholine
PI	L-α-Phosphatidylinositol
PE	L-α-Phosphatidylethanolamine
Arf	ADP-ribosylation factor
BLI	Bio-layer interferometry

Thesis Format and Manuscript Claims

This thesis was written to follow the format of a manuscript. Chapter one summarizes relevant background information and the thesis' rationale and objectives. Chapter two also follows a manuscript format and contains an abstract, introduction, materials and methods, results, and discussion sections. The last chapter highlights the findings of the thesis, provides a conclusion, and suggests possible future directions for this work.

Chapter two adapted from: Harris NJ, Jenkins ML, Dalwadi U, Fleming KD, Nam SE, Parson M.AH, Yip CK, Burke JE. 2021. Biochemical insight into novel Rab-GEF activity of the mammalian TRAPPIII complex. 2021. Journal of Molecular Biology, 443(18).

Chapter 1 – Introduction

1.1 Overview

Trafficking of cellular material between organelles is an intricate and organized process involving an interplay of numerous different proteins that have distinct roles. One of the most important family of proteins involved in regulating this process are the Rab GTPases. Ras-related in brain (Rabs) act as “molecular switches” that alternate between a GTP-bound “on” state and a GDP-bound “off” state. The state that a given Rab exists in determines the effector molecules they recruit and therefore the role it plays in membrane trafficking. Guanine nucleotide exchange factors (GEFs) are responsible for flipping the switch on, or activating Rabs by catalyzing the exchange of GDP with GTP. Conversely, GTPase activating proteins (GAPs) are responsible for inactivating Rabs by catalyzing the hydrolysis of GTP to GDP [1–5]. This strict regulation of Rabs by GEFs and GAPs is extremely important to ensure membrane trafficking functions seamlessly. Studying the molecular basis underlying how Rabs are activated by GEFs is crucial for understanding their role in membrane trafficking.

The multi-subunit Transport Protein Particle (TRAPPII/III) complexes are well conserved and established class of GEFs [6–12]. In metazoans, two different complexes exist: TRAPPII and TRAPPIII. TRAPP complexes share a catalytic core that is responsible for binding Rab, but they differ by the presence of complex specific subunits. Each complex has its own Rab specificity so it’s clear that they are involved in diverse trafficking processes but the exact molecular mechanism for this Rab specificity is unknown. This thesis therefore focuses on investigating the molecular mechanism of the

different TRAPP complexes using a variety of powerful biochemical and biophysical techniques.

1.2 Rab GTPases

Rabs are one of the major protein families involved in regulating a multitude of cellular events. For this reason, Rabs are a fascinating family of proteins and very important to study. The first section of this thesis will go into more detail covering the activation of Rabs through their “molecular switch” and their regulation by GEFs and GAPs, and finally, the key Rabs involved in this thesis: Rab1, Rab11, Rab19 and Rab43 will be introduced.

1.2.1 Activation and Regulation of Rabs

As cells evolved and developed distinct intracellular compartments and therefore more complex membrane trafficking pathways there was a growing demand for proteins capable of regulating this process. The Rab protein family emerged to take on the responsibility of coordinating this transportation of cellular cargo with upwards of 60 different Rabs identified in humans controlling distinct trafficking pathways [2,13–15]. Like other GTPases, Rabs act as “molecular switches” that alternate between a GDP-bound “inactive” state and a GTP-bound “active” state with the GTP-bound state recruiting effector molecules that regulate downstream signaling. The activation of Rabs is mediated by GEFs which aid in the release of GDP and binding of GTP. GEFs catalyze nucleotide release via several different mechanisms. In general, GEFs stabilize the nucleotide-free state of the GTPase by recognizing residues in the switch I and switch II

which make up two of three important regions within the Rab [3,5,16]. Switch I and Switch II contain important residues that form interactions with both the phosphate groups of the nucleotide and with the magnesium ion in the binding pocket. As the GEF binds to GDP-Rab, the switch regions rearrange which move them away from the nucleotide binding site. The rearrangement of switch regions decreases the Rab's affinity for GDP while increasing the GEF's affinity for Rab ultimately resulting in nucleotide release [1,17–21]. Other GEFs directly attack the magnesium ion present at the nucleotide binding site by inserting residues that sterically hinder the magnesium thus destabilizing the Rab-GDP complex [1,5]. Magnesium is present to help coordinate the phosphate groups of the nucleotide in the binding pocket and form interactions with residues in the switch regions. For these reasons, an "attack" on the magnesium ion would destabilize nucleotide binding and promote GDP release [3]. In the cell, GTP is present at a much higher concentration compared to GDP and therefore will bind Rab as soon as GDP has been displaced. The result from GTP binding is GEF dissociation and an activated Rab. Many different effector molecules such as molecular motors, tethers, and even other GEFs can be recruited and interact with active Rabs to control specific trafficking pathways [15,22–24].

The ability of Rabs to work properly relies on an interplay between the activation by GEFs at the appropriate time and place but also the inactivation by GAPs to ensure the "switch" does not stay on when unneeded. The inactivation of Rabs occurs through hydrolysis of GTP back into GDP. In general, GTPases have an intrinsic rate of GTP hydrolysis [2,3]. However, for some Rabs, this occurs too slowly and in a physiologically irrelevant timeframe. To address this, the cell has evolved to ensure these processes can

happen within a timely manner and this hydrolysis is accelerated by GAPs. One of the most common domains present in proteins that function as Rab GAPs are the Tre-2, Bub2 and Cdc16 (TBC) domains [25]. TBC domains utilize a conserved catalytic arginine and glutamine residue to stabilize both the transition state and a nucleophilic water molecule at the active site which ultimately results in the hydrolysis of GTP into GDP [26–28]. A figure summarizing the Rabs molecular switch activity is shown in Figure 1-1.

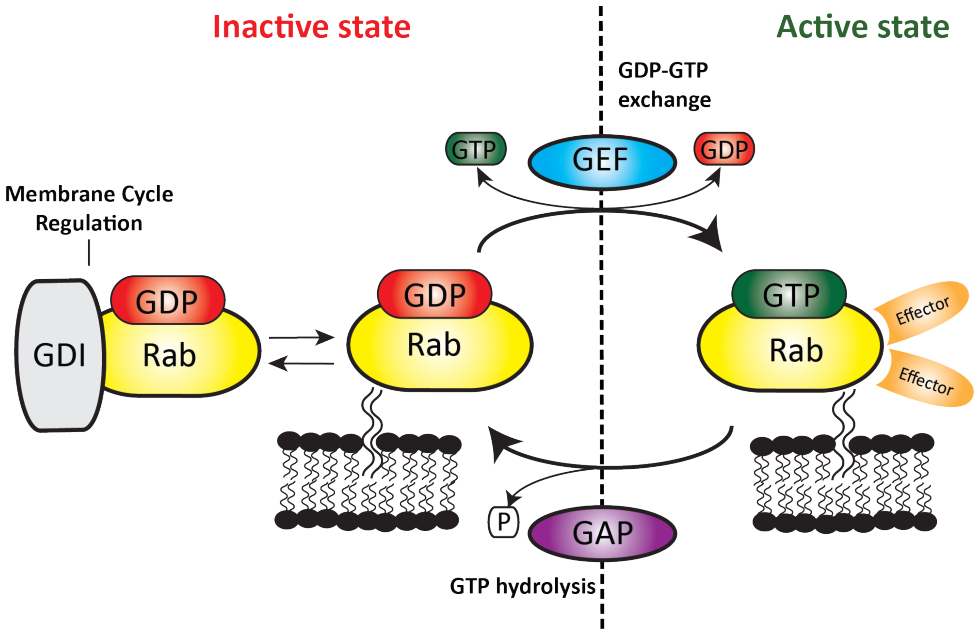

Figure 1-1. The Rabs "molecular switch" activity. Rabs alter between two different states: an inactive GDP-bound state and an active GTP-bound state. GEFs control the activation of Rabs while GAPs control the inactivation through hydrolysis of GTP back into GDP. GDI's can sequester Rabs off a particular membrane. Figure adapted from [29]

Because Rabs control many essential functions, they themselves need to be tightly regulated. This regulation is controlled by an interplay of GEFs and GAPs activating and inactivating Rabs ensuring that the right material is where it needs to be at the appropriate time. It's easy to imagine how Rabs can work in tandem where one active Rab recruits

the GEF of a downstream Rab in a certain trafficking pathway. However, the following Rab, once activated, may then recruit a GAP for the previous Rab thus inactivating the previous trafficking step. It is this organized and controlled feedback loop or Rab cascade that contributes to maintaining the integrity of our intracellular compartments and the trafficking between them [4].

In addition to the switchI and switchII regions, the last important structural region that make up Rabs is the C-terminal hyper-variable tail (HVT). This region is variable amongst Rabs thus can help distinguish different members of the Rab family [30,31]. Unfortunately, HVTs are often removed in structural studies due to their unstructured and flexible nature. The HVT is not required for GDP/GTP binding and usually is not involved in effector binding but is an important part in associating the GTPase to a membrane [21,31,32]. In addition to Rabs "molecular switch" activity cycling between on and off states, Rabs also cycle between cytosolic and membrane-bound states. In order for membrane association to occur the Rab must be prenylated at C-terminal cysteines [33]. A newly synthesized Rab-GDP is recognized by a Rab escort protein (REP) which presents the Rab-GDP to a geranylgeranyl transferase (GGTase) which prenylates the Rab at two of its C-terminal cysteine residues. Once prenylated, the GGTase dissociates from the Rab-REP complex and the Rab can associate with a particular membrane [34]. In order to be removed from the membrane, membrane bound Rab is recognized by a Rab GDP dissociation inhibitor (GDI). GDI's only interact with prenylated, GDP-bound Rab and therefore can sequester the Rab from a particular membrane [3]. There is still some ambiguity related to how Rabs are located to distinct membranes and several

possible mechanisms exist. GDI displacement factors (GDFs) putatively target Rab-GDI to specific membranes and were shown to promote dissociation of the Rab-GDI complex [35]. However, because GDIs only interact with Rabs bound to GDP, others have argued that GEFs could also be a major factor in determining membrane localization by catalyzing the release of GDP and thus locking the active GTP-bound Rab at a particular membrane [36]. For example, a particular Rab (specific examples outlined in section 1.2.2) can sample different membranes and only when it encounters its GEF, GTP will bind and "lock" the Rab on its current membrane. It's clear that the process of recruiting Rabs to specific membranes is likely more complex and perhaps involves a combination GDIs, GEFs and GAPs working together.

1.2.2 Rabs trafficking between ER/Golgi and in Autophagy

Rab GTPases are undoubtably critical regulators of membrane trafficking. They have become the largest subfamily within the Ras superfamily of small GTPases with over 60 members identified in humans and only about 13 members identified in yeast. This large expansion across yeast to humans has presented a need to understand how Rabs are regulated and how they can mediate distinct trafficking events. This sub-section will introduce four important Rabs involved in this thesis: Rab1, Rab11, Rab19 and Rab43. These Rabs control important trafficking steps including ER-Golgi transport, autophagy, recycling endosomes, ciliogenesis, and GPCR trafficking. This diverse set of pathways requires many different binding partners, and effectors that mediate their specific function and thus a particular biological response.

Rab1 is well-studied and a master regulator of ER-golgi transport also playing roles in autophagy [2,15,37–40]. Yeast has a single Rab1 gene: Ypt1 while in humans there are seven related genes: Rab1a, Rab1b, Rab19, Rab30, Rab33a, Rab33b, Rab35, Rab43 (also known as Rab19b) [41]. Of this group Rab1 is the only one conserved back to the last eukaryotic common ancestor (LECA) highlighting its conservation and importance throughout evolution. Active Rab1 is principally found at the ER and the Golgi but has also been found on autophagosomes consistent with its role in ER-Golgi transport and autophagy. Rab1 like other GTPases is regulated by a combination of specific effectors, GEFs, and GAPs. Of this list, the most well-studied GEF mediating activation for Rab1 is the Transport protein particle complex III (TRAPPIII) [38,42,43]. TRAPPIII has been shown to activate Rab1 in ER-Golgi transport and autophagy and is discussed further in section 1.3 of this thesis. An important GAP that catalyzes the inactivation of Rab1 is TBC1D20 [44]. Overexpression of TBC1D20 causes disruption of the Golgi highlighting the importance of proper Rab1 activation and inactivation in maintaining a functional Golgi [44].

Some important effectors that bind active Rab1 include Atg1, p115, and Vps34. Atg1 (autophagy related gene) is a critical serine/threonine kinase involved in phagophore assembly and initiation. Rab1's link to Atg1 and autophagy is through interactions with TRAPPIII and Atg17 (a scaffold that mediates other Atg proteins at the phagophore assembly site (PAS)) [45]. The Rab1 GEF TRAPPIII is recruited to the PAS via Atg17 which results in the activation of Rab1 and recruitment of Atg1 to the PAS. P115 is a tether mediating ER-Golgi, and intra-Golgi transport. Active Rab1 recruits p115 to coat

protein complex II (COPII) vesicles at the ER which ultimately directs these vesicles to the Golgi for fusion [37]. Vps34 is a member of the phosphoinositide 3-kinase (PI3K) family and forms two heterotetrametric complexes: complex I and II. Complex I functions in autophagosome formation, and complex II functions in endosome sorting. Interestingly, Rab1a binds and potently activates complex I with no alteration of complex II activity [46]. This is consistent with Rab1 playing important roles during the initial steps of autophagy. These different GEFs, GAPs and effectors are examples of how Rab1 can mediate different specific cellular functions.

Rab11 is an important regulator of recycling endosomes and has also been implicated to play roles in ciliogenesis and cytokinesis [47–50]. Yeast have two Rab11 genes: Ypt31/32 and in humans there are three: Rab11a, Rab11b, Rab25 (also known as Rab11c) [41]. Of this family, Rab11 is the most important member and is conserved back to the LECA. Rab11 principally localizes to the trans-Golgi network (TGN) and to endosomes in the secretory pathway. To mediate Rab11's specific functions it must be regulated by various GEFs, GAPs, and effectors. Two of the most important and well-studied Rab11 GEFs are the TRAPPII complex and SH3BP5 [43,51–53]. The most well studied Rab11 GAP is Evi5 which is required for tight regulation of Rab11-mediated cell migration and the recycling of endosomes [54]. Rab11 has several known effectors including class V myosins, the Rab11-family interacting proteins (Rab11-FIPs), and PI4KIIIβ [55–57]. The class V myosins are well studied molecular motors which help to transport vesicles to their destination and specifically function in cell polarity and membrane trafficking. Rab11 interacts with Myosin Vb and plays an important role in

plasma membrane and receptor recycling which highlights the important role of Rab11 in maintaining membrane integrity [55]. FIPs are Rab11 interacting proteins with functions that not surprisingly overlap with those of Rab11. FIPs can link Rab11 to motor proteins and are important for cell division, cytokinesis, and ciliogenesis. As examples, Rab11-FIP3 complex plays an important role in vesicle transport during cytokinesis [58] and the Rab11-FIP3-Rabin8 complex plays an important role in delivering vesicles during ciliogenesis [49]. PI4KIIIβ is a kinase that primarily resides at the Golgi and is crucial for proper Golgi function. Rab11 interacts with its effector PI4KIIIβ at an interface that doesn't involve the switch region which allows for an additional interaction between Rab-PI4KIIIβ and FIP3 [57],

Rab19 and Rab43 (Rab19b) are less characterised but evolutionarily similar Rabs only diverging in vertebrata and make up part of the Rab1 sub-family. Rab19 and Rab43 have been implicated in ciliogenesis and trafficking of GPCRs respectively [59,60]. Because these Rabs are poorly characterized, the proteins they interact with are also unclear. TRAPPII is one known GEF that activates Rab19 and Rab43 at relatively equal rates [52]. Active Rab19 plays a role in ciliary membrane growth through multiple interactions with a Rab-GAP TBC1D4 and an effector known as the HOPS-tethering complex [59]. Rab43 plays important roles in ER-Golgi trafficking and in sorting of GPCRs and it has also been shown to interact directly with α2B-Adrenergic receptor and angiotensin II type 1 receptor [60,61]. Rab43 has one known Rab-GAP RN-tre which regulates transport from endosomes to the Golgi [44].

This short introduction of Rabs highlights the complexity of membrane trafficking and the multitude of different effectors, GEFs, GAPs that help regulate and control their localization and activation. Studying how Rabs are activated by GEFs is one important way to investigate and understand the specific functions of different Rabs.

1.3 Transport Protein Particle Complexes

Transport protein particle (TRAPP) complexes are well established and potent Rab GEFs and the primary focus of this thesis. This section will introduce the TRAPP complexes in yeast including their history and their controversy, followed by present day TRAPP complexes in yeast and metazoans and finally the role of TRAPP complexes in human disease.

1.3.1 TRAPP complexes – history and controversy

The multi-subunit TRAPPI and TRAPPII complexes were originally discovered in yeast as molecular tethers that mediate fusion during membrane trafficking but were subsequently found to act as potent Rab GEFs. TRAPP complexes have now become one of the most well studied and well characterised Rab-GEFs.

Originally, only two TRAPP complexes were identified by size exclusion chromatography and immunoblotting experiments: TRAPPI and TRAPPII [62–64]. These two complexes shared six core subunits (Bet3A/B, Bet5, Trs20, Trs23, Trs31 and Trs33). TRAPPI is the simplest complex being composed of only the shared core subunits while TRAPPII contains the core subunits and three additional complex specific subunits:

Trs65, Trs120, Trs130. A table highlighting the different TRAPP subunits across yeast and metazoans is summarized in Table 1-1. TRAPPI was found to function in ER-Golgi trafficking by tethering vesicles intended for the Golgi by an interaction with TRAPPI's Bet3 subunit and COPII's Sec23 subunit [64,65]. TRAPPII was found to act as a tether during trafficking events within the Golgi and from endosomes to the late Golgi [66]. It was thought that the presence of additional complex specific subunits prevented the interaction of Bet3 and COPII in TRAPPII supporting its previously described role in Golgi trafficking.

Table 1-1 TRAPP subunits in yeast and associate subunits in metazoans/humans

Subunit in Yeast	Subunit in metazoans/humans	Subunit Group
Bet5	TRAPPC1	Core (TRAPPI)
Trs20	TRAPPC2	Core/adaptor (TRAPPI)
Tca17	TRAPPC2L	Mammalian core/adaptor
Bet3	TRAPPC3	Core (TRAPPI)
Trs23	TRAPPC4	Core (TRAPPI)
Trs31	TRAPPC5	Core (TRAPPI)
Trs33	TRAPPC6	Core (TRAPPI)
Trs120	TRAPPC9	TRAPPII specific
Trs130	TRAPPC10	TRAPPII specific
Trs85	TRAPPC8	TRAPPIII specific
n/a	TRAPPC11	TRAPPIII specific
n/a	TRAPPC12	TRAPPIII specific
Trs65	TRAPPC13	Stabilizes yeast TRAPPII dimer/TRAPPIII specific

Akin to TRAPP's tether functions, they were also found to have Ypt1 (Rab1 in mammals) GEF activity [67,68]. Structural analyses showed that the core TRAPP subunits: Bet5, Trs23, Trs31 and Bet3A/B were minimally required for GEF activity [69]. The crystal structure of the core subunits bound to Ypt1 was solved and showed direct interactions between Bet3, Bet5 and Trs23 with Ypt1 suggesting a mechanism for how both TRAPPI and TRAPPII can activate Ypt1 through the same subunits [69]. It was unclear whether Ypt1 was the only substrate activated by TRAPPI/TRAPPII and if so, what are the exact functions of these redundant GEFs. Several studies investigated genetic interactions with TRAPPII specific subunits and Ypt31/32 (Rab11 homologues in mammals) and suggested the possibility that TRAPPII swaps its GEF activity from Ypt1 to Ypt31/32 [70,71]. It was proposed that the complex-specific subunits of TRAPPII: Trs120 and Trs130 combine with TRAPP at the Golgi to alter activity towards Ypt31/32 possibly by blocking Ypt1 binding [72].

The idea of TRAPPII being a GEF for Ypt31/32 was the center of the TRAPP controversy for many years. Pulldown assays with TRAPPII showed interactions between TRAPPII and Ypt1 but not Ypt31/32 [73], while others demonstrated that TRAPPII had *in-vitro* GEF activity for Ypt31 [72]. The electron microscopy (EM) structure of yeast TRAPPII released in 2010 by Yip *et al.,* provided strong evidence against the hypothesis that the TRAPPII specific subunits mask the Ypt1 binding site [73]. The structure showed that TRAPPII subunits together dimerize to form a compact diamond shape. Importantly, in this structure the Ypt1 binding site appears to be unrestricted and accessible to Ypt1.

The model that both TRAPPI and TRAPPII only activate Ypt1 was soon broken based on several elegant studies. First, Ypt1 and Ypt31 were shown to localize to opposite ends of the Golgi: Ypt1 to the early Golgi and Ypt31 to the late Golgi [74] where TRAPPI and TRAPPII had been discovered to work respectively. Second, in fungus, TRAPPII was shown to act as a GEF for the Ypt31 homolog RabE at the late Golgi in solution and in cells [75]. However, possibly the most definitive evidence was a study by Thomas & Fromme published in 2016 where they produced several key pieces of information strongly suggesting that TRAPPII is a GEF for Ypt31/32 [51]. First, they tested the activity of TRAPPI and TRAPPII against Ypt1 and Ypt31/32 in the presence and absence of membranes. This was one of the first attempts at measuring the activity of the TRAPP complexes when the Rab was presented on a membrane surface like how it would exist in a cell. They found that TRAPPII potently activated Ypt31/32 in the presence of membranes while TRAPPI was unable to activate Ypt31/32. They further recapitulated these results *in-vivo* demonstrating that mutations in TRAPPII specific subunits resulted in Ypt31/32 being completely cytosolic. In addition, some Ypt1 was did not localize at the late Golgi suggesting that TRAPPII can assist in activating Ypt1 in addition to Ypt31 at the late Golgi which is consistent with its established ability to activate Ypt1 *in-vitro*.

A third complex was later identified named TRAPPIII which was composed of the core subunits and one additional complex specific subunit: Trs85. TRAPPIII was proposed to work solely during the early events of autophagy where it recruits and activates Ypt1 at the PAS [38,76]. TRAPPIII contains all the machinery required to

activate Ypt1 and its EM structure depicts an elongated rod like structure similar to that of TRAPPI with additional length from the Trs85 subunit at one end of the rod [77]. A figure of cartoon models based off the yeast structural evidence of TRAPPI, TRAPPII and TRAPPIII is shown in Figure 1-2. At this point, it appeared that yeast had three TRAPP complexes activating either Ypt1 or Ypt31 during distinct trafficking events. The reason for why the cell had these redundant GEFs was still unclear and thus highlighted an important area of study surrounding the functions of the TRAPP complexes and specifically the molecular mechanism of Rab activation.

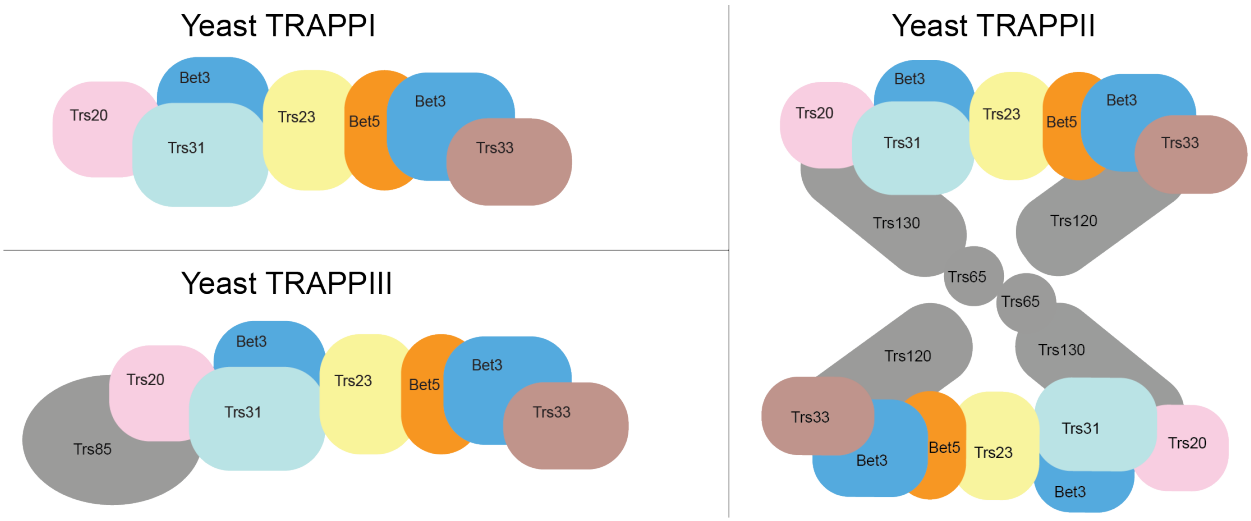

Figure 1-2. Cartoon models of yeast TRAPP complexes. TRAPPI contains only core subunits (multi-color) and is essentially a long rod-like structure. The core subunits and complex specific subunits of TRAPPII: trs120 and trs130 (grey) dimerize to form a diamond-shaped complex. TRAPPIII contains the core subunits and TRAPPIII specific subunit trs85 (grey). TRAPPIII is comparable to TRAPPI with additional length from trs85.

1.3.2 Yeast TRAPP complexes – present day

To date, evidence suggests that the two most important TRAPP complexes that exist in yeast are TRAPPII and TRAPPIII which activate Ypt31/32 and Ypt1 respectively

[42,51,78]. TRAPPI is currently thought to be less important for Rab activity for the following reasons: Firstly, TRAPPI was first discovered based on size exclusion chromatography and immunoblots and found to activate Ypt1, however, the relative abundance of the TRAPP subunits was not thoroughly investigated at this time. In addition, studies have shown that TRAPPI levels increase in the presence of high salt or in TRAPPII/TRAPPIII complex disrupting mutants [79]. This information brought into question the biological relevance of TRAPPI and hinted that it may be a biproduct produced when purifying either TRAPPII or TRAPPIII. Further supporting the idea that TRAPPII and TRAPPIII are the primary TRAPP complexes, it was found that TRAPPIII is a potent Ypt1 GEF in yeast activating Ypt1 much faster than TRAPPI in the presence of membranes [42]. Moreover, *in-vivo* assays demonstrated that Ypt1 was cytosolic in Trs85 mutant cells suggesting that TRAPPIII not TRAPPI is the primary activator of Ypt1 at the Golgi [42]. It is important to note that Trs85 mutants do not completely compromise Ypt1 activation and that the TRAPPI complex (that forms in Trs85 mutants) can sustain a low level of activated Ypt1 required for survival.

Since both TRAPP complexes are activating their substrates using the same subunits, there was a need for understanding a mechanism that controls GEF specificity. In yeast, specificity is achieved through a steric gating mechanism in which the varying length of the HVT in combination with the heights of the TRAPP complexes control the substrates specificity [80]. The shorter HVT of Ypt1 allows access to the TRAPPIII binding site while the longer HVT of Ypt31can access the same binding site on the taller TRAPPII complex.

The structural architecture of the yeast TRAPPIII complex has been well defined and illustrates how Ypt1 binds to TRAPPIII at the core [78]. The structure includes the important HVT of Ypt1 (not included in previous structural analyses) and suggests a mechanism for how the TRAPPIII complex associates with membranes. In brief, the cryo-EM structure of TRAPPIII takes on a rod-like structure which resembles that of the original negative stain EM structure and highlights the important interaction between the HVT of Ypt1 and core subunit Trs31. This structure also shows the interface between the complex specific subunit Trs85 with core subunits Trs20/Trs31 and identifies a conserved amphipathic helix in Trs85 that is important for membrane binding and Ypt1 activation.

1.3.3 Metazoan TRAPP complexes

Most of the original research regarding TRAPP complexes were carried out with the yeast variants which is important because when comparing TRAPP complexes across yeast and metazoans as there are some prominent differences. Metazoans, like yeast, have two well established TRAPP complexes: TRAPPII and TRAPPIII. However, the subunit composition of these complexes differs from that of the yeast complexes. TRAPPII and TRAPPIII share seven (six in yeast) core subunits (TRAPPC1, TRAPPC2, TRAPPC2L, TRAPPC3A/B, TRAPPC4, TRAPPC5, TRAPPC6a), with two complex specific subunits for TRAPPII (TRAPPC9 and TRAPPC10) and four complex specific subunits for TRAPPIII (TRAPPC8, TRAPPC11, TRAPPC12, TRAPPC13) [81] (Table 1-1). The core subunits that are required for activity in yeast are also essential in metazoans: TRAPPC1, TRAPPC3, TRAPPC4, TRAPPC5 [8,82]. The TRAPPIII specific

subunit Trs85 is not essential in yeast while the homolog TRAPPC8 is essential in humans. TRAPP activity is conserved *in-vitro* with TRAPPII activating Rab1 with its primary role being to activate Rab11 [43,52]. TRAPPIII activates Rab1 and has no activity on Rab11 [43,83]. Mammalian TRAPPII has additional activity on Rab19, and Rab43 [52].

At the beginning of this thesis, there was little structural information regarding the metazoan TRAPP complexes. We knew the conserved core subunits are arranged in a similar manner to yeast complexes with structures of subcomplexes TRAPPC1,TRAPPC3, TRAPPC4, TRAPPC6 and TRAPPC2, TRAPPC3, TRAPPC5 being solved [82]. However, there was little insight into how the additional complex specific subunits (primarily the additional subunits present in TRAPPIII) were arranged. The negative stain EM structures of mammalian TRAPPII revealed that the subunits come together to form a monomer distinct from yeast TRAPPII that forms a dimer [52,83]. In yeast, the dimer is stabilized by the Trs65 subunit [79,84] which is not conserved in metazoans agreeing with the inability of the mammalian complex to dimerize. The monomer contains an elongated rod (core subunits) along the bottom, two “arms” (complex specific subunits) attaching to either end of the rod and meeting at the top to form a triangular shaped structure. Only low-resolution structural studies exist investigating the mammalian TRAPPII complex which limits our structural understanding of TRAPPII’s complex specific subunits in relation to the core.

Galindo *et al.,* 2021 unambiguously resolved how Drosophila TRAPPIII subunits are arranged within the complex by showing the arrangement of the complex specific subunits using Cryo-EM and cross-linking mass spectrometry [83]. The Cryo-EM

structure of Drosophila TRAPPIII is made up of an elongated rod-like region like TRAPPII which is reminiscent of the core subunits, two “arms” which cap the ends of the rod and meet above. Cross linking mass spectrometry showed that TRAPPC8 attaches to one end of the rod via multiple cross-links with TRAPPC2 and that TRAPPC11 attaches to the other end via TRAPPC2L. TRAPPC12 and TRAPPC13 exist at the top where the two arms meet. A cartoon image summarizing the general structures of TRAPPII and TRAPPIII in metazoans is highlighted in Figure 1-3.

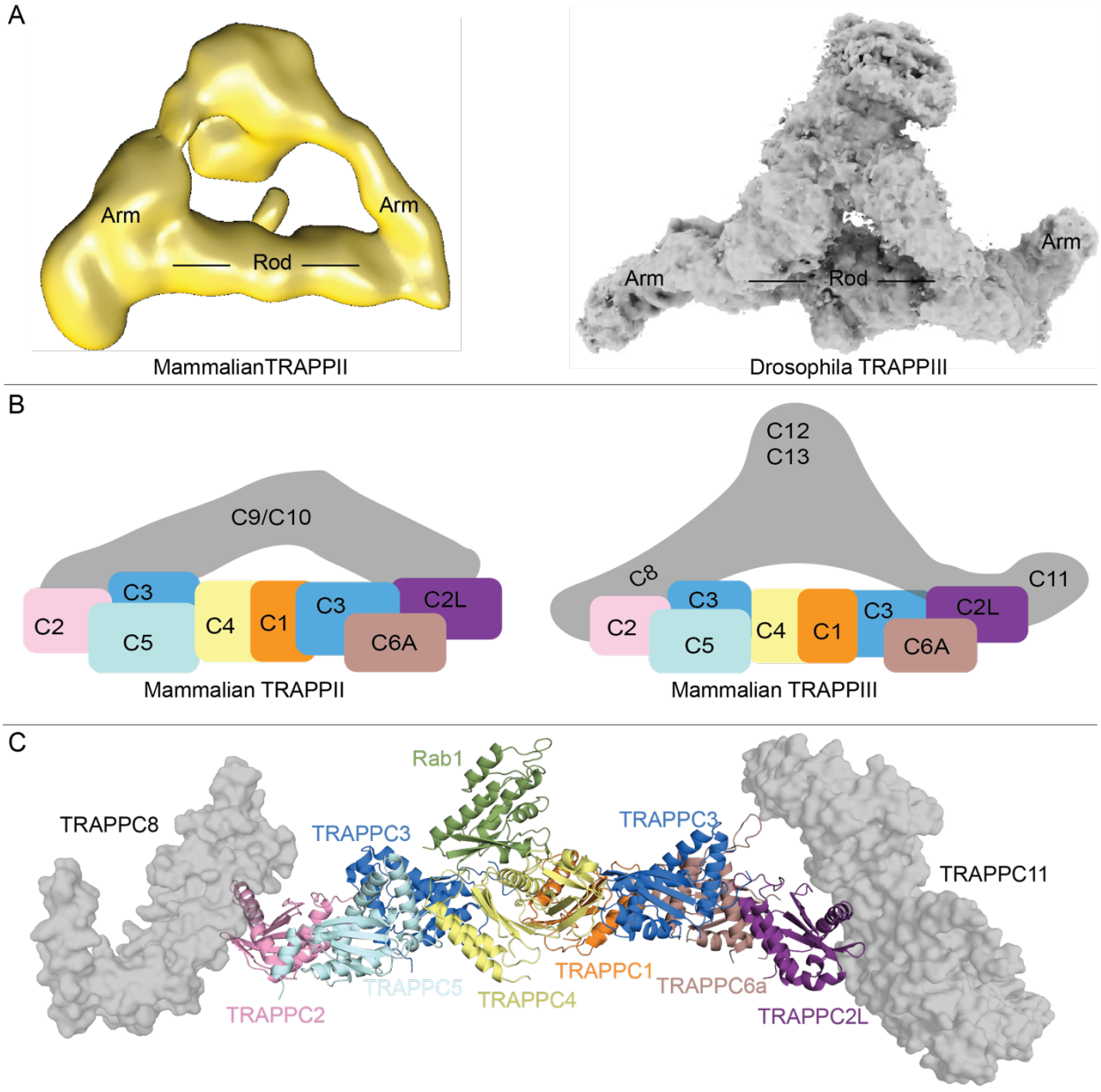

Figure 1-3. Mammalian/metazoan TRAPP complex architecture.

A. (left) Mammalian TRAPPII negative stain EM structure from [52]. **(right)** Metazoan TRAPPIII cryo-EM structure from [83]. The "rod" region refers to the core subunits and the arms refer to the complex specific subunits.

B. (left) Mammalian TRAPPII cartoon model based off panel A. TRAPPII is composed of core subunits and complex specific subunits: TRAPPC9 and TRAPPC10 that meet above the core. **(right)** Mammalian/metazoan TRAPPIII cartoon model based off panel A. TRAPPIII is composed core subunits and complex specific subunits TRAPPC8, TRAPPC11, TRAPPC12, TRAPPC13. TRAPPC8 is located at the TRAPPC2 interface of

the core, TRAPPC11 is located at the TRAPPC2L interface on the opposite end of the core and TRAPPC12 and TRAPPC13 form together at the top.
C. Mammalian TRAPPIII model with Rab bound generated using a combination of the core model in figure 2-2 and Phyre2 models based on PDB:7B6R.

In metazoans Rab-TRAPP specificity is not as well defined. In yeast, specificity is determined via the steric gating mechanism. However, the length of the HVT in mammalian homologs of Rabs differs. Further, the presence of additional complex specific subunits in metazoan TRAPPIII present a possible implication for allosteric or physical regulation. To date, the focus of mammalian/metazoan TRAPPs have been solidifying structural information and defining specificity for Rab1 and Rab11. However, the lack of detailed investigations regarding a mechanism of specificity in combination with activity against other untested Rabs sheds light to the possible unknown functions of the TRAPP complexes.

1.3.4 TRAPP complexes and diseases

Highlighting the important roles that TRAPP complexes have in important cellular processes are the discoveries of various human diseases that arise when mutations occur within TRAPP subunits [7,8,11]. Diseases associated with these mutations including the skeletal disorder: spondyloepiphyseal dysplasia tarda (SEDT), neurodevelopmental delay, intellectual disability, and muscular disorders [85–89]. These diseases are caused by mutations in different TRAPP subunits including TRAPPC2, TRAPPC2L, TRAPPC6, TRAPPC9, and TRAPPC11. Specific mutations in both TRAPPII and TRAPPIII complex specific subunits highlights the importance of both complexes in disease. Many of these mutations act to completely destabilize the complex or they lie at the interface between

the core and complex specific subunits thus destabilizing their interaction [85,86]. More research is needed to completely understand how these mutations function in disease. A table and figure highlighting TRAPP subunits and their mutations is summarized in Table 1-2 and Appendix J.

Table 1-2. Examples of TRAPP subunits and their disease-linked mutations

TRAPP subunit	Mutation	Disease	Reference
TRAPPC2	D47Y, H80R, F83S, S73L	SEDT	[11,90–92]
TRAPPC2L	D37Y	Neurodevelopmental delay	[87]
TRAPPC6	Y107N	Intellectual disability	[93]
TRAPPC9	L178P	Intellectual disability	[88]
TRAPPC11	Q284P, Q777P	Muscular disorder, elevated creatine Kinase	[89,94]

1.4 Research Objectives

TRAPP complexes are large multi-subunit complexes and well established/potent Rab GEFs. Although the yeast and metazoan complexes are well characterised both structurally and biochemically, the mechanism for how the complex specific subunits alter GEF activity towards different Rabs is unknown. The objective of this thesis is to understand the molecular basis of Rab-GEF specificity and activity of the mammalian TRAPP complexes. The analysis of these large, complicated complexes is highlighted in a single thesis objective and further summarized below.

1.4.1 Thesis Objective: Determine the specificity of the mammalian TRAPP complex and investigate the molecular mechanism of Rab specificity

The goal of this objective is to determine the activity and specificity of the TRAPPIII complex. Once the specificity is known, a combination of powerful biophysical and

biochemical techniques are used to compare what we know about both TRAPPII and TRAPPIII complexes, determine how Rabs bind and are subsequently activated, and finally to determine the conformational differences between the complexes and ultimately understand how these complexes achieve Rab specificity.

Altogether, this work will improve our understanding of the activity and specificity of the mammalian TRAPP complexes while generating an important starting point for future structural and biochemical studies investigating the functions of the TRAPP complexes and how they mediate Rab specificity. This data chapter has been published in the Journal of Molecular Biology and is thus presented as a manuscript in Chapter 2. To conclude, Chapter 3 will summarize findings and discuss some possible future directions.

Chapter 2 – Biochemical insight into novel Rab-GEF activity of the mammalian TRAPPIII complex

Noah J Harris[1], Meredith L Jenkins[1], Udit Dalwadi[2], Kaelin D Fleming[1], Sung-Eun-Nam[2], Matthew AH Parson[1], Calvin K Yip[2], John E Burke[1,2]

[1]Department of Biochemistry and Microbiology, University of Victoria, Victoria, British Columbia, Canada V8W 2Y2

[2]Life sciences Institute, Department of Biochemistry and Molecular Biology, The University of British Columbia, Vancouver, British Columbia V6T 1Z3, Canada

Adapted from: Harris NJ, Jenkins ML, Dalwadi U, Fleming KD, Nam SE, Parson M.AH, Yip CK, Burke JE. 2021. Biochemical insight into novel Rab-GEF activity of the mammalian TRAPPIII complex. 2021. Journal of Molecular Biology, 443(18).

Contributions:

JEB, **Noah J Harris** and MLJ designed all biophysical/biochemical experiments. **NJH** cloned the TRAPPIII complex. **NJH** carried out all protein expression/purification with some assistance from MP, and MLJ. **NJH** carried out all biochemical studies with some assistance from MLJ. **NJH** set all HDX-MS experiments and performed data analysis with assistance from MLJ, KDF and MP. UD SEN and CKY carried out electron microscopy studies presented in Fig. 2-2 C+D and supplied methods for the electron microscopy experiments. **NJH**, MLJ, and JEB wrote the manuscript with input from all authors.

2.1 Abstract

Transport Protein Particle complexes (TRAPP) are evolutionarily conserved regulators of membrane trafficking, with this mediated by their guanine nucleotide exchange factor (GEF) activity towards Rab GTPases. In metazoans evidence suggests that two different TRAPP complexes exist, TRAPPII and TRAPPIII. These two complexes share a common core of subunits, with complex specific subunits (TRAPPC9 and TRAPPC10 in TRAPPII and TRAPPC8, TRAPPC11, TRAPPC12, TRAPPC13 in TRAPPIII). TRAPPII and TRAPPIII have distinct specificity for GEF activity towards Rabs, with TRAPPIII acting on Rab1, and TRAPPII acting on Rab1 and Rab11. The molecular basis for how these complex specific subunits alter GEF activity towards Rab GTPases is unknown. Here we have used a combination of biochemical assays, hydrogen deuterium exchange mass spectrometry (HDX-MS) and electron microscopy to examine the regulation of TRAPPII and TRAPPIIII complexes in solution and on membranes. GEF assays revealed that the TRAPPIII has GEF activity against Rab1 and Rab43, with no detectable activity against the other 18 Rabs tested. The TRAPPIII complex had significant differences in protein dynamics at the Rab binding site compared to TRAPPII, potentially indicating an important role of accessory subunits in altering the active site of TRAPP complexes. Both the TRAPPII and TRAPPIII complexes had enhanced GEF activity on lipid membranes, with HDX-MS revealing numerous conformational changes that accompany membrane association. HDX-MS also identified a membrane binding site in TRAPPC8. Collectively, our results provide insight into the functions of TRAPP complexes and how they can achieve Rab specificity.

2.2 Introduction

Membrane trafficking is an essential process in all eukaryotic cells and requires tightly coordinated transport of cellular material to distinct intracellular organelles. Numerous different proteins are involved in regulating this pathway but one of the most important protein families involved are Rab GTPases. Rabs act as molecular switches that cycle between GTP-bound active and GDP-bound inactive states. Rabs recruit downstream effector molecules depending on their nucleotide binding state, including molecular motors, and tethers which control membrane trafficking events. The activation of Rabs is catalyzed by Guanine nucleotide exchange factors (GEFs) [1,3,4] which mediate the exchange of GDP for GTP. Defining how Rabs are targeted by GEFs is important in understanding their function in membrane trafficking. The Transport Protein Particle (TRAPP) complexes are evolutionarily conserved in all eukaryotic cells, and are potent Rab GEFs playing important roles in secretion, autophagy, and Golgi trafficking [6–11].

Metazoans are proposed to form two different TRAPP complexes: TRAPPII and TRAPPIII. TRAPPII can activate Rab1, but it has been proposed that its main role is to activate Rab11, therefore playing key roles in secretion from the Golgi [43,51,52,72]. TRAPPIII does not have activity against Rab11, and instead is proposed to primarily mediate activation of Rab1, an important regulator in ER-Golgi, intra-Golgi trafficking and autophagy [38,42,43,76]. The mammalian TRAPPII complex has additional activity on Rab19 and Rab43 [52]. Rab19 and Rab43 are both Golgi-localised Rabs, with Rab43 being involved in mediating GPCR trafficking and Rab19 being involved in ciliogenesis

[59,60]. Defining the molecular mechanisms that mediate GEF specificity of mammalian TRAPP complexes will be critical in understanding their roles in membrane trafficking.

TRAPPII and TRAPPIII all share seven conserved subunits that make up the TRAPP "core" (TRAPPC1, TRAPPC2, TRAPPC2L, TRAPPC3A/B, TRAPPC4, TRAPPC5, TRAPPC6A/B) [82]. Mammalian TRAPPII is composed of the core and two additional complex specific subunits (TRAPPC9, TRAPPC10) with mammalian TRAPPIII composed of the core and four additional complex specific subunits (TRAPPC8, TRAPPC11, TRAPPC12, TRAPPC13) [43,81,95]. The importance of TRAPPIII as a Rab1 GEF is highlighted by TRAPPC8 and TRAPPC11 being essential for cell survival and Rab1 activation [40,43]. Highlighting the critical role of TRAPP complexes in human disease is that mutations or deletions in TRAPP specific subunits have been found to be involved in several neurodevelopmental disorders collectively known as "TRAPPopathies" [7,8,11].

Structural studies using X-ray crystallography and electron microscopy have revealed the architecture of the conserved core of the TRAPP complexes and how they associate with Rab GTPases (Fig. 2-2A, Appendix B) [69,82]. The structure of the yeast TRAPP core complex bound to Ypt1 (Rab1 homolog) revealed the Rab binding interface, which is composed of TRAPPC1, TRAPPC3, and TRAPPC4 [69,82]. The cryo-electron microscopy (cryo-EM) structure of the yeast TRAPPIII complex revealed the interactions of the core with TRAPPC8, with an additional interaction of TRAPPC5 with the hyper-variable tail (HVT) of Ypt1 (Rab1 homolog) [78]. The cryo-EM structure of the Drosophila TRAPPIII complex bound to Rab1 shows how the additional TRAPPIII complex specific

subunits are arranged in relation to the core, with a novel interaction between TRAPPC8 and Rab1 [83]. Despite these insights into the assembly of TRAPPIII complexes, it is still not understood how the TRAPPIII complex specific subunits change the way the conserved subunits interact with Rab substrates, and how substrate selectivity is controlled.

Here we have carried out biochemical and biophysical analysis of the mammalian TRAPPIII complex using a combination of in-vitro GEF assays, electron microscopy, and hydrogen deuterium exchange mass spectrometry (HDX-MS). We have purified both mammalian TRAPPII (composed of TRAPPC1, TRAPPC2, TRAPPC2L, TRAPPC3, TRAPPC4, TRAPPC5, TRAPPC6A, TRAPPC9, TRAPPC10) and TRAPPIII (composed of TRAPPC1, TRAPPC2, TRAPPC2L, TRAPPC3, TRAPPC4, TRAPPC5, TRAPPC6A, TRAPPC8, TRAPPC11, TRAPPC12, TRAPPC13). Single-particle electron microscopy analysis of the purified TRAPPIII revealed an overall architecture resembling that of TRAPPIII isolated from Drosophila. We characterised TRAPPIII GEF activity against 20 different Rab GTPases both in solution and on membranes. We found TRAPPIII mediated GEF activity for Rab1 and Rab43, but no activity towards other any other Rab GTPases tested. HDX-MS comparing the TRAPPII and TRAPPIII complexes showed extensive differences at the Rab binding site, revealing a potential role of complex specific subunits in reshaping the GEF catalytic site. GEF activity of both TRAPPII and TRAPPIII was enhanced on membranes, with HDX-MS revealing extensive conformational changes upon membrane binding and identifying a conserved membrane binding site in the TRAPPIII specific subunit TRAPPC8. Overall, this work provides unique insight into the

architecture and dynamics of TRAPP complexes, and the mechanisms by which their GEF activity is regulated.

2.3 Materials and Methods

2.3.1 Plasmids and antibodies

The full length TRAPPII, and Rab genes were used as described previously [52]. TRAPPC8, TRAPPC11, and TRAPPC12 genes, were purchased from DNASU (C8- HsCD00347731 & HsCD00399392, C11- HsCD00082480, C12- HsCD324976) and TRAPPC13 was ordered from Thermofisher Geneart. Genes were subcloned into pLIB vectors, and in the case of TRAPPC12 a TEV cleavable c-term 2x strep tag was added while a TEV cleavable c-term 6x his tag was added to the c-term of TRAPPC11. Genes were subsequently amplified following the biGBac protocol to generate 2 plasmids that together contain all the TRAPPIII genes [96]. A table summarizing the plasmids used is outlined in Appendix K. A figure summarizing the cloning process of the mammalian TRAPPIII complex is highlighted in Figure 2-1.

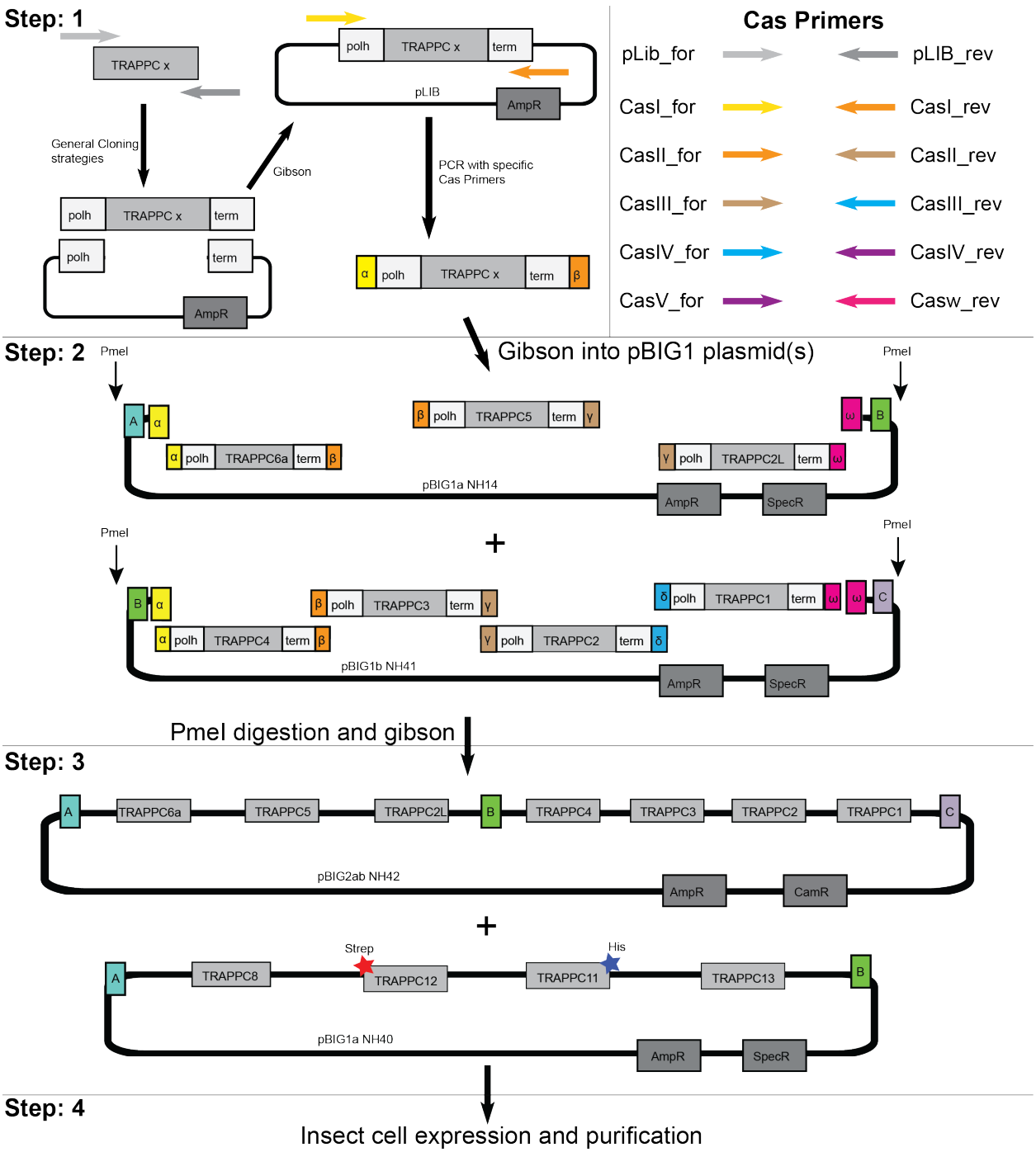

Figure 2-1. Cloning strategy for the mammalian TRAPPIII complex.
The mammalian TRAPPIII cloning strategy is complex but can be summarized into 4 steps and was designed based on the protocol from [96]. The first step is to generate library vectors (pLIB) for each individual TRAPP gene. pLIBs are generated using general cloning strategies (i.e Q5 PCR and Gibson assembly). The second step uses specific Cas primers (top left) to generate unique overlapping ends on each TRAPP gene. Overlapping

genes can be combined into the second plasmid: pBIG1 using Gibson assembly. Five different pBIG1 plasmids exist (with unique linkers: A, B, C, D, E, F; pBIG1a and pBIG1b are only shown here) and up to five genes can be combined into a single pBIG1 plasmid. The third step utilizes the PmeI cutsite on pBIG1 plasmids and their specific linkers to release the set of genes from pBIG1. Each set of genes and linkers released from pBIG1 plasmids can be combined using Gibson assembly into a final plasmid: pBIG2. Two plasmids (pBIG2ab NH42: core subunits and pBIg1a NH40: TRAPPIII specific subunits) were co-expressed in insect cells and purified as described below. Figure adapted from [97].

2.3.2 Protein expression

TRAPPII complexes were expressed as previously described [52]. In short, to express TRAPPII/TRAPPIII complexes, an optimized ratio of baculovirus was used to co-infect *Spodoptera frugiperda* (Sf9) cells between 1-2×10^6 cells/mL. Co-infections were harvested at ~66-hours and washed with ice-cold PBS before snap-freezing in liquid nitrogen. Rab constructs were all expressed in BL21 C41 DE3 *E.coli,* induced with 0.5mM IPTG and grown at 37°C for 4hrs. Pellets were washed with ice-cold phosphate-buffered saline (PBS), flash frozen in liquid nitrogen, and stored at -80°C until use.

2.3.3 Protein purification

TRAPP complexes and Rabs were purified as described previously [52]. TRAPP cell pellets were lysed by sonication for 1.5 minutes in lysis buffer (20mM Tris pH 8.0, 100mM NaCl, 5% (v/v) glycerol, 2mM ß–mercaptoethanol (BME), and protease inhibitors (Millipore Protease Inhibitor Cocktail Set III, Animal-Free)). Triton X-100 was added to 0.1% v/v, and the solution was centrifuged for 45 minutes at 20,000 x g at 1°C. The supernatant was then loaded onto a 5 mL HisTrap™ FF column (GE Healthcare) that had been equilibrated in NiNTA A buffer (20 mM Tris pH8.0, 100 mM NaCl, 10 mM imidazole

pH 8.0, 5% (v/v) glycerol, 2 mM bME). The column was washed with 20 mL of NiNTA buffer, 20 mL of 6% NiNTA B buffer (20 mM Tris pH 8.0, 100 mM NaCl, 200 mM imidazole pH 8.0, 5% (v/v) glycerol, 2 mM bME) before being eluted with 100% NiNTA B. The eluate was subsequently loaded on a 5ml Strep™ column and washed with 10ml SEC buffer (20mM HEPES pH 7.5, 100mM NaCl, 0.5mM TCEP). The Strep-tag was cleaved by adding SEC buffer containing 10mM BME and TEV protease to the column and incubating overnight at 4°C. Protein was pooled and concentrated using Amicon 50K concentrator and size exclusion chromatography (SEC) was performed using a Superose 6 increase 10/300 column equilibrated in SEC Buffer. Yield can be improved by taking pooled TRAPP complex before SEC and manually running protein through a 1 mL HisTrap™ FF column (GE Healthcare) that had been equilibrated in NiNTA A buffer followed by buffer exchange into SEC buffer using a 5 mL HiTrap® Desalting Column (GE Healthcare). Fractions containing protein of interest were pooled, concentrated, flash frozen in liquid nitrogen and stored at -80°C.

For Rab purification, cell pellets were lysed by sonication for 5 minutes in lysis buffer (20mM Tris pH 8.0, 100mM NaCl, 5% (v/v) glycerol, 2mM ß–mercaptoethanol (BME), and protease inhibitors (Millipore Protease Inhibitor Cocktail Set III, Animal-Free)). Triton X-100 was added to 0.1% v/v, and the solution was centrifuged for 45 minutes at 20,000 x g at 1°C. Supernatant was loaded onto a 5ml GSTrap 4B column (GE Healthcare) in a superloop for 1.5 hours and the column was washed in Buffer A (20mM Tris pH 8.0, 100mM NaCl, 5% (v/v) glycerol, 2mM BME) to remove non-specifically bound proteins. The GST-tag was cleaved by adding Buffer A containing 10mM BME and TEV

protease to the column and incubating overnight at 4°C. Cleaved protein was eluted with Buffer A. Protein was further purified by separating on a 5ml HiTrap Q column with a gradient of Buffer A and Buffer B (20mM Tris pH 8.0, 1M NaCl, 5% (v/v) glycerol, 2mM BME). Protein was pooled and concentrated using an Amicon 30K concentrator, and were flash frozen in liquid nitrogen and stored at -80°C.

2.3.4 Lipid vesicle preparation

Nickelated lipid vesicles were made with 10% phosphatidylserine (bovine brain PS, Sigma), 10% L-α-phosphatidylinositol-4-phosphate (PI4P, Avanti) 30% phosphatidylcholine (egg yolk PC, Sigma), 10% L-α-Phosphatidylinositol (Liver PI, Avanti), 15% L-α-Phosphatidylethanolamine (egg yolk PE, Sigma), and 10% DGS-NTA(Ni) (18:1 DGSNTA(Ni), Avanti). Vesicles were prepared by combining liquid chloroform stocks together at appropriate concentrations and evaporating away the chloroform with nitrogen gas. The resulting lipid film layer was desiccated for 20 min before being resuspended in lipid buffer (20mM HEPES (pH 7.5) and 100mM KCl) to a concentration of 1mg/ml. The lipid solution was vortexed for 5 min, bath sonicated for 10 min, and flash frozen in liquid nitrogen. Vesicles were then subjected to three freeze thaw cycles using a warm water bath. Vesicles were extruded 11 times through a 150nm NanoSizer Liposome Extruder (T&T Scientific) and stored at -80°C.

2.3.5 In-vitro GEF assays

C-terminally His-tagged Rabs were purified, and nucleotide loaded as described previously [52]. Reactions were conducted in 10μl volumes with a final concentration of 4 μM Mant-GDP loaded Rab, 100 μM GTPγS, the appropriate amount of TRAPP (4.5 – 300

μM) and vesicles (0.2mg/ml). Rab and membrane were aliquoted into a 384-well, black, low-volume plate (Corning 3676). To start the reaction, TRAPP and GTPγS were added simultaneously to the wells and a SpectraMax® M5 Multi-Mode Microplate Reader was used to measure the fluorescent signal for 1hr (Excitation λ = 366nm; Emission λ = 443nm). Data was analyzed using GraphPad Prism 7 Software, and k_{cat}/K_m analysis was carried out according to the protocol of. GEF curves were fit to a non-linear dissociate one phase exponential decay using the formula $I(t)=(I_0-I_\infty)*\exp(-k_{obs}*) + I_\infty$ (GraphPad Software), where I(t) is the emission intensity as a function of time, and I_0 and I_∞ are the emission intensities at t=o and t=∞. The catalytic efficiency k_{cat}/K_m was obtained by a slope of a linear least squares fit to $k_{obs}=k_{cat}/K_m*[GEF]+ k_{intr}$, where k_{intr} is the rate constant in the absence of GEF.

2.3.6 Hydrogen deuterium exchange (HDX) experiments

TRAPPII vs TRAPPIII

HDX reactions comparing both complexes were conducted in 50μl reaction volumes with a final concentration of 160nM for TRAPPII or TRAPPIII. Exchange was carried out in triplicate for five time points (3s at 4°C and 3s, 30s, 300s and 3000s at 20°C). Hydrogen deuterium exchange was initiated by the addition of 40μl of D_2O buffer solution (10mM HEPES pH 7.5, 50mM NaCl, 97% D_2O) to give a final concentration of 78% D_2O. Exchange was terminated by the addition of acidic quench buffer at a final concentration 0.6M guanidine-HCl and 0.9% formic acid. Samples were immediately frozen in liquid nitrogen at -80°C.

Hydrogen deuterium exchange (HDX) TRAPPII and TRAPPIII apo vs Membrane

HDX reactions comparing both complexes bound to membranes were conducted in 50μl reaction volumes with a final concentration of 120nM for TRAPPII or TRAPPIII and 0.1mg/ml membranes. Exchange was carried out in triplicate for three time points (3s, 100s and 3000s at 20°C). Prior to the addition of D_2O, TRAPP was incubated at 20°C with vesicles for one minute to facilitate TRAPP-membrane interactions. Hydrogen deuterium exchange was initiated by the addition of 32.1μl of D_2O buffer solution (10mM HEPES pH 7.5, 50mM NaCl, 97% D_2O) to the protein/membrane solutions, to give a final concentration of 62% D_2O. Exchange was terminated by the addition of acidic quench buffer at a final concentration 0.6M guanidine-HCl and 0.9% formic acid. Samples were immediately frozen in liquid nitrogen at -80°C.

Hydrogen deuterium exchange (HDX) TRAPPIII apo vs Rab bound

HDX reactions comparing TRAPPIII and TRAPPIII-Rab1 complex were conducted in 50μl reaction volumes with a final concentration 100nM TRAPPIII per sample and 560 nM Rab1. Exchange was carried out in triplicate for four time points (3s, 30s, 300s and 3000s at 20°C). Prior to the addition of D_2O, proteins were incubated on ice in the presence of 20mM EDTA for 30 minutes to facilitate release of nucleotide. Hydrogen deuterium exchange was initiated by the addition of 43.1μl of D_2O buffer solution (10mM HEPES pH 7.5, 50mM NaCl, 97% D_2O) to give a final concentration of 82% D_2O. Exchange was terminated by the addition of acidic quench buffer at a final concentration 0.6M guanidine-HCl and 0.9% formic acid. Samples were immediately frozen in liquid nitrogen at -80°C.

2.3.7 HDX-MS data Analysis

Protein samples were rapidly thawed and injected onto an integrated fluidics system containing a HDx-3 PAL liquid handling robot and climate-controlled (2°C) chromatography system (LEAP Technologies), a Dionex Ultimate 3000 UHPLC system, as well as an Impact HD QTOF Mass spectrometer (Bruker). The protein was run over one (at 10°C) immobilized pepsin column (Trajan; ProDx protease column, 2.1 mm x 30 mm PDX.PP01-F32) at 200 μL/min for 3 minutes. The resulting peptides were collected and desalted on a C18 trap column (Acquity UPLC BEH C18 1.7mm column (2.1 x 5 mm); Waters 186003975). The trap was subsequently eluted in line with an ACQUITY 1.7 µm particle, 100 × 1 mm2 C18 UPLC column (Waters), using a gradient of 3-35% B (Buffer A 0.1% formic acid; Buffer B 100% acetonitrile) over 11 minutes immediately followed by a gradient of 35-80% over 5 minutes. Mass spectrometry experiments acquired over a mass range from 150 to 2200 m/z using an electrospray ionization source operated at a temperature of 200C and a spray voltage of 4.5 kV. The resulting MS/MS datasets were analyzed using PEAKS7 (PEAKS), and a false discovery rate was set at 1% using a database of purified proteins and known contaminants. HDExaminer Software (Sierra Analytics) was used to automatically calculate the level of deuterium incorporation into each peptide. All peptides were manually inspected for correct charge state and presence of overlapping peptides. Deuteration levels were calculated using the centroid of the experimental isotope clusters. Differences in exchange were in a peptide were considered significant if they met all three of the following criteria: >5% change in exchange, >0.5 Da difference in exchange, and a p value <0.01 using a two tailed student t-test. Samples

were only compared within a single experiment and were never compared to experiments completed at a different time with a different final D_2O level.

The data analysis statistics for all HDX-MS experiments are in Appendices L-N according to the guidelines of [98]. The mass spectrometry proteomics data have been deposited to the ProteomeXchange Consortium via the PRIDE partner repository [99] with the dataset identifier PXD025928.

2.3.8 Negative stain single-particle electron microscopy (EM) and image analysis of TRAPPIII

Purified TRAPPIII complex was adsorbed to glow discharged carbon coated grids and stained with uranyl formate. The stained specimens were examined using a Talos L120C transmission electron microscope (ThermoFisher Scientific) operated at an accelerating voltage of 120 kV and equipped with a Ceta charged-coupled-device (CCD) camera. 100 micrographs were acquired at a nominal magnification of 45,000x at a defocus of ~1.2µm and binned twice to obtain a final pixel size of 4.53 Å/pixel. Contrast transfer function (CTF) estimation for each micrograph was carried out using CTFFind4 [100]. 200 particles were manually picked then aligned to generate 2D class averages for template-based autopicking in Relion 3.0 [101]. 38,062 particles were autopicked and extracted with a box size of 148 pixels. Particles were then subjected to 2D classification and 1034 particles which did not classify well were discarded. The remaining particles were transferred to cryoSPARC v2.14 [102] for *ab initio* reconstruction using 2 classes which were refined by heterogenous refinement. A final particle stack of 32,429 particles was used to carry out homogenous refinement of the better model, yielding a final map

at 14.2Å resolution based on the gold-standard 0.143 Fourier Shell Correlation criterion (Appendix B). The EM data have been deposited to the EMDB with the accession code: EMD-23997.

2.4 Results

2.4.1 Purification and architecture of the mammalian TRAPPIII complex

We recombinantly purified TRAPPII and TRAPPIII using a similar approach to our previous work on TRAPPII [52]. TRAPPII and TRAPPIII complexes were generated using the biGBac multi-promoter system [96] in *Sf9* insect cells and protein purification was carried out using HisTrap and StrepTrap affinity columns followed by gel filtration (Fig. 2-2B). The details outlining the specific plasmids and TRAPP subunit boundaries used can be found in Appendix K. TRAPPIII eluted at a size consistent with one copy of all subunits (exception being two copies of TRAPPC3) on size exclusion chromatography. Tandem mass spectrometry (MS/MS) analysis of the purified TRAPPII and TRAPPIII complexes identified peptides covering all expressed subunits.

To investigate the architecture of the mammalian TRAPPIII complex we subjected purified mammalian TRAPPIII to negative stain single particle electron microscopy (EM) analysis (Fig. 2-2C-D, Appendix B). Raw images revealed triangular-shaped particles similar to Drosophila TRAPPIII [83] (Fig. 2-2C-D) but distinct from the smaller-sized yeast TRAPPIII [78]. Two-dimensional (2D) analysis and 3D reconstruction revealed mammalian TRAPPIII is composed of an elongated rod-like region reminiscent of the TRAPP core (TRAPPC1, TRAPPC2, TRAPPC3A/B, TRAPPC4, TRAPPC5,

TRAPPC6A), two “arms” capping the ends of the putative TRAPP core, and a peripheral region extending from the core (Fig. 2-2D, Appendix B). The ultrastructure of mammalian TRAPPIII is consistent with the cryo-EM structure of Drosophila TRAPPIII (Appendix B) which identified a triangular-shaped complex with a similar rod-like TRAPP core that contains TRAPPC8 and TRAPPC11 “arms” on either end of the core with a peripheral TRAPPC12/C13 region extending from this core region. This suggests a highly conserved architecture between TRAPPIII complexes in metazoans.

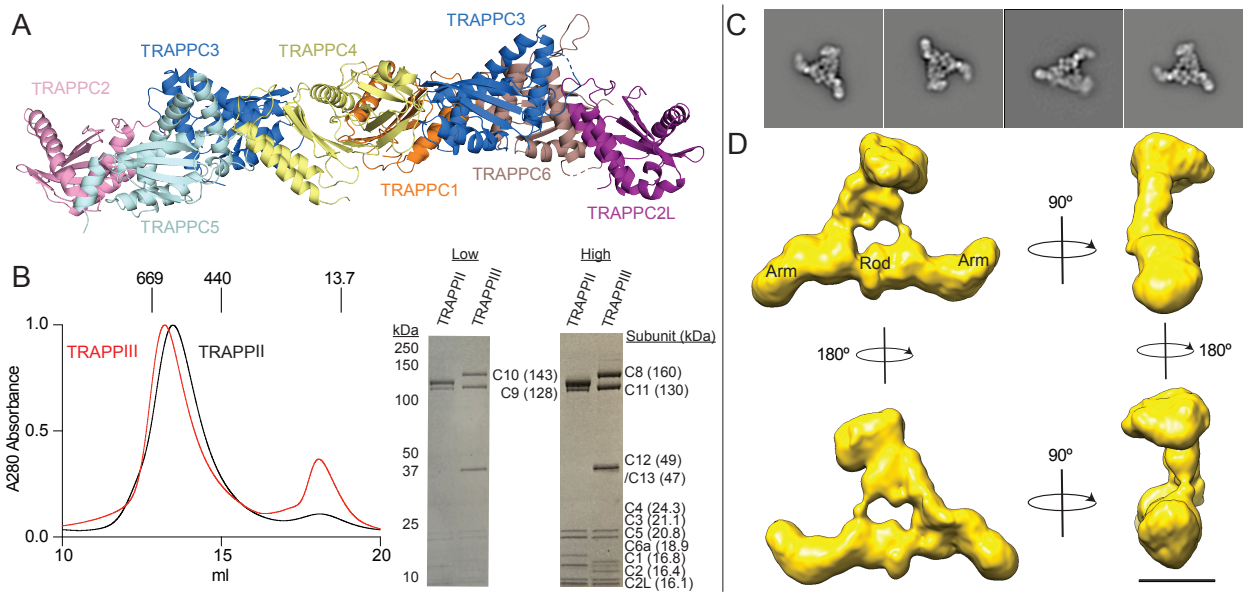

Figure 2-2. Purification and Architecture of the mammalian TRAPPIII complex

A. Model of the mammalian TRAPP conserved subunits. The model was generated through a combination of the following structures (PDB: 2J3T, 2J3W, 3CUE, 7B6R) Phyre2 was used to generate structures of mammalian TRAPP subunits with no solved crystal structure [103]. A model of the TRAPPIII mammalian complex based on the Drosophila Cryo-EM structure is shown in Fig S2C.

B. left: Size Exclusion Chromatography (SEC) trace of TRAPPII and TRAPPIII on a Superose 6 gel filtration column with molecular weight markers indicated in kDa. Absorbance is normalized to max absorbance. Right: SDS-PAGE gel of purified mammalian TRAPPII and TRAPPIII complex. Protein composition is shown on the right. High and low labels refer to protein amount loaded (high=3.6 μg and low= 1.4 μg), uncropped image is shown in Appendix A.

C. Representative 2D negative stain electron microscopy class averages of the TRAPPIII complex. Box edge length is 670 Å.

D. 3D EM reconstruction of TRAPPIII with different orientations of the complex. Scale bar represents 100 Å.

2.4.2 Determination of mammalian TRAPPIII Rab Specificity

To examine the specificity of the GEF activity of the mammalian TRAPPIII complex we tested 20 different Rab GTPases. We focused on Rab GTPases that are evolutionarily similar to Rab1 and Rab11, to identify possibly overlooked Rabs. GEF assays were carried out using Rabs preloaded with the fluorescent GDP analog 3-(N-methyl-anthraniloyl)-2-deoxy-GDP (Mant-GDP) and nucleotide exchange was determined as a function of TRAPP concentration. Rab GTPases were designed with a C-terminal his tag which allowed for GEF activity to be measured in the presence of NiNTA containing membranes.

In solution, the TRAPPIII complex had GEF activity on Rab1 with a catalytic efficiency of ~$1.7x10^3$ $M^{-1}s^{-1}$ which is similar to the catalytic efficiency that we previously determined for TRAPPII on Rab1 ($2.9x10^3$ $M^{-1}s^{-1}$) and consistent with TRAPPIII's role as a Rab1 GEF [42,43] (Fig. 2-3C). Like TRAPPII, we found TRAPPIII mediated activity towards Rab43. TRAPPIII showed increased catalytic efficiency for Rab43 compared to Rab1 ($5.2x10^3$ $M^{-1}s^{-1}$ vs $1.7x10^3$ $M^{-1}s^{-1}$, respectively) which was a similar trend to what was observed with the mammalian TRAPPII complex (Fig. 2-3C) [52]. However, this activity against Rab43 appeared to be logarithmic, which was not observed in Rab1. There was no detectable TRAPPIII mediated GEF activity for any other Rab GTPase tested including Rab11a, Rab11b, or Rab19 which are substrates for mammalian TRAPPII (Fig. 2-3D). This is consistent with TRAPPIII having GEF activity for Rab1 but

not Rab11 in both metazoans and yeast [43,80]. The lack of GEF activity for TRAPPIII with Rab19 was striking because Rab43 and Rab19 are very evolutionarily similar to each other, only diverging in vertebrata with TRAPPII being able to activate both Rab19 and Rab43. A conservational alignment of these GTPases is shown in Appendix C. Collectively, our *in-vitro* analysis of TRAPPIII shows that TRAPPIII is a specific GEF for Rab1a and Rab43 in solution and reveals insight into an unexpected difference in GEF activity between TRAPPII and TRAPPIII towards Rab19. There is no clear sequence relationship explaining the selectivity of why TRAPPII, but not TRAPPIII, is active on Rab19/Rab11 (Appendix C), presenting a need for further high-resolution structural studies to determine Rab selectivity.

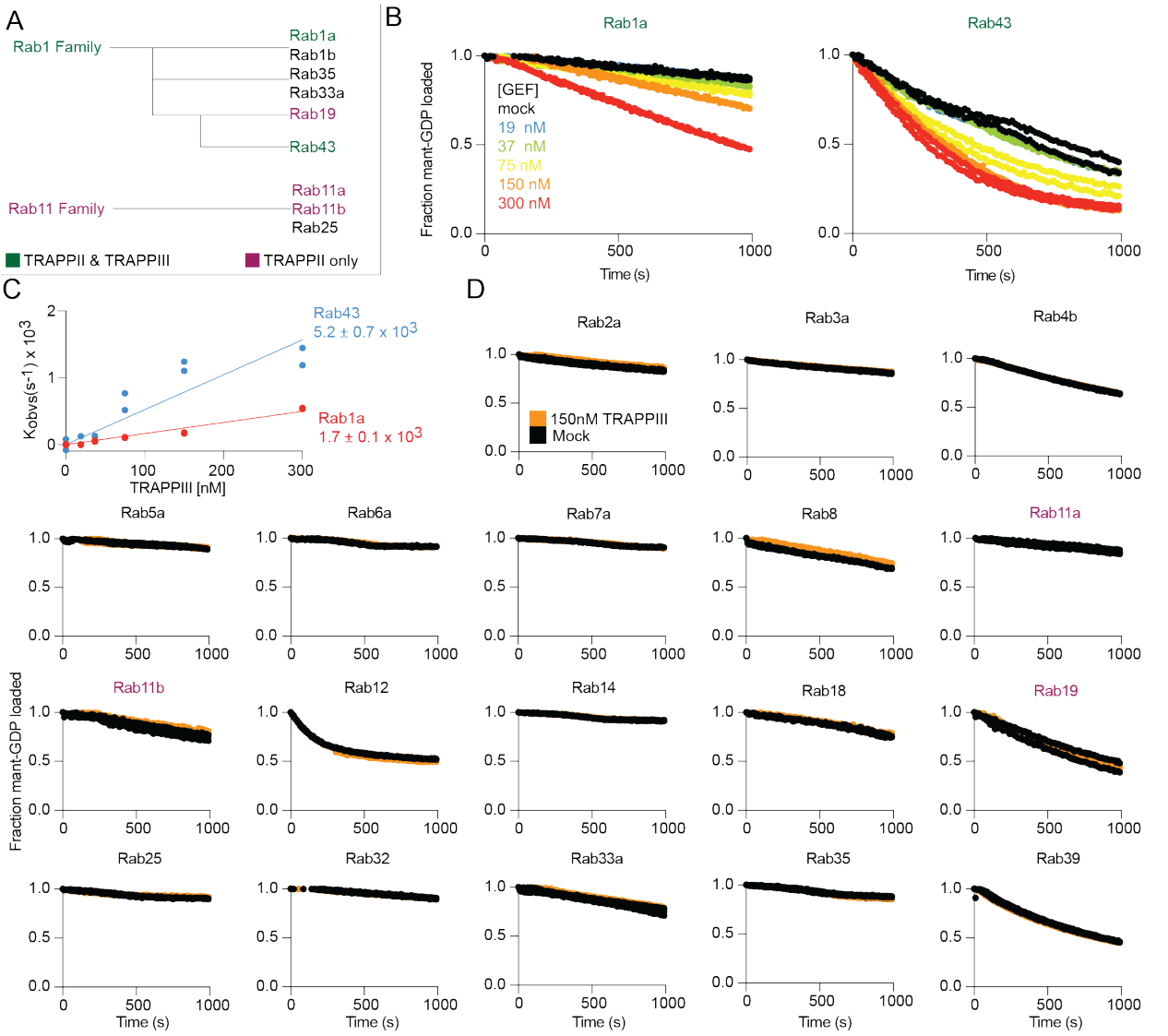

Figure 2-3. Biochemical analysis of the mammalian TRAPPIII complex against a panel of different Rab GTPases.

A. A simplified Rab evolutionary schematic (based on [41]) . Rabs are colored according to their TRAPPII and TRAPPIII GEF activity.

B. In-vitro GEF assay of TRAPPIII on Rab1a and Rab43. Nucleotide exchange was monitored by measuring the fluorescent signal during the TRAPPIII (19 nM-300 nM) catalyzed release of Mant-GDP from 4 μM of Rab-His6 in the presence of 100 μM GTPγS. Each concentration was conducted in duplicate (n=2).

C. Nucleotide exchange rates of Rab1 and Rab43 plotted as a function of TRAPPIII concentration (n=2).

D. In vitro GEF assay of TRAPPIII on the panel of Rab GTPases. 4 μM Rab was loaded with Mant-GDP in the presence of 150nM TRAPPIII. Each concentration was either

conducted in duplicate or triplicate (n=3 for Rab11a, Rab11b, Rab18, Rab19, Rab33, Rab35, n=2 for the others).

2.4.3 Determination of conformational differences upon Rab1 binding to mammalian TRAPPIII

We carried out HDX-MS experiments of TRAPPIII binding to Rab1 to understand the molecular basis for how TRAPPIII binds to and activates Rab1. HDX-MS measures the deuterium incorporation of backbone amide hydrogens in solution, with this being primarily determined by stability of secondary structure. It is a powerful tool to measure protein conformational dynamics. Deuterium incorporation in HDX-MS requires the generation of pepsin peptide fragments spanning the entire complex. We obtained peptide maps spanning 58-97% of the entire complex (**Core**: TRAPPC1, TRAPPC2, TRAPPC2L, TRAPPC3, TRAPPC4, TRAPPC5, TRAPPC6A; **TRAPPII specific**: TRAPPC9, TRAPPC10; **TRAPPIII specific**: TRAPPC8, TRAPPC11, TRAPPC12, TRAPPC13), with specific coverage values listed in Appendix L-N. The majority of proteins had coverage >80%, with TRAPPC3 being the subunit with the poorest coverage (58-69%). Significant differences in exchange between conditions were defined as differences at any timepoint fitting the following three criteria (>5%, >0.5 Da, and two tailed T-test p value <0.01).

HDX-MS experiments were performed in the presence of EDTA to generate a nucleotide free stabilised Rab-GEF complex. Experiments were carried out under three conditions: EDTA treated Rab, TRAPPIII alone, and TRAPPIII bound to Rab1. We observed decreased exchange upon formation of the Rab-TRAPPIII complex in

TRAPPC4 (5-19, 112-136, 180-191) and Rab1a (49-79) (Fig. 2-4B-D). There were multiple regions with increased exchange in Rab1a (12-40, 91-108, 116-165), likely driven by GEF mediated nucleotide loss. The full HDX-MS data for all subunits and Rab1a can be found in [104]. Decreases in exchange in TRAPPC4 (180-191) mapped onto the putative Rab binding site consistent with this peptide being protected when Rab was incubated with TRAPPII [52]. Decreases in exchange in Rab1 were observed in the interswitch and switchII regions upon binding the complex (49-79) (Fig. 2-4B-D). There was no difference in the hyper-variable tail (HVT) of Rab1, as this region was fully deuterated at the earliest time points both apo and when bound to TRAPPIII. Rab1 was also destabilized in the nucleotide binding pocket as would be expected with the loss of nucleotide upon binding its GEF. No other significant changes were observed in the TRAPPIII complex upon Rab binding. These results suggest that both mammalian TRAPPII and TRAPPIII complexes are binding Rabs at a similar interface.

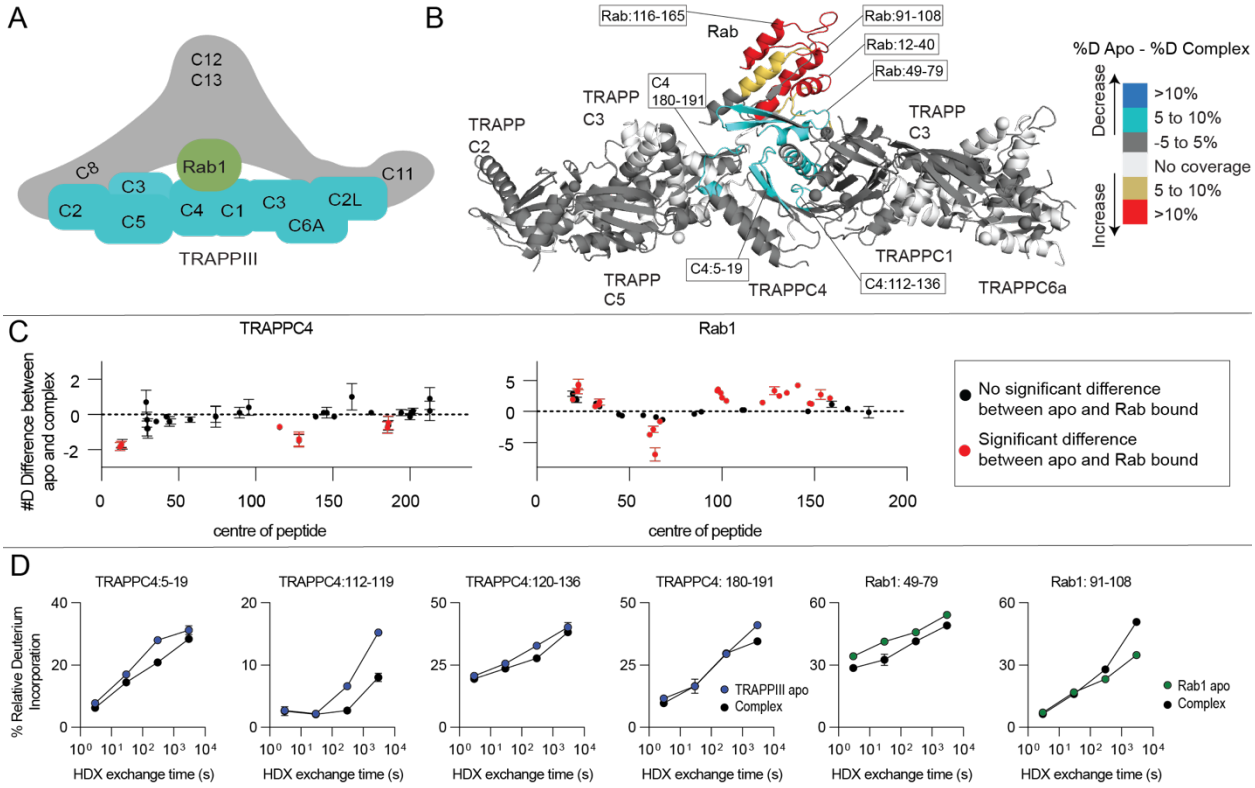

Figure 2-4. Defining the Rab binding site in the mammalian TRAPPIII complex

A. Cartoon schematic highlighting TRAPPIII with bound Rab GTPase.

B. Significant differences in HDX observed across all time points when Rab1 was incubated with TRAPPIII are mapped onto the predicted model of the TRAPP core. Regions with differences are coloured according to the legend.

C. The number of deuteron differences for all analysed peptides over the entire deuterium exchange time course for TRAPPIII in the presence of Rab1 (n=3). Only subunits with significant differences (defined as >5%, >0.5 Da, two tailed T-test p value <0.01), are shown. Every point represents the central residue of an individual peptide with significant differences being indicated by points colored red.

D. Changes in percent deuterium exchange for selected peptides in TRAPPIII and Rab. Error bars represent SD (n=3). The full set of peptide graphs can be found in Appendix E.

2.4.4 Dynamic differences exist at the Rab binding site of the core subunits in the mammalian TRAPPII and TRAPPIII complexes

We carried out hydrogen deuterium exchange mass spectrometry (HDX-MS) experiments comparing TRAPPII vs TRAPPIII to understand any conformational differences that occur in the core between the two complexes. H/D exchange differences between TRAPPII and TRAPPIII can be analyzed only in the shared core components. Multiple different subunits had significant differences in deuterium exchange. TRAPPIII was more protected than TRAPPII in TRAPPC2L (72-80, 100-135), and TRAPPC4 (137-155, 170-204) (Fig. 2-5B-D). TRAPPII was more protected than TRAPPIII in TRAPPC2 (47-53, 59-70), TRAPPC2L (17-25, 37-66, 81-99), TRAPPC4 (65-83) and TRAPPC5 (58-69, 180-188) (Fig. 2-5B-D). The full HDX-MS data for all subunits can be found in [104]. The TRAPPIII complex was more protected than TRAPPII at the canonical Rab interface in TRAPPC4 (170-204). This region in TRAPPC4 would likely be in contact with the N and C termini of the Rab substrate (Fig. 2-5C). Intriguingly, this is in the same region that was protected in TRAPPC4 (181-191) with Rab1a (Fig. 2-4C+D). The large protections observed in the TRAPPC2L subunit are likely due to interactions with TRAPPIII specific subunits which is consistent with cryo-EM data showing TRAPPC2L being at the interface with TRAPPC11 in the Drosophila TRAPPIII complex [83]. Regions of TRAPPC2 were more protected in the TRAPPII complex, which is unexpected since this is the putative binding interface for the TRAPPIII specific subunit TRAPPC8. Together these data suggest that TRAPPII and TRAPPIII have dynamic differences in their core subunits that are involved in Rab binding, which may be playing a role in mediating Rab specificity.

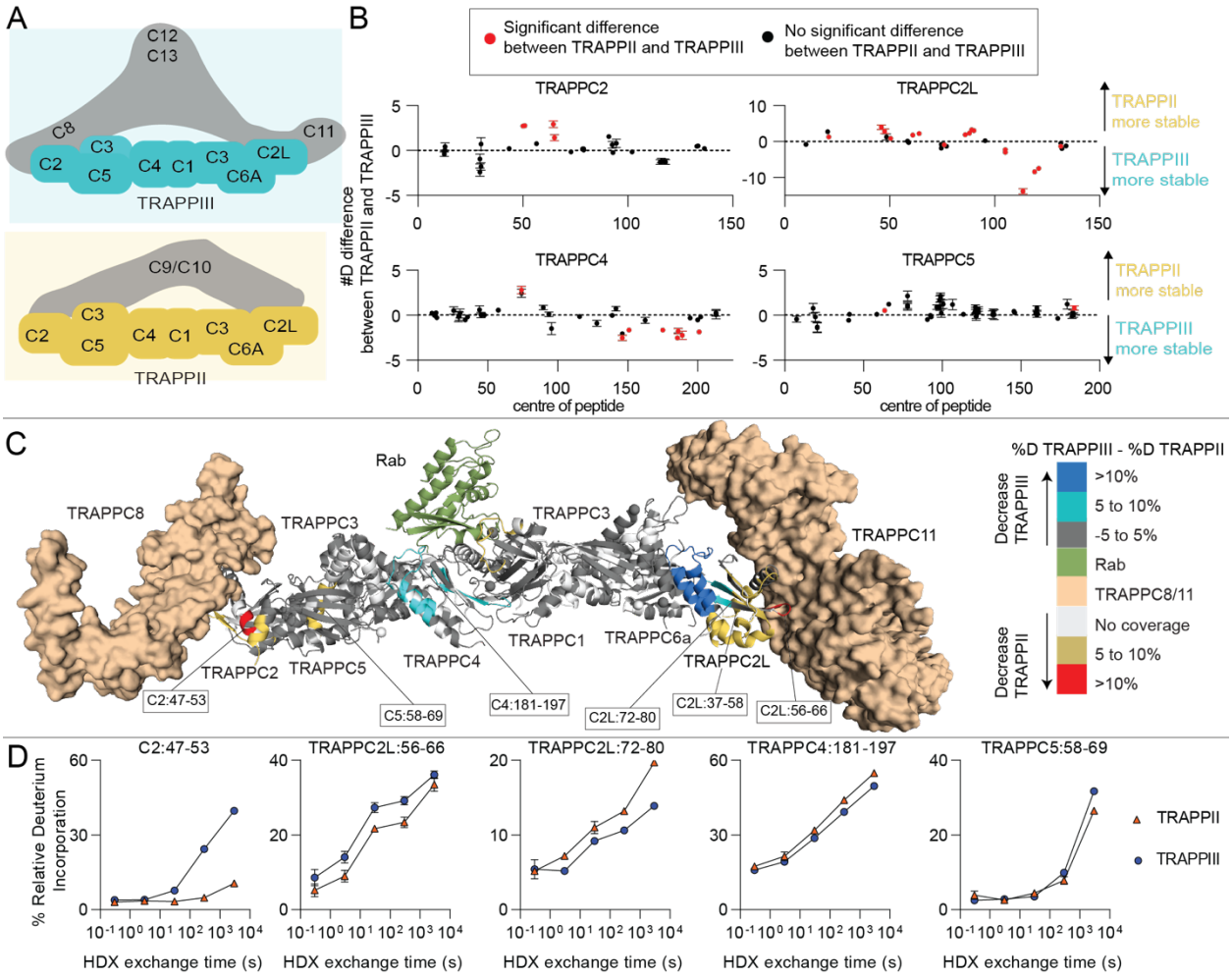

Figure 2-5. Comparative HDX-MS reveals dynamic differences within the core of TRAPPIII compared to TRAPPII

A. Cartoon schematic highlighting protections or destabilisations in TRAPPII and TRAPPIII.

B. The number of deuteron differences for all analysed peptides over the entire deuterium exchange time course for TRAPPIII compared to TRAPPII (n=3). Red points indicate peptides with significant differences (defined as >5%, >0.5 Da, two tailed T-test p value <0.01) in HDX. Only subunits with significant differences between complexes are shown. The full H/D exchange data can be found in [104]. Increases in the number of deuterons indicates a stabilization in TRAPPII while a decrease in the number of deuterons indicates a stabilization in TRAPPIII. Every point represents the central residue of an individual peptide.

C. Significant differences in HDX between the TRAPP complexes are mapped on to the TRAPPIII model (based on PDB: 7B6R), with Rab shown to illustrate the binding interface. Increases in exchange are regions that are more stable in TRAPPII, with

decreases in exchange representing regions that are more stable in TRAPPIII. Regions with differences are coloured according to the legend.
D. Changes in percent deuterium exchange for selected peptides in the conserved subunits between TRAPPII and TRAPPIII. Error bars represent SD (n=3). The full set of peptide graphs can be found in Appendix F.

2.4.5 The C-terminus of Rab GTPases is not the sole determinant of selectivity for mammalian TRAPP complexes

The conformational differences observed in the TRAPPC4 subunit between TRAPPII and TRAPPIII at a region that interacts with the N-terminus and C-terminus of Rab substrates led us to investigate the potential role of the Rab C-terminus in controlling substrate specificity. We generated two chimeras of both Rab1 and Rab11 where we replaced part of the C-terminal helix and the entire hyper-variable tail (Fig. 2-6A+B). We conducted GEF assays using TRAPPIII against the four different constructs and found that changing the C-terminus of Rabs did not alter the substrate specificity, with no activity at all against Rab11 with different C-termini, and slightly increased activity with toward Rab1A with the chimeric Rab11A C-termini (Fig. 2-6C). The hyper-variable tail of Rabs play an essential role in controlling Rab selectivity in the yeast TRAPPII and TRAPPIII complexes, with this mediated by a steric gating mechanism [80]. The chimera data with mammalian TRAPP complexes reveals that there is some determinant of Rab selectivity that is independent of the C-termini and may be driven either by conformational changes in the Rab binding site, or additional interactions between the TRAPPII or TRAPPIII specific subunits and the substrate Rabs.

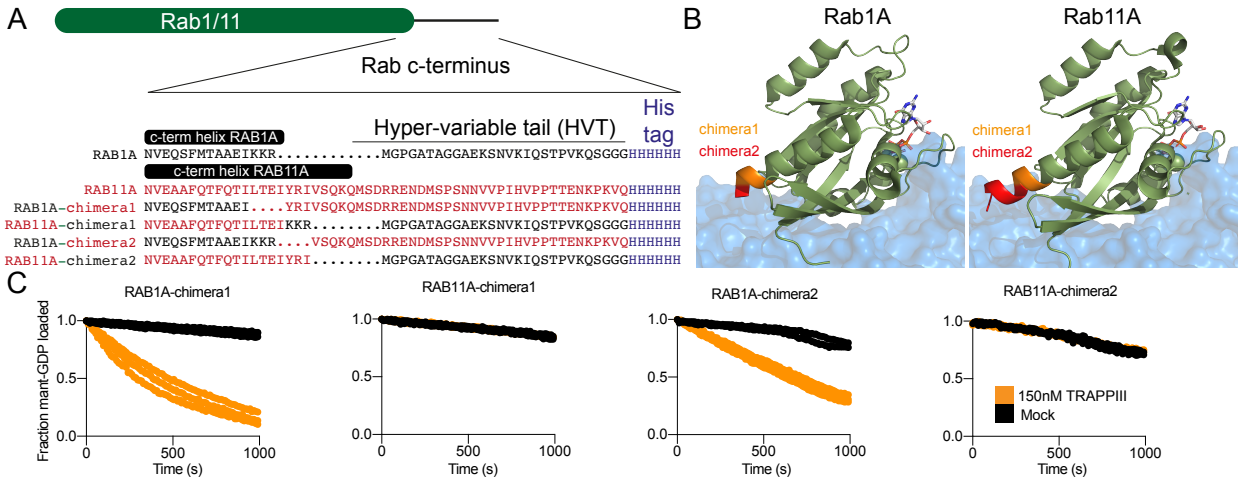

Figure 2-6. The C-terminus of Rab1A and Rab11 is not the major determinant of Rab selectivity for mammalian TRAPPIII

A. Alignment of the C-terminus of Rab1A and Rab11A, covering the C-terminal helix of the Nucleotide binding domain, and the hyper-variable tail. The lipidated cysteine residue is replaced by a his-tag, to allow for Ni-NTA mediated coupling to membranes. Chimeras of Rab1 and Rab11 were generated replacing the C-terminus of Rabs as indicated by the sequence alignment. Rab1A sequence is in black, with the Rab11A sequence in red.

B. Structures of Rab1A (pdb: 3tkl) [105] and Rab11A (pdb: 6djl) [53] with the approximate position of the TRAPP core as described in Cai et al (pdb: 3cue) [69]. The colors indicate the locations where the sequence is swapped for the two chimeras.

C. In vitro GEF assay of TRAPPIII against Rab1a and Rab11a c-terminal chimeras. 4 μM Rab was loaded with Mant-GDP in the presence of 150 nM TRAPPIII. Control experiments without GEF present were conducted in duplicate for Rab1A and Rab11A chimera1 (n=2), all other concentrations and controls for all other experiments were done in triplicate (n=3).

2.4.6 Membrane binding enhances GEF activity of TRAPPII and TRAPPIII, and leads to extensive conformational changes

To investigate the role that membranes play in altering TRAPPII and TRAPPIII Rab activity we compared TRAPPII and TRAPPIII mediated GEF activity of Rab1 on extruded liposomes and conducted HDX-MS experiments examining conformational changes that occur upon membrane binding for both TRAPII and TRAPPIII. We tested TRAPPII's and

TRAPPIII's ability to activate Rab1a on membranes, with both having enhanced GEF activity. The TRAPPIII complex was more active than TRAPPII with membrane localised Rab1a (43.2 x 10^3 $M^{-1}s^{-1}$ vs 8.8 x 10^3 $M^{-1}s^{-1}$ respectively, Fig. 2-7A+B, Fig. 2-8A+B). This is consistent with TRAPPIII being the primary activator of Rab1 *in-vivo* and further validates that TRAPP complexes are more efficient GEFs when their substrates are presented on a membrane surface.

Increased GEF activity on membrane surfaces could be mediated by a multitude of mechanisms. Activity could be enhanced by increased local concentration of GEF and substrate on membranes, and/or conformational changes in the TRAPP complex may occur upon membrane binding. We compared differences in HDX-MS upon membrane binding for both TRAPPII and TRAPPIII. Liposomes were composed of 45% PC, 10% PI, 15% PE, 10% PS, 10% DGS NTA, 10% PI(4)P, mimicking the composition of the trans Golgi network (TGN).

Numerous differences were observed in multiple subunits of TRAPPIII (Fig. 2-7) and TRAPPII (Fig. 2-8) in the presence of liposomes. There was decreased exchange in TRAPPIII in TRAPPC8 (5-21, 115-126, 376-421, 440-457, 471-487, 492-498) and increased exchange was observed in TRAPPC4 (181-191), TRAPPC8 (24-62, 340-350, 588-620, 643-647, 710-720, 759-767, 981-992, 1105-1139, 1159-1198, 1266-1284, 1369-1380), TRAPPC11 (13-25, 74-96, 120-139, 152-161, 193-259, 266-281, 312-338, 349-373, 405-477, 612-621, 773-852, 882-889, 1056-1066), TRAPPC12 (341-358, 382-399, 701-716), and TRAPPC13 (119-127, 311-327, 375-387) (Fig. 2-7D-F, Appendix

G+H). The full list of HDX-MS data for all subunits is compiled in [104], with exchange data for peptides with differential exchange shown in Appendix G+H.

The decreased exchange observed in TRAPPC8 upon membrane binding (5-21, 115-126, 376-421, 440-457, 471-487, 492-498) could be contact sites between TRAPPC8 and membrane or interactions between TRAPPC8 and different subunits that are enhanced in the presence of membranes. The protection in TRAPPC8 (376-421) in the presence of liposomes is consistent with a conserved amphipathic helix present in the yeast TRAPPC8 homolog trs85 (368-409) that was found to be important for membrane binding [78]. This region is highly conserved (Appendix D) and reveals a key role of TRAPPC8 in driving membrane binding of TRAPPIII. Increased exchange was observed in the TRAPPIII complex specific subunits (TRAPPC8, TRAPPC11, TRAPPC12, TRAPPC13), and the conserved TRAPPC4 subunit. The increased exchange in the core subunits of TRAPPIII (TRAPPC4) include regions that span the Rab binding site (TRAPPC4 181-191) and reveal a possible conformational driven mechanism of activation of TRAPP GEF activity on membranes.

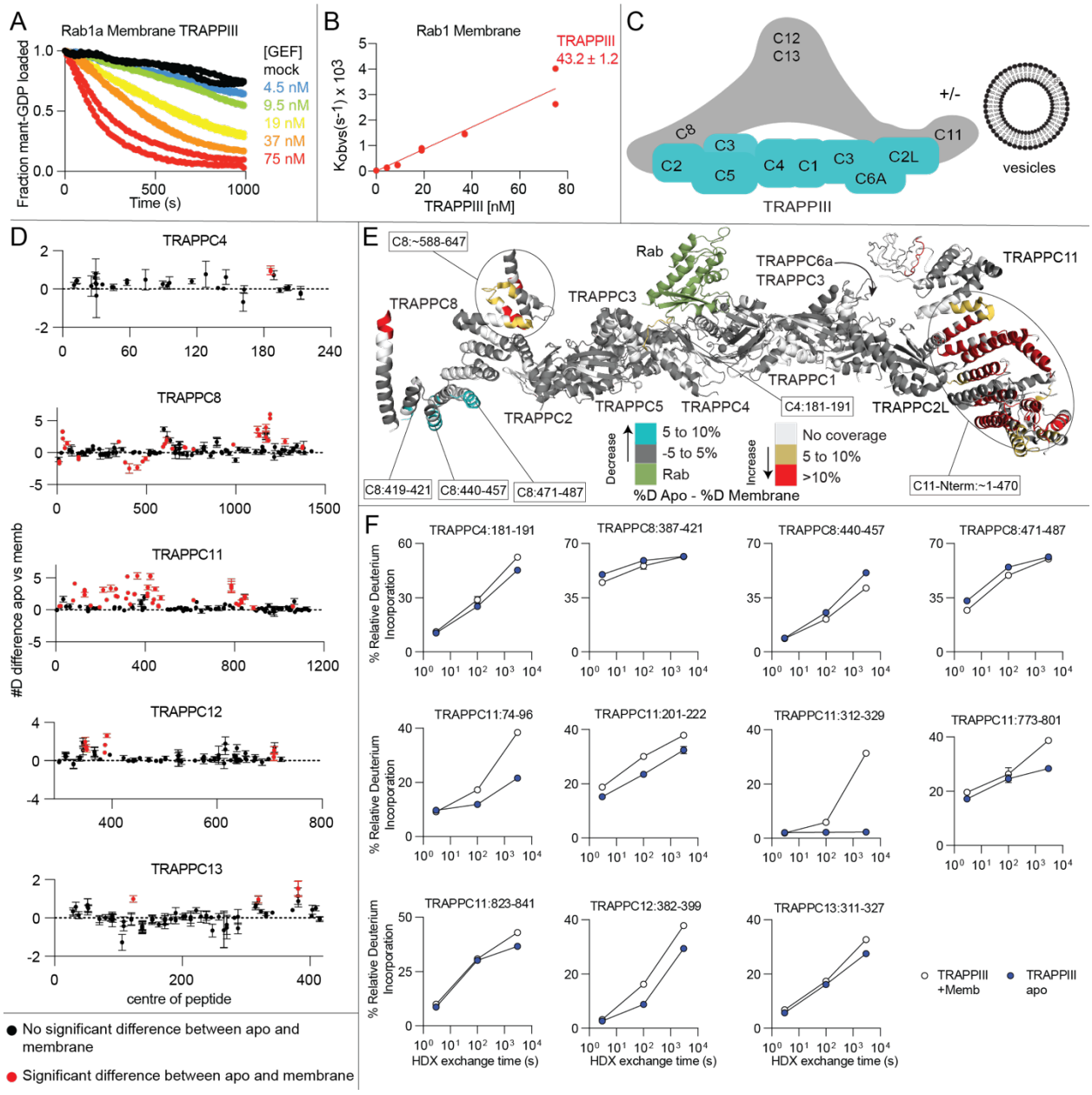

Figure 2-7. Membrane binding increases TRAPPIII-GEF activity and leads to large scale conformational changes

A. In vitro GEF assay of TRAPPIII at various concentrations (4.5nM – 75nM) against Rab1a (4 μM) in the presence or absence of 150 nm extruded liposomes at 0.2mg/ml (45% PC, 10% PI, 15% PE, 10% PS, 10% DGS NTA, 10% PI(4)P, n=2).

B. Nucleotide exchange rates of Rab1 plotted as a function of TRAPP concentration (n=2)

C. Cartoon schematic of TRAPPIII-membrane experiments.

D. The number of deuteron difference for all analysed peptides over the entire deuterium exchange time course for TRAPPIII in the presence and absence of 150 nm extruded

liposomes (45% PC, 10% PI, 15% PE, 10% PS, 10% DGS NTA, 10% PI(4)P) (n=3). Only subunits with significant differences are shown (defined as >5%, >0.5 Da, two tailed T-test p value <0.01). Every point represents the central residue of an individual peptide with significant differences indicated in red.
E. HDX changes with TRAPPIII and membranes are mapped onto the mammalian TRAPPIII model (based on PDB: 7B6R). Regions with differences are coloured according to the legend.
F. Changes in percent deuterium exchange for selected TRAPPIII peptides with and without membranes. Error bars represent SD (n=3). The full set of peptide graphs for TRAPPIII can be found in Appendix G+H.

Differences were observed in multiple subunits of TRAPPII (Fig. 2-8) in the presence of liposomes, however, distinct from TRAPPIII all differences were increases in exchange rates. We observed increased exchange in TRAPPII upon membrane binding in TRAPPC2L (8-16, 56-66), TRAPPC5 (51-69), TRAPPC9 (68-80, 87-99, 160-180, 311-322, 352-363, 890-896, 1006-1033) and TRAPPC10 (30-37, 95-124, 149-162, 272-310, 374-381, 397-423, 469-487, 489-562, 740-760, 1093-1112, 1133-1147) (Fig. 2-8D-E, Appendix I). The full list of HDX-MS data for all subunits is compiled in [104], with exchange data for peptides with differential exchange shown in Appendix I. Changes were observed in TRAPPII specific subunits (TRAPPC9, TRAPPC10) as well as in the core subunits TRAPPC2L and TRAPPC5 suggesting that large conformational changes occur upon membrane binding, suggesting a potential reorientation of subunits relative to each other on membrane surfaces.

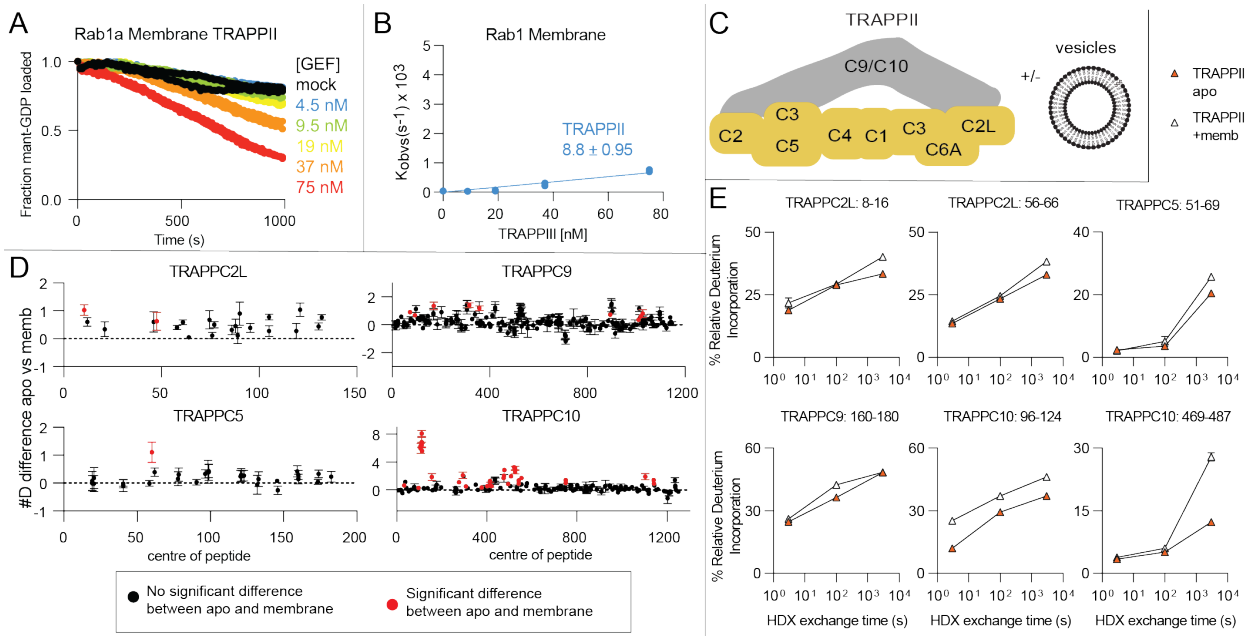

Figure 2-8. Membrane binding increases TRAPPII-GEF activity and leads to large scale conformational changes

A. In vitro GEF assay of TRAPPIII at various concentrations (4.5nM – 75nM) against Rab1a (4 μM) in the presence or absence of 150 nm extruded liposomes at 0.2mg/ml (45% PC, 10% PI, 15% PE, 10% PS, 10% DGS NTA, 10% PI(4)P, n=2).

B. Nucleotide exchange rates of Rab1 plotted as a function of TRAPP concentration (n=2)

C. Cartoon schematic of TRAPPII-membrane experiments.

D. The number of deuteron difference for all analysed peptides over the entire deuterium exchange time course for TRAPPII in the presence and absence of 150 nm extruded liposomes (45% PC, 10% PI, 15% PE, 10% PS, 10% DGS NTA, 10% PI(4)P) (n=3). Only subunits with significant differences are shown (defined as >5%, >0.5Da, two tailed T-test p value <0.01). Every point represents the central residue of an individual peptide with significant differences indicated in red.

E. Changes in percent deuterium exchange for selected TRAPPII peptides with and without membranes. Error bars represent SD (n=3). The full set of peptide graphs for TRAPPII can be found in Appendix I.

2.5 Discussion

The TRAPPII and TRAPPIII complexes play critical roles in activating Rab GTPases during membrane trafficking processes, with these complexes being conserved

in all Eukaryotes. They have well established roles in a diverse set of pathways including secretion, ER-Golgi transport and autophagy [38,42,72,76,106]. Many biochemical and structural studies have revealed the architecture of these complexes in both yeast and metazoans showing how these complexes are assembled and how they bind and activate Rab GTPases [42,69,73,77,82,84]. However, the exact molecular details for TRAPP complex Rab substrate selectivity and membrane activation are still ambiguous. Our biophysical and biochemical analysis of the mammalian TRAPPIII complex has revealed novel insight into TRAPPIII substate specificity, how complex specific subunits alter the Rab binding interface of the core, and how membranes lead to large scale conformational changes in both TRAPPII and TRAPPIII.

The mammalian TRAPPII complex has activity towards Rab1, Rab11a/b, Rab19 and Rab43 [52]. The TRAPPIII complex is a well validated GEF for Rab1a, however, the substrate specificity towards other Rab GTPases for mammalian TRAPPIII is unknown. We find that mammalian TRAPPIII has activity towards Rab1a and a novel activity towards Rab43. There was no detectable GEF activity for Rab19 or the other 17 Rab GTPases tested. The observation that TRAPPIII is a GEF for Rab43 but not Rab19 is intriguing since Rab43 and Rab19 are in the Rab1a family and are very evolutionarily similar [41]. TRAPPII was equally active against both Rab43 and Rab19, revealing an additional substrate selectivity between TRAPPII and TRAPPIII. Extensive sequence analysis between Rab1/Rab43 with Rab19/Rab11 does not reveal a simple difference for how TRAPPII and TRAPPIII obtain substrate selectivity. Further biochemical and high-

resolution structural data will be required to decipher the exact molecular mechanism of Rab specificity.

Multiple conformational differences were observed between TRAPPII and TRAPPIII in the shared subunits. TRAPPIII was more stable at the Rab-binding interface compared with TRAPPII, which suggests initial insight into a possible mechanism for how these complexes can mediate Rab specificity. The C-terminus of TRAPPC4 was more stable in TRAPPIII, with these being very similar regions to those protected upon Rab binding in TRAPPIII and TRAPPII (180-191 in TRAPPC4) [52]. It's possible that this alteration in the conformation of the putative Rab binding site prevents association with either Rab11 or Rab19 for TRAPPIII. The recent Cryo-EM structure of Drosophila TRAPPIII allowed for a comparison between the two complexes seen in the mammalian complexes [83]. Intriguingly, the interfaces identified between TRAPPC2 with TRAPPC8 and TRAPPC2L with TRAPPC11 identified in the Drosophila TRAPPIII cryo-EM structure were more protected from H/D exchange in TRAPPII compared to TRAPPIII. This suggests that there are shared interfaces between the core and the TRAPPII and TRAPPIII unique subunits. Further details of the differences will require high resolution structural data of the TRAPPII complex.

Rab substrates had increased activity in the presence of membranes for both TRAPPII and TRAPPIII, consistent with studies of the yeast TRAPPII and TRAPPIII complexes [42]. The TRAPPIII complex activated Rab1a significantly faster in the presence of membranes compared to TRAPPII which is consistent with TRAPPIII being the primary activator of Rab1 *in-vivo*. This increased activity may be driven by the

membrane binding site identified in HDX-MS studies in TRAPPC8. We found multiple peptides with significant protections spanning TRAPPC8 including the region 376-421. This region corresponds to an amphipathic helix (368-409) discovered in yeast Trs85, where mutants of this region decreased membrane recruitment and Rab activation [78]. This highlights a conserved role throughout evolution of the TRAPPC8 subunit in mediating membrane association and activation of Rab1. Multiple TRAPPII and TRAPPIII specific subunits were destabilised upon membrane binding. These increases in exchange are likely driven by conformational rearrangements of the subunit-subunit interacting regions. Further detailed structural studies will help interpret how these changes may mediate membrane binding or alter GEF activity.

The emerging set of clinical mutations in either TRAPP core or complex specific subunits demonstrates the important roles that both TRAPPII and TRAPPIII play in membrane trafficking [7,8,11,12]. Interestingly, our HDX-MS experiments revealed conformational differences between TRAPPII and TRAPPIII located at or near these sites of mutations (Appendix J). These differences occurred in TRAPPC2 and TRAPPC2L. The mutations D47Y, H80R, and F83S in TRAPPC2 have been associated with the skeletal disorder spondyloepiphyseal dysplasia tarda (SEDT; also abbreviated SEDL) [85,86]. TRAPPII was protected compared to TRAPPIII in peptides spanning 47-53 and 59-70 of TRAPPC2. The D47Y mutation has been shown to disrupt both the TRAPPIII and TRAPPII complexes through disrupting the interactions between TRAPPC2 with TRAPPC9 or TRAPPC8 [86] with the equivalent D46Y mutation in yeast only disrupting the TRAPPIII complex [85]. The mutation D37Y in TRAPPC2L has been associated with

neurodevelopmental delay [87]. The equivalent yeast mutant (D45Y) disrupts the interaction between TRAPPC2L and the TRAPPII specific subunit TRAPPC10 [87]. We found large stabilisations in TRAPPII compared to TRAPPIII in a peptide spanning 37-58 which would be consistent with this mutation disrupting the TRAPPC2L-TRAPPC10 interaction. This mutant is at the interface of TRAPPC2L with TRAPPC11 in the Drosophila TRAPPIII complex [83], however, the differences between TRAPPII and TRAPPIII at these important residues indicate that the clinical mutants could possibly target TRAPPII and TRAPPIII differently depending on unique interactions with complex specific subunits.

HDX-MS experiments examining differences upon membrane binding revealed secondary structure differences at or near regions mutated in human disease, specifically in TRAPPC9 and TRAPPC11. The mutation L178P in TRAPPC9 has been implicated with severe intellectual disability [88]. HDX-MS experiments comparing apo-TRAPPII to membrane bound TRAPPII showed an exposure in a peptide spanning 160-180. Furthermore, the mutations Q284P and Q777P of TRAPPC11 have been implicated in muscular disorders by elevated creatine kinase levels and cerebral atrophy [89,94] and we found that TRAPPC11 was exposed in the peptides 266-281 and 773-801. The peptide spanning 266-281 lies extremely close to the Q284 residue and the peptide spanning 773-801 completely contains the Q777 residue. These secondary structure differences could indicate that these clinical mutants alter the membrane activation of both TRAPPII and TRAPPIII complexes. More research is needed to investigate the exact molecular mechanisms of these clinical mutants and how they alter TRAPP's function.

The TRAPP complexes are some of the most important regulators of membrane trafficking and activators of Rabs at the Golgi. Our data highlights the critical dynamic differences between the two complexes at the Rab binding site which likely has a role in regulating Rab specificity and is highlighted in Figure 2-9. Continued biochemical and structural studies will be required to decipher the exact mechanism of this specificity with this work helping provide a strong start point for these future studies.

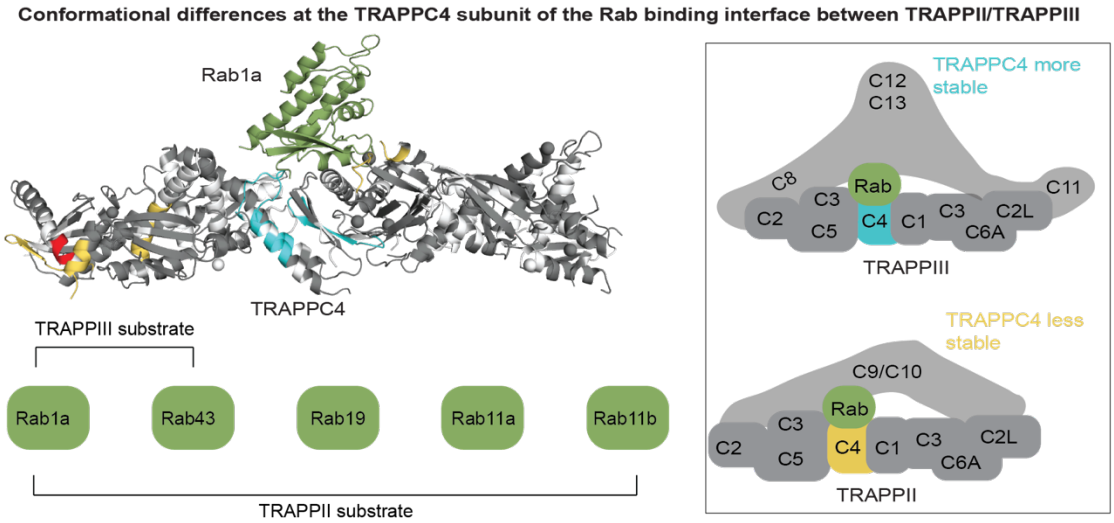

Figure 2-9. TRAPPIII activity summary figure showing the activity of TRAPPII/TRAPPIII and the conformational differences that exist at the Rab binding site.

Chapter 3 - Conclusions and Future Directions

3.1 Conclusions

Rab GTPases are critical regulators of membrane trafficking and therefore must be strictly controlled by their appropriate GEFs and GAPs. Understanding how Rabs are activated by GEFs is fundamental to advancing our understanding of the role they play in membrane trafficking. The large multi-subunit TRAPPII and TRAPPIII complexes are potent Rab GEFs and play roles in secretion, autophagy and trafficking at the Golgi. TRAPPII and TRAPPIII share a conserved core that binds and activates Rab GTPases. However, even though the same subunits in TRAPPII and TRAPPIII are responsible for binding Rabs, the two complexes have differential Rab selectivity. This thesis was centered around investigating these large multi-subunit machines and determining the molecular mechanism of this intriguing TRAPP-Rab specificity.

To address this thesis' objective, we utilized a combination of powerful biophysical and biochemical techniques. In summary, we were able to purify mammalian TRAPPII and TRAPPIII using the biGBac method [96]. We revealed the architecture of the mammalian TRAPPIII complex using electron microscopy which closely resembled the triangular-shaped Drosophila TRAPPIII complex [83]. We characterised the GEF activity of the TRAPPIII complex against a panel of 20 different Rab GTPases and found activity for Rab1 and Rab43 but not for any other Rab tested. The lack of activity with TRAPPIII towards Rab19 revealed an unexpected selectivity difference between TRAPPII and TRAPPIII. HDX-MS revealed the Rab binding site within the TRAPP core composed of TRAPPC4, and that this binding site was more stable in TRAPPIII compared with

TRAPPII. This difference between TRAPPII and TRAPPIII suggested a potential role of the complex specific subunits in reshaping the Rab binding site to permit and inhibit specific Rabs. HDX-MS revealed large conformational changes in both TRAPPII and TRAPPIII upon membrane binding and identified a conserved membrane binding region in the TRAPPC8 subunit of TRAPPIII. Finally, GEF activity was enhanced when the substrate is presented on a membrane surface. Overall, this thesis provides valuable insight to the field with regards to the different dynamics of these complexes and how they can mediate Rab specificity providing a fundamental start point for future studies.

3.2 Future Directions

The findings from this thesis reveal several new and exciting aspects to how these large, complicated TRAPP complexes regulate Rab activity. We now have evidence towards the dynamics of the Rab binding site which could mediate Rab specificity. Despite what we now know, some questions remain unanswered.

3.2.1 Further investigating specificity

Our GEF assays revealed activity with TRAPPIII towards Rab1 and Rab43, but no other Rab tested. This was intriguing because TRAPPII had no preference in activating Rab43 or Rab19. Further, we know that TRAPPII can activate Rab1 in solution which shows that TRAPPII can activate the same Rabs TRAPPIII activates in solution. This unanswered question relates to determining the exact residues (either in TRAPP or Rab) involved dictating Rab specificity. In yeast, specificity is controlled via a steric gating

mechanism regulated by the HVTs of Rabs [80], however this does not seem to be entirely the case for mammalian TRAPPs. For example, HVTs are slightly different lengths in mammalian Rabs, the chimeras we generated in Figure 2-5 in chapter 2 showed no alteration of activity and the low HDX signal we observed in the HVT when Rab1 was incubated with TRAPPIII (Figure 2-3) show that there may be some other factors designating specificity.

With the release of the metazoan TRAPPIII structure, Galindo *et al.,* 2021 proposed that the TRAPPC8 arm could serve to mediate Rab specificity and/or enhance activity by directly interacting with bound Rab [83]. Additionally, it's been proposed that the flexibility of the TRAPPC8 and TRAPPC11 arms could allow for the TRAPPC8 arm to physically interfere or block Rab binding [83]. TRAPPIII activity could then in theory be mediated by an allosteric event that caused movement of the TRAPPC8 arm to expose/block the Rab binding site. Additionally, TRAPPC8 and TRAPPC11 arms make some contact with core subunits which supports the possibility presented in this thesis of an allosteric or conformationally driven mechanism [83].

The architecture of the metazoan TRAPPIII complex is relatively well defined. However, there seems to be a lack of high-resolution structural information for the metazoan TRAPPII complex. A high-resolution structure of metazoan TRAPPII would allow for direct comparison between TRAPPII and TRAPPIII giving valuable structural insight into the TRAPPII complex specific subunits and importantly determine how they are arranged around the core subunits. This would be helpful information for answering

the question presented in this thesis relating to how the complex specific subunits of TRAPPII might play a role in membrane binding or Rab activation.

Further investigating Rab specificity between TRAPPII and TRAPPIII would require detailed structural analysis of both complexes with and without Rab bound. Assuming adequate structural information is available, one could compare the structures of both complexes in combination with using the regions identified in TRAPPC4, TRAPPC8, and Rab from this thesis as start points to investigate exact residues involved in mediating specificity. Detailed structural analyses within these regions of both TRAPP complexes along with a thorough sequence analysis across various Rabs would identify key putative residues. The key residues determined can be used to generate chimeras or mutant variants of Rabs that “swap” their GEF specificity (i.e., Rab11 variant that can be activated by TRAPPIII) and would unambiguously show how Rab specificity is achieved, and which residues are essential. The mutant Rab’s GEF activity could be determined using the same GEF assay used in this thesis and *in-vitro* activity could be recapitulated *in-vivo* by observing the localization of mutant Rabs with the different TRAPP complexes to distinct membranes.

It has also been proposed that TRAPP complexes can be recruited to specific membranes. Active Arf1 can recruit TRAPPII to anionic membranes in yeast [51] with TRAPPII having increased activity in the presence of anionic membranes in yeast and mammalian cells [52]. TRAPPIII also has several potential effectors such as COP proteins Sec23/24, Sec13/31, and the autophagy protein Atg9 that could recruit TRAPPIII to the appropriate membrane to activate a particular Rab [40,65]. Further, this recruitment and

activity could also be in part mediated by the Rab GDI which is partially responsible for the membrane localisation of Rabs.

To date, Rab19 has generally been a poorly understood Rab. However, recently Jewett *et al.,* 2021 found that Rab19 associates with the Rab-GAP: TBC1D4 and the HOPS-tethering complex to regulate ciliary membrane growth [59]. In this thesis we illustrated the ability for TRAPPII to activate Rab1, Rab11, Rab19 and Rab43 with TRAPPIII being specific to only Rab1 and Rab43. The finding that TRAPPIII was able to activate Rab43 but unable to activate the evolutionary similar GTPase Rab19 was an unexpected result from this thesis since TRAPPII had no preference for either Rab19 or Rab43 [52]. Rab11 already has an established role in ciliogenesis through the Rab11-Rab8 cascade which helps mediate the formation of ciliary vesicles [50]. The observation of Rab19 being involved in ciliogenesis potentially highlights TRAPPII's important role in activating Rabs that control this process in addition to its established roles in secretion. Moreover, this gives some insight into why TRAPPII but not TRAPPIII has activity towards Rab19. To support this, in 2019, an additional putative TRAPPII specific subunit was identified named TRAPPC14 [107]. TRAPPC14 was found to interact with Rabin8 (a Rab8 GEF) and to be involved in ciliogenesis. Further investigation into TRAPPII's role in ciliogenesis would be interesting, specifically looking into known and unknown Rabs and effectors involved that could play a role in recruiting TRAPP complexes to distinct membranes thus controlling specificity.

These large complexes clearly have the capacity to interact with a multitude of different effectors which highlights the potential unknown roles of the TRAPP complexes

that have yet to be completely discovered. Further investigation of these proteins that interact with or recruit TRAPP is important, and more work is needed to understand if they play a role in mediating Rab specificity. For example, identifying TRAPP putative binding partners (i.e. TRAPPC14) using pull-down assays, bio-layer interferometry (BLI), or isothermal titration calorimetry (ITC), investigating binding interfaces and/or conformational differences within the core subunits in the presences of a binding partner using HDX-MS, then using mutations to verify and disrupt these potential interfaces, and reconstituting of TRAPP complexes with binding partners on membranes or in solution to investigate activity.

Bibliography

[1] J. Cherfils, M. Zeghouf, Regulation of Small GTPases by GEFs, GAPs, and GDIs, Physiological Reviews. 93 (2013) 269–309. https://doi.org/10.1152/physrev.00003.2012.

[2] H. Stenmark, Rab GTPases as coordinators of vesicle traffic, Nat Rev Mol Cell Biol. 10 (2009) 513–525. https://doi.org/10.1038/nrm2728.

[3] M.P. Müller, R.S. Goody, Molecular control of Rab activity by GEFs, GAPs and GDI, Small GTPases. 9 (2018) 5–21. https://doi.org/10.1080/21541248.2016.1276999.

[4] P. Novick, Regulation of membrane traffic by Rab GEF and GAP cascades, Small GTPases. 7 (2016) 252–256. https://doi.org/10.1080/21541248.2016.1213781.

[5] A. Delprato, E. Merithew, D.G. Lambright, Structure, exchange determinants, and family-wide rab specificity of the tandem helical bundle and Vps9 domains of Rabex-5, Cell. 118 (2004) 607–617. https://doi.org/10.1016/j.cell.2004.08.009.

[6] J. Barrowman, D. Bhandari, K. Reinisch, S. Ferro-Novick, TRAPP complexes in membrane traffic: convergence through a common Rab, Nature Reviews Molecular Cell Biology. 11 (2010) 759–763. https://doi.org/10.1038/nrm2999.

[7] S. Brunet, M. Sacher, In Sickness and in Health: The Role of TRAPP and Associated Proteins in Disease, Traffic. 15 (2014) 803–818. https://doi.org/10.1111/tra.12183.

[8] J.J. Kim, Z. Lipatova, N. Segev, TRAPP Complexes in Secretion and Autophagy, Front. Cell Dev. Biol. 4 (2016). https://doi.org/10.3389/fcell.2016.00020.

[9] Z. Lipatova, N. Segev, Ypt/Rab GTPases and their TRAPP GEFs at the Golgi, FEBS Letters. 593 (2019) 2488–2500. https://doi.org/10.1002/1873-3468.13574.

[10] M. Sacher, Y.-G. Kim, A. Lavie, B.-H. Oh, N. Segev, The TRAPP Complex: Insights into its Architecture and Function, Traffic. 9 (2008) 2032–2042. https://doi.org/10.1111/j.1600-0854.2008.00833.x.

[11] M. Sacher, N. Shahrzad, H. Kamel, M.P. Milev, TRAPPopathies: An emerging set of disorders linked to variations in the genes encoding transport protein particle (TRAPP)-associated proteins, Traffic. 20 (2019) 5–26. https://doi.org/10.1111/tra.12615.

[12] Z. Lipatova, N.V. Bergen, D. Stanga, M. Sacher, J. Christodoulou, N. Segev, TRAPPing a neurological disorder: from yeast to humans, Autophagy. 16 (2020) 965–966. https://doi.org/10.1080/15548627.2020.1736873.

[13] S.L. Schwartz, C. Cao, O. Pylypenko, A. Rak, A. Wandinger-Ness, Rab GTPases at a glance, Journal of Cell Science. 120 (2007) 3905–3910. https://doi.org/10.1242/jcs.015909.

[14] J.B. Pereira-Leal, M.C. Seabra, Evolution of the rab family of small GTP-binding proteins11Edited by J. Thornton, Journal of Molecular Biology. 313 (2001) 889–901. https://doi.org/10.1006/jmbi.2001.5072.

[15] M. Zerial, H. McBride, Rab proteins as membrane organizers, Nat Rev Mol Cell Biol. 2 (2001) 107–117. https://doi.org/10.1038/35052055.

[16] L. Langemeyer, R. Nunes Bastos, Y. Cai, A. Itzen, K.M. Reinisch, F.A. Barr, Diversity and plasticity in Rab GTPase nucleotide release mechanism has

consequences for Rab activation and inactivation, ELife. 3 (2014) e01623. https://doi.org/10.7554/eLife.01623.

[17] S. Toma-Fukai, T. Shimizu, Structural Insights into the Regulation Mechanism of Small GTPases by GEFs, Molecules. 24 (2019) 3308. https://doi.org/10.3390/molecules24183308.

[18] J.L. Bos, H. Rehmann, A. Wittinghofer, GEFs and GAPs: Critical Elements in the Control of Small G Proteins, Cell. 129 (2007) 865–877. https://doi.org/10.1016/j.cell.2007.05.018.

[19] L. Renault, B. Guibert, J. Cherfils, Structural snapshots of the mechanism and inhibition of a guanine nucleotide exchange factor, Nature. 426 (2003) 525–530. https://doi.org/10.1038/nature02197.

[20] F. Barr, D.G. Lambright, Rab GEFs and GAPs, Current Opinion in Cell Biology. 22 (2010) 461–470. https://doi.org/10.1016/j.ceb.2010.04.007.

[21] J.J. Dumas, Z. Zhu, J.L. Connolly, D.G. Lambright, Structural basis of activation and GTP hydrolysis in Rab proteins, Structure. 7 (1999) 413-s2. https://doi.org/10.1016/S0969-2126(99)80054-9.

[22] A.K. Gillingham, R. Sinka, I.L. Torres, K.S. Lilley, S. Munro, Toward a Comprehensive Map of the Effectors of Rab GTPases, Developmental Cell. 31 (2014) 358–373. https://doi.org/10.1016/j.devcel.2014.10.007.

[23] B.L. Grosshans, D. Ortiz, P. Novick, Rabs and their effectors: Achieving specificity in membrane traffic, PNAS. 103 (2006) 11821–11827. https://doi.org/10.1073/pnas.0601617103.

[24] Y. Zhen, H. Stenmark, Cellular functions of Rab GTPases at a glance, Journal of Cell Science. 128 (2015) 3171–3176. https://doi.org/10.1242/jcs.166074.

[25] M. Fukuda, TBC proteins: GAPs for mammalian small GTPase Rab?, Bioscience Reports. 31 (2011) 159–168. https://doi.org/10.1042/BSR20100112.

[26] X. Pan, S. Eathiraj, M. Munson, D.G. Lambright, TBC-domain GAPs for Rab GTPases accelerate GTP hydrolysis by a dual-finger mechanism, Nature. 442 (2006) 303–306. https://doi.org/10.1038/nature04847.

[27] K. Gavriljuk, E.-M. Gazdag, A. Itzen, C. Kötting, R.S. Goody, K. Gerwert, Catalytic mechanism of a mammalian Rab·RabGAP complex in atomic detail, PNAS. 109 (2012) 21348–21353. https://doi.org/10.1073/pnas.1214431110.

[28] M.A.M. Frasa, K.T. Koessmeier, M.R. Ahmadian, V.M.M. Braga, Illuminating the functional and structural repertoire of human TBC/RABGAPs, Nat Rev Mol Cell Biol. 13 (2012) 67–73. https://doi.org/10.1038/nrm3267.

[29] H. Stenmark, V.M. Olkkonen, The Rab GTPase family, Genome Biology. 2 (2001) reviews3007.1. https://doi.org/10.1186/gb-2001-2-5-reviews3007.

[30] S.R. Pfeffer, Structural Clues to Rab GTPase Functional Diversity*, Journal of Biological Chemistry. 280 (2005) 15485–15488. https://doi.org/10.1074/jbc.R500003200.

[31] P. Chavrier, J.-P. Gorvel, E. Stelzer, K. Simons, J. Gruenberg, M. Zerial, Hypervariable C-termmal domain of rab proteins acts as a targeting signal, Nature. 353 (1991) 769–772. https://doi.org/10.1038/353769a0.

[32] O. Steele-Mortimer, M.J. Clague, L.A. Huber, P. Chavrier, J. Gruenberg, J.P. Gorvel, The N-terminal domain of a rab protein is involved in membrane-membrane recognition and/or fusion., The EMBO Journal. 13 (1994) 34–41. https://doi.org/10.1002/j.1460-2075.1994.tb06232.x.

[33] R.S. Goody, A. Rak, K. Alexandrov, The structural and mechanistic basis for recycling of Rab proteins between membrane compartments, CMLS, Cell. Mol. Life Sci. 62 (2005) 1657–1670. https://doi.org/10.1007/s00018-005-4486-8.

[34] N.H. Thomä, A. Iakovenko, A. Kalinin, H. Waldmann, R.S. Goody, K. Alexandrov, Allosteric Regulation of Substrate Binding and Product Release in Geranylgeranyltransferase Type II, Biochemistry. 40 (2001) 268–274. https://doi.org/10.1021/bi002034p.

[35] A.B. Dirac-Svejstrup, T. Sumizawa, S.R. Pfeffer, Identification of a GDI displacement factor that releases endosomal Rab GTPases from Rab–GDI, The EMBO Journal. 16 (1997) 465–472. https://doi.org/10.1093/emboj/16.3.465.

[36] J. Blümer, J. Rey, L. Dehmelt, T. Mazel, Y.-W. Wu, P. Bastiaens, R.S. Goody, A. Itzen, RabGEFs are a major determinant for specific Rab membrane targeting, Journal of Cell Biology. 200 (2013) 287–300. https://doi.org/10.1083/jcb.201209113.

[37] B.B. Allan, B.D. Moyer, W.E. Balch, Rab1 Recruitment of p115 into a cis-SNARE Complex: Programming Budding COPII Vesicles for Fusion, Science. 289 (2000) 444–448. https://doi.org/10.1126/science.289.5478.444.

[38] M.A. Lynch-Day, D. Bhandari, S. Menon, J. Huang, H. Cai, C.R. Bartholomew, J.H. Brumell, S. Ferro-Novick, D.J. Klionsky, Trs85 directs a Ypt1 GEF, TRAPPIII, to the phagophore to promote autophagy, PNAS. 107 (2010) 7811–7816. https://doi.org/10.1073/pnas.1000063107.

[39] X. Ao, L. Zou, Y. Wu, Regulation of autophagy by the Rab GTPase network, Cell Death Differ. 21 (2014) 348–358. https://doi.org/10.1038/cdd.2013.187.

[40] C.A. Lamb, S. Nühlen, D. Judith, D. Frith, A.P. Snijders, C. Behrends, S.A. Tooze, TBC1D14 regulates autophagy via the TRAPP complex and ATG9 traffic, The EMBO Journal. 35 (2016) 281–301. https://doi.org/10.15252/embj.201592695.

[41] T.H. Klöpper, N. Kienle, D. Fasshauer, S. Munro, Untangling the evolution of Rab G proteins: implications of a comprehensive genomic analysis, BMC Biol. 10 (2012) 71. https://doi.org/10.1186/1741-7007-10-71.

[42] L.L. Thomas, A.M.N. Joiner, J.C. Fromme, The TRAPPIII complex activates the GTPase Ypt1 (Rab1) in the secretory pathway, Journal of Cell Biology. 217 (2017) 283–298. https://doi.org/10.1083/jcb.201705214.

[43] F. Riedel, A. Galindo, N. Muschalik, S. Munro, The two TRAPP complexes of metazoans have distinct roles and act on different Rab GTPases, Journal of Cell Biology. 217 (2017) 601–617. https://doi.org/10.1083/jcb.201705068.

[44] A.K. Haas, S. Yoshimura, D.J. Stephens, C. Preisinger, E. Fuchs, F.A. Barr, Analysis of GTPase-activating proteins: Rab1 and Rab43 are key Rabs required to maintain a functional Golgi complex in human cells, Journal of Cell Science. 120 (2007) 2997–3010. https://doi.org/10.1242/jcs.014225.

[45] J. Wang, S. Menon, A. Yamasaki, H.-T. Chou, T. Walz, Y. Jiang, S. Ferro-Novick, Ypt1 recruits the Atg1 kinase to the preautophagosomal structure, PNAS. 110 (2013) 9800–9805. https://doi.org/10.1073/pnas.1302337110.

[46] S. Tremel, Y. Ohashi, D.R. Morado, J. Bertram, O. Perisic, L.T.L. Brandt, M.-K. von Wrisberg, Z.A. Chen, S.L. Maslen, O. Kovtun, M. Skehel, J. Rappsilber, K. Lang, S. Munro, J.A.G. Briggs, R.L. Williams, Structural basis for VPS34 kinase activation by Rab1 and Rab5 on membranes, Nat Commun. 12 (2021) 1564. https://doi.org/10.1038/s41467-021-21695-2.

[47] C.J. Westlake, L.M. Baye, M.V. Nachury, K.J. Wright, K.E. Ervin, L. Phu, C. Chalouni, J.S. Beck, D.S. Kirkpatrick, D.C. Slusarski, V.C. Sheffield, R.H. Scheller, P.K. Jackson, Primary cilia membrane assembly is initiated by Rab11 and transport protein particle II (TRAPPII) complex-dependent trafficking of Rabin8 to the centrosome, PNAS. 108 (2011) 2759–2764. https://doi.org/10.1073/pnas.1018823108.

[48] V. Walia, A. Cuenca, M. Vetter, C. Insinna, S. Perera, Q. Lu, D.A. Ritt, E. Semler, S. Specht, J. Stauffer, D.K. Morrison, E. Lorentzen, C.J. Westlake, Akt Regulates a Rab11-Effector Switch Required for Ciliogenesis, Developmental Cell. 50 (2019) 229-246.e7. https://doi.org/10.1016/j.devcel.2019.05.022.

[49] M. Vetter, R. Stehle, C. Basquin, E. Lorentzen, Structure of Rab11–FIP3–Rabin8 reveals simultaneous binding of FIP3 and Rabin8 effectors to Rab11, Nat Struct Mol Biol. 22 (2015) 695–702. https://doi.org/10.1038/nsmb.3065.

[50] A. Knödler, S. Feng, J. Zhang, X. Zhang, A. Das, J. Peränen, W. Guo, Coordination of Rab8 and Rab11 in primary ciliogenesis, PNAS. 107 (2010) 6346–6351. https://doi.org/10.1073/pnas.1002401107.

[51] L.L. Thomas, J.C. Fromme, GTPase cross talk regulates TRAPPII activation of Rab11 homologues during vesicle biogenesis, Journal of Cell Biology. 215 (2016) 499–513. https://doi.org/10.1083/jcb.201608123.

[52] M.L. Jenkins, N.J. Harris, U. Dalwadi, K.D. Fleming, D.S. Ziemianowicz, A. Rafiei, E.M. Martin, D.C. Schriemer, C.K. Yip, J.E. Burke, The substrate specificity of the human TRAPPII complex's Rab-guanine nucleotide exchange factor activity, Communications Biology. 3 (2020) 1–12. https://doi.org/10.1038/s42003-020-01459-2.

[53] M.L. Jenkins, J.P. Margaria, J.T.B. Stariha, R.M. Hoffmann, J.A. McPhail, D.J. Hamelin, M.J. Boulanger, E. Hirsch, J.E. Burke, Structural determinants of Rab11 activation by the guanine nucleotide exchange factor SH3BP5, Nat Commun. 9 (2018) 3772. https://doi.org/10.1038/s41467-018-06196-z.

[54] T. Welz, J. Wellbourne-Wood, E. Kerkhoff, Orchestration of cell surface proteins by Rab11, Trends in Cell Biology. 24 (2014) 407–415. https://doi.org/10.1016/j.tcb.2014.02.004.

[55] L.A. Lapierre, R. Kumar, C.M. Hales, J. Navarre, S.G. Bhartur, J.O. Burnette, D.W. Provance, J.A. Mercer, M. Bähler, J.R. Goldenring, Myosin Vb Is Associated with Plasma Membrane Recycling Systems, MBoC. 12 (2001) 1843–1857. https://doi.org/10.1091/mbc.12.6.1843.

[56] C.P. Horgan, M.W. McCaffrey, The dynamic Rab11-FIPs, Biochemical Society Transactions. 37 (2009) 1032–1036. https://doi.org/10.1042/BST0371032.

[57] J.E. Burke, A.J. Inglis, O. Perisic, G.R. Masson, S.H. McLaughlin, F. Rutaganira, K.M. Shokat, R.L. Williams, Structures of PI4KIIIβ complexes show simultaneous recruitment of Rab11 and its effectors, Science. 344 (2014) 1035–1038. https://doi.org/10.1126/science.1253397.

[58] C.P. Horgan, M. Walsh, T.H. Zurawski, M.W. McCaffrey, Rab11-FIP3 localises to a Rab11-positive pericentrosomal compartment during interphase and to the cleavage furrow during cytokinesis, Biochemical and Biophysical Research Communications. 319 (2004) 83–94. https://doi.org/10.1016/j.bbrc.2004.04.157.

[59] C.E. Jewett, A.W.J. Soh, C.H. Lin, Q. Lu, E. Lencer, C.J. Westlake, C.G. Pearson, R. Prekeris, RAB19 Directs Cortical Remodeling and Membrane Growth for Primary Ciliogenesis, Developmental Cell. 56 (2021) 325-340.e8. https://doi.org/10.1016/j.devcel.2020.12.003.

[60] C. Li, Z. Wei, Y. Fan, W. Huang, Y. Su, H. Li, Z. Dong, M. Fukuda, M. Khater, G. Wu, The GTPase Rab43 Controls the Anterograde ER-Golgi Trafficking and Sorting of GPCRs, Cell Rep. 21 (2017) 1089–1101. https://doi.org/10.1016/j.celrep.2017.10.011.

[61] S.Y. Dejgaard, A. Murshid, A. Erman, Ö. Kızılay, D. Verbich, R. Lodge, K. Dejgaard, T.B.N. Ly-Hartig, R. Pepperkok, J.C. Simpson, J.F. Presley, Rab18 and Rab43 have key roles in ER-Golgi trafficking, Journal of Cell Science. 121 (2008) 2768–2781. https://doi.org/10.1242/jcs.021808.

[62] M. Sacher, Y. Jiang, J. Barrowman, A. Scarpa, J. Burston, L. Zhang, D. Schieltz, J.R. Yates III, H. Abeliovich, S. Ferro-Novick, TRAPP, a highly conserved novel complex on the cis-Golgi that mediates vesicle docking and fusion, The EMBO Journal. 17 (1998) 2494–2503. https://doi.org/10.1093/emboj/17.9.2494.

[63] M. Sacher, J. Barrowman, D. Schieltz, J.R. Yates, S. Ferro-Novick, Identification and characterization of five new subunits of TRAPP, European Journal of Cell Biology. 79 (2000) 71–80. https://doi.org/10.1078/S0171-9335(04)70009-6.

[64] M. Sacher, J. Barrowman, W. Wang, J. Horecka, Y. Zhang, M. Pypaert, S. Ferro-Novick, TRAPP I Implicated in the Specificity of Tethering in ER-to-Golgi Transport, Molecular Cell. 7 (2001) 433–442. https://doi.org/10.1016/S1097-2765(01)00190-3.

[65] H. Cai, S. Yu, S. Menon, Y. Cai, D. Lazarova, C. Fu, K. Reinisch, J.C. Hay, S. Ferro-Novick, TRAPPI tethers COPII vesicles by binding the coat subunit Sec23, Nature. 445 (2007) 941–944. https://doi.org/10.1038/nature05527.

[66] H. Cai, Y. Zhang, M. Pypaert, L. Walker, S. Ferro-Novick, Mutants in trs120 disrupt traffic from the early endosome to the late Golgi, Journal of Cell Biology. 171 (2005) 823–833. https://doi.org/10.1083/jcb.200505145.

[67] S. Jones, C. Newman, F. Liu, N. Segev, The TRAPP Complex Is a Nucleotide Exchanger for Ypt1 and Ypt31/32, MBoC. 11 (2000) 4403–4411. https://doi.org/10.1091/mbc.11.12.4403.

[68] W. Wang, M. Sacher, S. Ferro-Novick, Trapp Stimulates Guanine Nucleotide Exchange on Ypt1p, Journal of Cell Biology. 151 (2000) 289–296. https://doi.org/10.1083/jcb.151.2.289.

[69] Y. Cai, H.F. Chin, D. Lazarova, S. Menon, C. Fu, H. Cai, A. Sclafani, D.W. Rodgers, E.M. De La Cruz, S. Ferro-Novick, K.M. Reinisch, The Structural Basis for Activation of the Rab Ypt1p by the TRAPP Membrane-Tethering Complexes, Cell. 133 (2008) 1202–1213. https://doi.org/10.1016/j.cell.2008.04.049.

[70] C. Zhang, J.B. Bowzard, M. Greene, A. Anido, K. Stearns, R.A. Kahn, Genetic interactions link ARF1, YPT31/32 and TRS130, Yeast. 19 (2002) 1075–1086. https://doi.org/10.1002/yea.903.

[71] K. Yamamoto, Y. Jigami, Mutation of TRS130, which encodes a component of the TRAPP II complex, activates transcription of OCH1 in Saccharomyces cerevisiae, Current Genetics. 42 (2002) 85–93. https://doi.org/10.1007/s00294-002-0336-5.

[72] N. Morozova, Y. Liang, A.A. Tokarev, S.H. Chen, R. Cox, J. Andrejic, Z. Lipatova, V.A. Sciorra, S.D. Emr, N. Segev, TRAPPII subunits are required for the specificity switch of a Ypt–Rab GEF, Nature Cell Biology. 8 (2006) 1263–1269. https://doi.org/10.1038/ncb1489.

[73] C.K. Yip, J. Berscheminski, T. Walz, Molecular architecture of the TRAPPII complex and implications for vesicle tethering, Nature Structural & Molecular Biology. 17 (2010) 1298–1304. https://doi.org/10.1038/nsmb.1914.

[74] J.J. Kim, Z. Lipatova, U. Majumdar, N. Segev, Regulation of Golgi Cisternal Progression by Ypt/Rab GTPases, Developmental Cell. 36 (2016) 440–452. https://doi.org/10.1016/j.devcel.2016.01.016.

[75] M. Pinar, H.N. Arst, A. Pantazopoulou, V.G. Tagua, V. de los Ríos, J. Rodríguez-Salarichs, J.F. Díaz, M.A. Peñalva, TRAPPII regulates exocytic Golgi exit by

mediating nucleotide exchange on the Ypt31 ortholog RabERAB11, PNAS. 112 (2015) 4346–4351. https://doi.org/10.1073/pnas.1419168112.

[76] K. Meiling-Wesse, U.D. Epple, R. Krick, H. Barth, A. Appelles, C. Voss, E.-L. Eskelinen, M. Thumm, Trs85 (Gsg1), a Component of the TRAPP Complexes, Is Required for the Organization of the Preautophagosomal Structure during Selective Autophagy via the Cvt Pathway*, Journal of Biological Chemistry. 280 (2005) 33669–33678. https://doi.org/10.1074/jbc.M501701200.

[77] D. Tan, Y. Cai, J. Wang, J. Zhang, S. Menon, H.-T. Chou, S. Ferro-Novick, K.M. Reinisch, T. Walz, The EM structure of the TRAPPIII complex leads to the identification of a requirement for COPII vesicles on the macroautophagy pathway, PNAS. 110 (2013) 19432–19437. https://doi.org/10.1073/pnas.1316356110.

[78] A.M. Joiner, B.P. Phillips, K. Yugandhar, E.J. Sanford, M.B. Smolka, H. Yu, E.A. Miller, J.C. Fromme, Structural basis of TRAPPIII-mediated Rab1 activation, The EMBO Journal. 40 (2021) e107607. https://doi.org/10.15252/embj.2020107607.

[79] C. Choi, M. Davey, C. Schluter, P. Pandher, Y. Fang, L.J. Foster, E. Conibear, Organization and Assembly of the TRAPPII Complex, Traffic. 12 (2011) 715–725. https://doi.org/10.1111/j.1600-0854.2011.01181.x.

[80] L.L. Thomas, S.A. van der Vegt, J.C. Fromme, A Steric Gating Mechanism Dictates the Substrate Specificity of a Rab-GEF, Developmental Cell. 48 (2019) 100-114.e9. https://doi.org/10.1016/j.devcel.2018.11.013.

[81] M.C. Bassik, M. Kampmann, R.J. Lebbink, S. Wang, M.Y. Hein, I. Poser, J. Weibezahn, M.A. Horlbeck, S. Chen, M. Mann, A.A. Hyman, E.M. LeProust, M.T.

McManus, J.S. Weissman, A Systematic Mammalian Genetic Interaction Map Reveals Pathways Underlying Ricin Susceptibility, Cell. 152 (2013) 909–922. https://doi.org/10.1016/j.cell.2013.01.030.

[82] Y.-G. Kim, S. Raunser, C. Munger, J. Wagner, Y.-L. Song, M. Cygler, T. Walz, B.-H. Oh, M. Sacher, The Architecture of the Multisubunit TRAPP I Complex Suggests a Model for Vesicle Tethering, Cell. 127 (2006) 817–830. https://doi.org/10.1016/j.cell.2006.09.029.

[83] A. Galindo, V.J. Planelles-Herrero, G. Degliesposti, S. Munro, Cryo-EM structure of metazoan TRAPPIII, the multi-subunit complex that activates the GTPase Rab1, The EMBO Journal. 40 (2021) e107608. https://doi.org/10.15252/embj.2020107608.

[84] M. Pinar, E. Arias-Palomo, V. de los Ríos, H.N.A. Jr, M.A. Peñalva, Characterization of Aspergillus nidulans TRAPPs uncovers unprecedented similarities between fungi and metazoans and reveals the modular assembly of TRAPPII, PLOS Genetics. 15 (2019) e1008557. https://doi.org/10.1371/journal.pgen.1008557.

[85] S. Brunet, N. Shahrzad, D. Saint-Dic, H. Dutczak, M. Sacher, A trs20 Mutation That Mimics an SEDT-Causing Mutation Blocks Selective and Non-Selective Autophagy: A Model for TRAPP III Organization, Traffic. 14 (2013) 1091–1104. https://doi.org/10.1111/tra.12095.

[86] M. Zong, X. Wu, C.W.L. Chan, M.Y. Choi, H.C. Chan, J.A. Tanner, S. Yu, The Adaptor Function of TRAPPC2 in Mammalian TRAPPs Explains TRAPPC2-

Associated SEDT and TRAPPC9-Associated Congenital Intellectual Disability, PLOS ONE. 6 (2011) e23350. https://doi.org/10.1371/journal.pone.0023350.

[87] M.P. Milev, C. Graziano, D. Karall, W.F.E. Kuper, N. Al-Deri, D.M. Cordelli, T.B. Haack, K. Danhauser, A. Iuso, F. Palombo, T. Pippucci, H. Prokisch, D. Saint-Dic, M. Seri, D. Stanga, G. Cenacchi, K.L.I. van Gassen, J. Zschocke, C. Fauth, J.A. Mayr, M. Sacher, P.M. van Hasselt, Bi-allelic mutations in TRAPPC2L result in a neurodevelopmental disorder and have an impact on RAB11 in fibroblasts, Journal of Medical Genetics. 55 (2018) 753–764. https://doi.org/10.1136/jmedgenet-2018-105441.

[88] S. Duerinckx, M. Meuwissen, C. Perazzolo, L. Desmyter, I. Pirson, M. Abramowicz, Phenotypes in siblings with homozygous mutations of TRAPPC9 and/or MCPH1 support a bifunctional model of MCPH1, Molecular Genetics & Genomic Medicine. 6 (2018) 660–665. https://doi.org/10.1002/mgg3.400.

[89] D.B. Fee, M. Harmelink, P. Monrad, E. Pyzik, Siblings With Mutations in TRAPPC11 Presenting With Limb-Girdle Muscular Dystrophy 2S, Journal of Clinical Neuromuscular Disease. 19 (2017) 27–30. https://doi.org/10.1097/CND.0000000000000173.

[90] A.K. Gedeon, G.E. Tiller, M. Le Merrer, S. Heuertz, L. Tranebjaerg, D. Chitayat, S. Robertson, I.A. Glass, R. Savarirayan, W.G. Cole, D.L. Rimoin, B.G. Kousseff, H. Ohashi, B. Zabel, A. Munnich, J. Gecz, J.C. Mulley, The Molecular Basis of X-Linked Spondyloepiphyseal Dysplasia Tarda, The American Journal of Human Genetics. 68 (2001) 1386–1397. https://doi.org/10.1086/320592.

[91] Y. Lin, S. Rao, Y. Yang, [A novel mutation in the SEDL gene leading to X-linked spondyloepiphyseal dysplasia tarda in a large Chinese pedigree], Zhonghua Yi Xue Yi Chuan Xue Za Zhi. 25 (2008) 150–153.

[92] E. Grunebaum, E. Arpaia, J.J. MacKenzie, J. Fitzpatrick, P.N. Ray, C.M. Roifman, A missense mutation in the SEDL gene results in delayed onset of X linked spondyloepiphyseal dysplasia in a large pedigree, Journal of Medical Genetics. 38 (2001) 409–411. https://doi.org/10.1136/jmg.38.6.409.

[93] H.S. Mohamoud, S. Ahmed, M. Jelani, N. Alrayes, K. Childs, N. Vadgama, M.M. Almramhi, J.Y. Al-Aama, S. Goodbourn, J. Nasir, A missense mutation in TRAPPC6A leads to build-up of the protein, in patients with a neurodevelopmental syndrome and dysmorphic features, Sci Rep. 8 (2018) 2053. https://doi.org/10.1038/s41598-018-20658-w.

[94] A.A. Larson, P.R. Baker, M.P. Milev, C.A. Press, R.J. Sokol, M.O. Cox, J.K. Lekostaj, A.A. Stence, A.D. Bossler, J.M. Mueller, K. Prematilake, T.F. Tadjo, C.A. Williams, M. Sacher, S.A. Moore, TRAPPC11 and GOSR2 mutations associate with hypoglycosylation of α-dystroglycan and muscular dystrophy, Skeletal Muscle. 8 (2018) 17. https://doi.org/10.1186/s13395-018-0163-0.

[95] P.J. Scrivens, B. Noueihed, N. Shahrzad, S. Hul, S. Brunet, M. Sacher, C4orf41 and TTC-15 are mammalian TRAPP components with a role at an early stage in ER-to-Golgi trafficking, MBoC. 22 (2011) 2083–2093. https://doi.org/10.1091/mbc.e10-11-0873.

[96] F. Weissmann, G. Petzold, R. VanderLinden, P.J.H. in ’t Veld, N.G. Brown, F. Lampert, S. Westermann, H. Stark, B.A. Schulman, J.-M. Peters, biGBac enables rapid gene assembly for the expression of large multisubunit protein complexes, PNAS. 113 (2016) E2564–E2569. https://doi.org/10.1073/pnas.1604935113.

[97] M.L. Jenkins, Structural and biochemical investigation of the regulation of Rab11a by the guanine nucleotide exchange factors SH3BP5 and TRAPPII, Thesis, 2019. https://dspace.library.uvic.ca/handle/1828/11343 (accessed July 29, 2021).

[98] G.R. Masson, J.E. Burke, N.G. Ahn, G.S. Anand, C. Borchers, S. Brier, G.M. Bou-Assaf, J.R. Engen, S.W. Englander, J. Faber, R. Garlish, P.R. Griffin, M.L. Gross, M. Guttman, Y. Hamuro, A.J.R. Heck, D. Houde, R.E. Iacob, T.J.D. Jørgensen, I.A. Kaltashov, J.P. Klinman, L. Konermann, P. Man, L. Mayne, B.D. Pascal, D. Reichmann, M. Skehel, J. Snijder, T.S. Strutzenberg, E.S. Underbakke, C. Wagner, T.E. Wales, B.T. Walters, D.D. Weis, D.J. Wilson, P.L. Wintrode, Z. Zhang, J. Zheng, D.C. Schriemer, K.D. Rand, Recommendations for performing, interpreting and reporting hydrogen deuterium exchange mass spectrometry (HDX-MS) experiments, Nature Methods. 16 (2019) 595–602. https://doi.org/10.1038/s41592-019-0459-y.

[99] Y. Perez-Riverol, A. Csordas, J. Bai, M. Bernal-Llinares, S. Hewapathirana, D.J. Kundu, A. Inuganti, J. Griss, G. Mayer, M. Eisenacher, E. Pérez, J. Uszkoreit, J. Pfeuffer, T. Sachsenberg, Ş. Yılmaz, S. Tiwary, J. Cox, E. Audain, M. Walzer, A.F. Jarnuczak, T. Ternent, A. Brazma, J.A. Vizcaíno, The PRIDE database and related

tools and resources in 2019: improving support for quantification data, Nucleic Acids Research. 47 (2019) D442–D450. https://doi.org/10.1093/nar/gky1106.

[100] A. Rohou, N. Grigorieff, CTFFIND4: Fast and accurate defocus estimation from electron micrographs, Journal of Structural Biology. 192 (2015) 216–221. https://doi.org/10.1016/j.jsb.2015.08.008.

[101] New tools for automated high-resolution cryo-EM structure determination in RELION-3 | eLife, (n.d.). https://elifesciences.org/articles/42166 (accessed May 14, 2021).

[102] A. Punjani, J.L. Rubinstein, D.J. Fleet, M.A. Brubaker, cryoSPARC: algorithms for rapid unsupervised cryo-EM structure determination, Nature Methods. 14 (2017) 290–296. https://doi.org/10.1038/nmeth.4169.

[103] L.A. Kelley, S. Mezulis, C.M. Yates, M.N. Wass, M.J.E. Sternberg, The Phyre2 web portal for protein modeling, prediction and analysis, Nature Protocols. 10 (2015) 845–858. https://doi.org/10.1038/nprot.2015.053.

[104] N.J. Harris, M.L. Jenkins, U. Dalwadi, K.D. Fleming, S.-E. Nam, M.A.H. Parson, C.K. Yip, J.E. Burke, Biochemical Insight into Novel Rab-GEF Activity of the Mammalian TRAPPIII Complex, Journal of Molecular Biology. 433 (2021) 167145. https://doi.org/10.1016/j.jmb.2021.167145.

[105] W. Cheng, K. Yin, D. Lu, B. Li, D. Zhu, Y. Chen, H. Zhang, S. Xu, J. Chai, L. Gu, Structural insights into a unique Legionella pneumophila effector LidA recognizing both GDP and GTP bound Rab1 in their active state, PLoS Pathog. 8 (2012) e1002528. https://doi.org/10.1371/journal.ppat.1002528.

[106] D. Taussig, Z. Lipatova, N. Segev, Trs20 is Required for TRAPP III Complex Assembly at the PAS and its Function in Autophagy, Traffic. 15 (2014) 327–337. https://doi.org/10.1111/tra.12145.

[107] A. Cuenca, C. Insinna, H. Zhao, P. John, M.A. Weiss, Q. Lu, V. Walia, S. Specht, S. Manivannan, J. Stauffer, A.A. Peden, C.J. Westlake, The C7orf43/TRAPPC14 component links the TRAPPII complex to Rabin8 for preciliary vesicle tethering at the mother centriole during ciliogenesis, Journal of Biological Chemistry. 294 (2019) 15418–15434. https://doi.org/10.1074/jbc.RA119.008615.

[108] X. Robert, P. Gouet, Deciphering key features in protein structures with the new ENDscript server, Nucleic Acids Res. 42 (2014) W320-324. https://doi.org/10.1093/nar/gku316.

Appendix

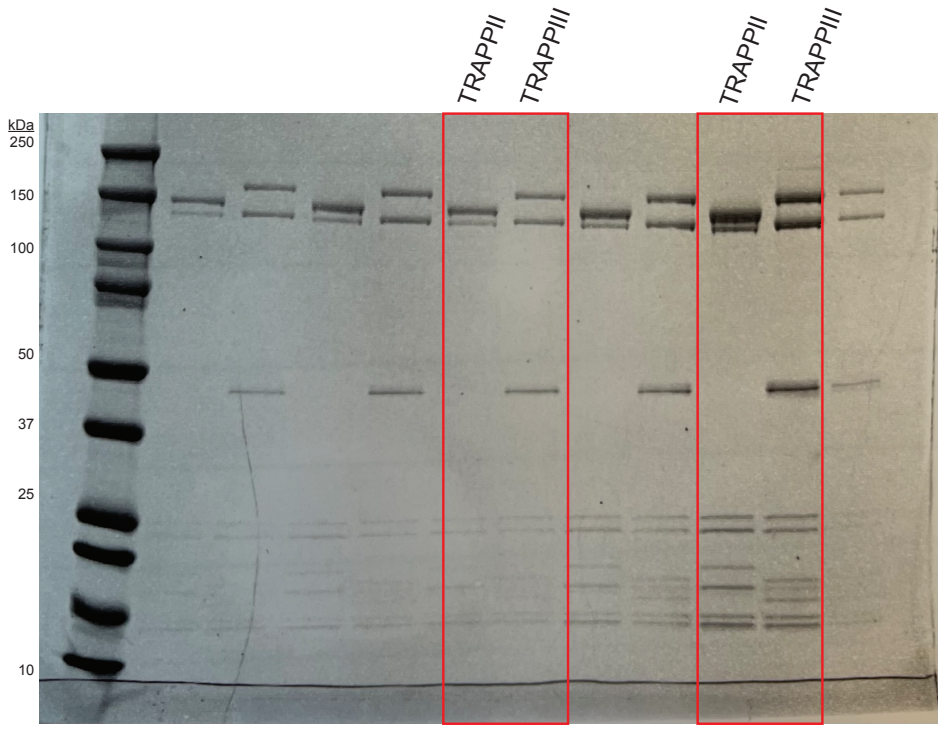

Appendix A. SDS-PAGE gel of purified TRAPP complexes.
Uncropped SDS-PAGE gel of TRAPPII and TRAPPIII used in figure 2-2. High and low refer to protein amount loaded (high=3.6ug and low= 1.4ug). 4-20% NuPAGE gradient gel run at 225V for 35 min and stained with Coomassie Brilliant Blue dye.

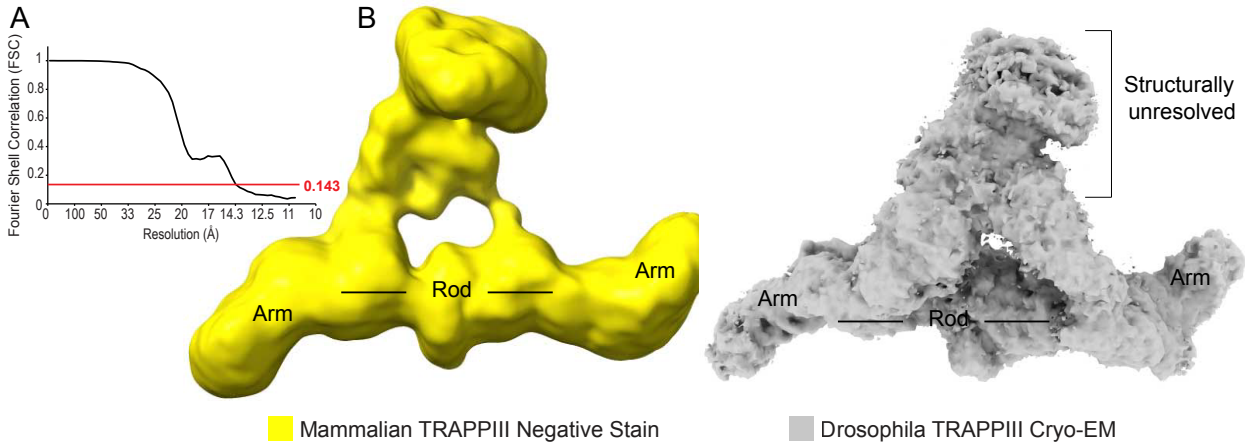

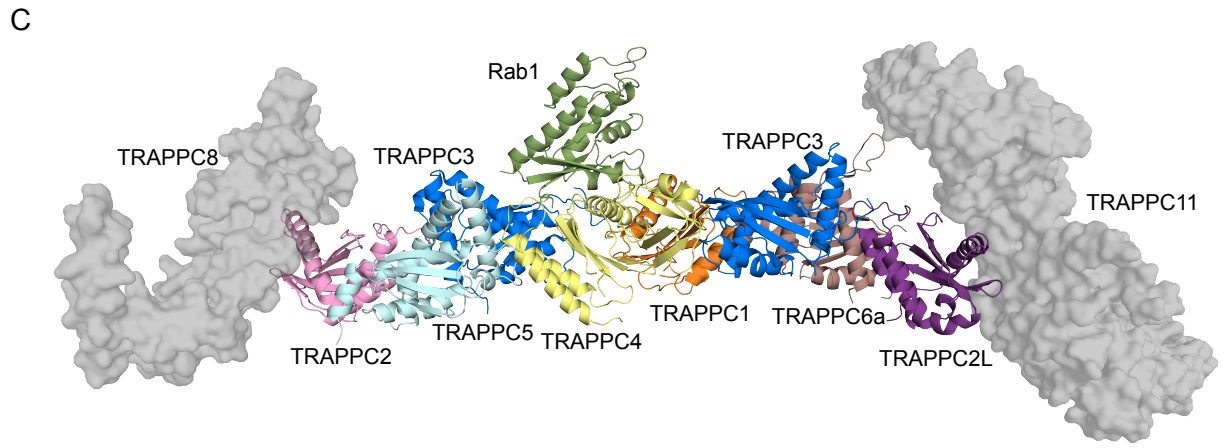

Appendix B. TRAPPIII Negative Stain EM and architecture comparison.

A. Gold-standard Fourier shell correlation curve showing the resolution of the TRAPPIII model in figure 2-2.

B. Architecture comparison between mammalian TRAPPIII negative stain (yellow, left) and Drosophila TRAPPIII cryo-EM (grey, right, PDB:7B6R) with their appropriate regions labelled according to the main text. Structurally unresolved refers to TRAPPC12/13 and the regions of TRAPPC8/C11 that were not mapped in panel C.

C. Mammalian TRAPPIII model with Rab generated using a combination of the core model in figure 2-2 and phyre models based on PDB:7B6R.

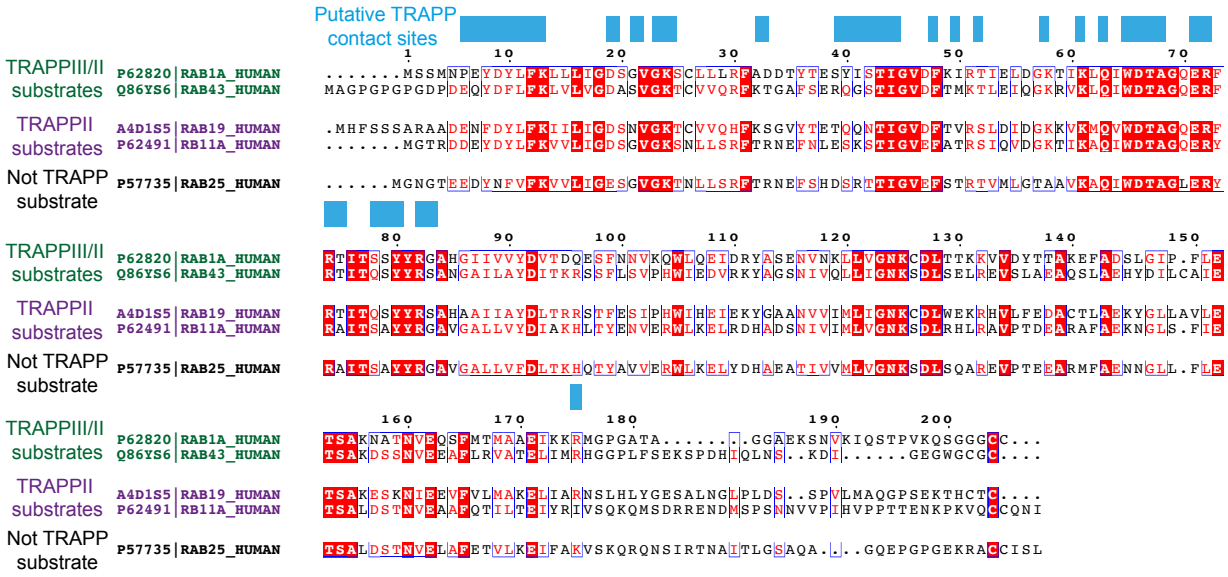

Appendix C. Alignment of substrate Rabs for mammalian TRAPP complexes. Alignment of Rab1, Rab43, Rab19, Rab11a, and Rab25. Putative contact sites with the TRAPP core are based on the pdb: 3CUE. Alignment was generated using Espript [108].

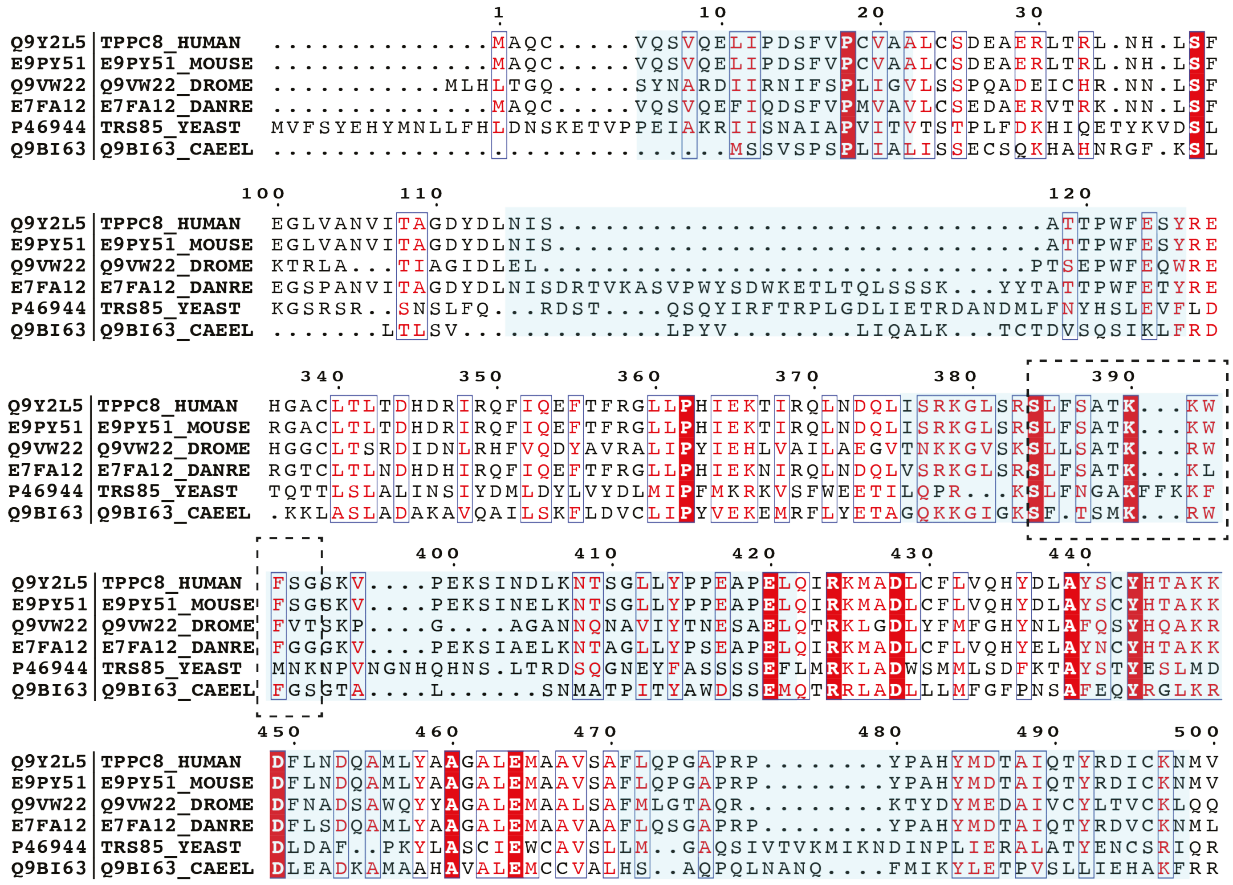

Appendix D. Alignment of TRAPPC8

Decreases in exchange upon membrane binding are highlighted in light blue. The putative amphipathic helix from Trs85 is indicated in the boxed dotted line. Alignment was generated using Espript [108].

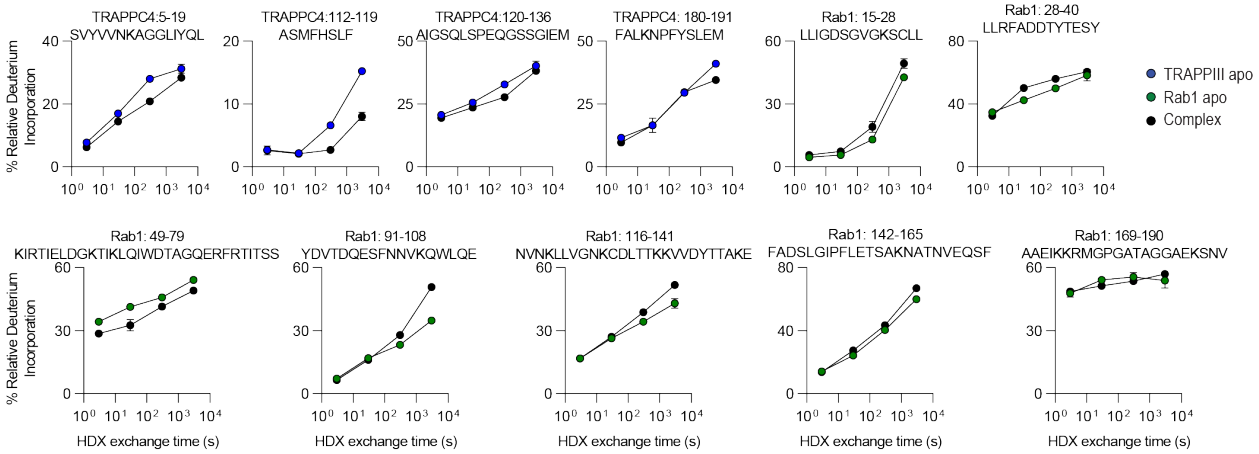

Appendix E. Time course of deuterium incorporation for a selection of peptides covering all regions that showed differences in HDX between TRAPPIII apo and TRAPPIII-Rab1 bound (Figure 2-4 HDX). Error is shown as standard deviation (n=3).

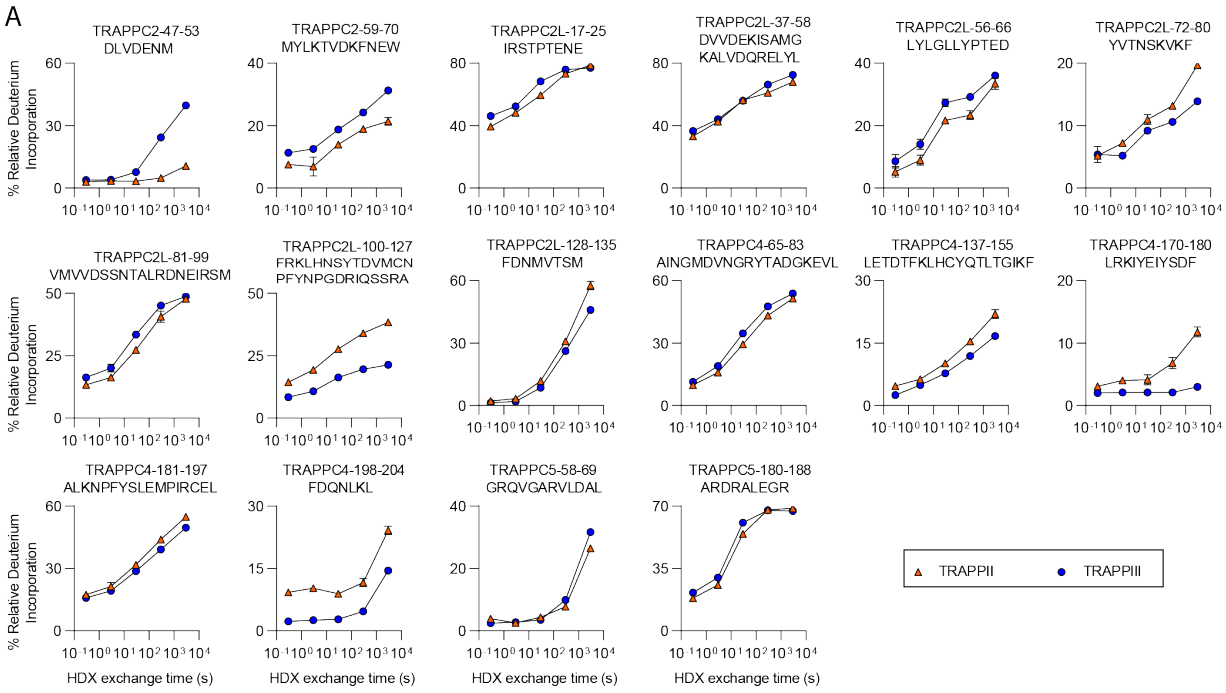

Appendix F. Time course of deuterium incorporation for a selection of peptides covering all regions that showed differences in HDX between TRAPPII and TRAPPIII (Figure 2-5 HDX). Error is shown as standard deviation (n=3).

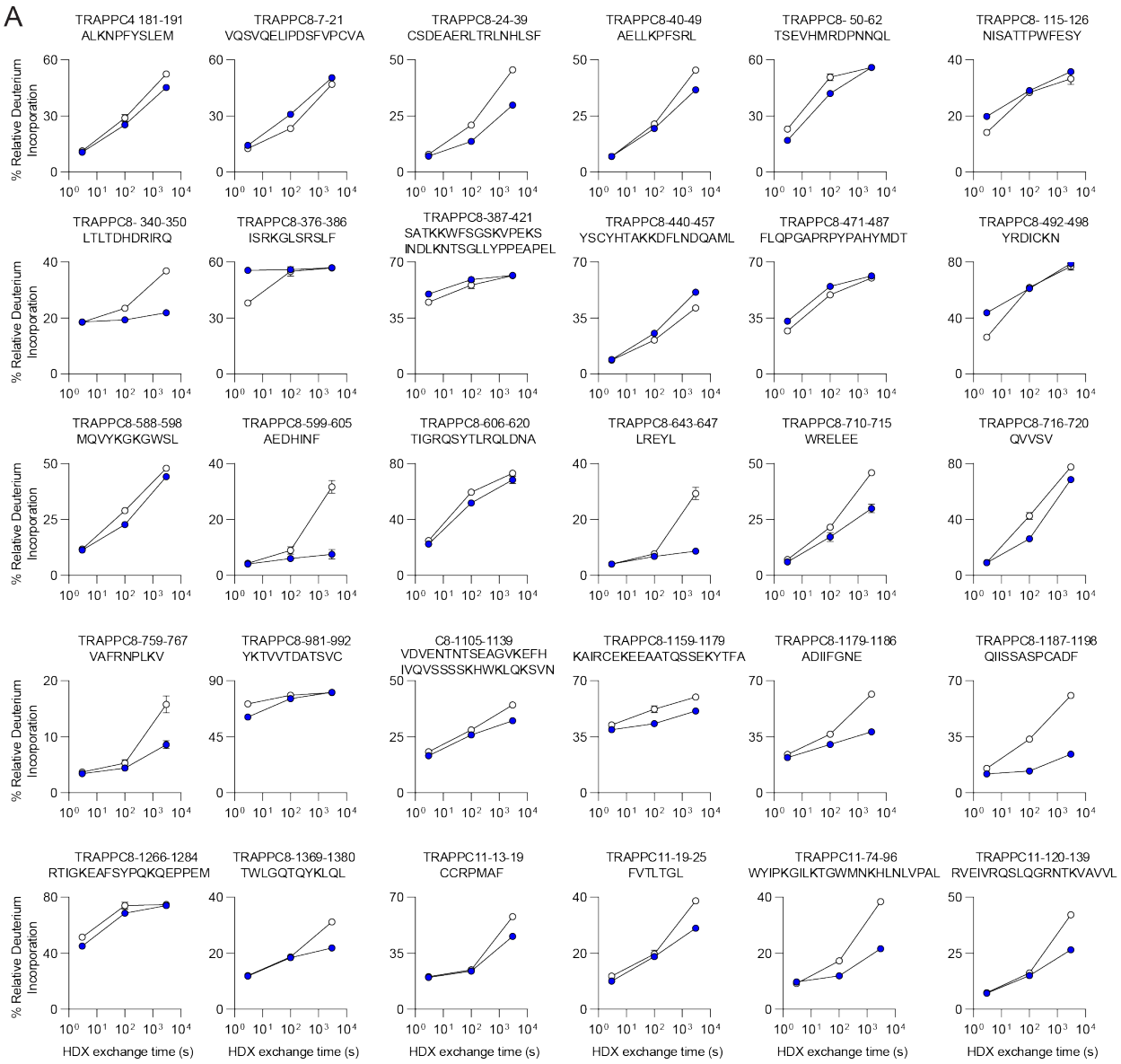

Appendix G. Time course of deuterium incorporation for a selection of peptides covering all regions that showed differences in HDX between TRAPPIII and TRAPPIII-membrane (1/2) (Figure 2-7). Error is shown as standard deviation (n=3).

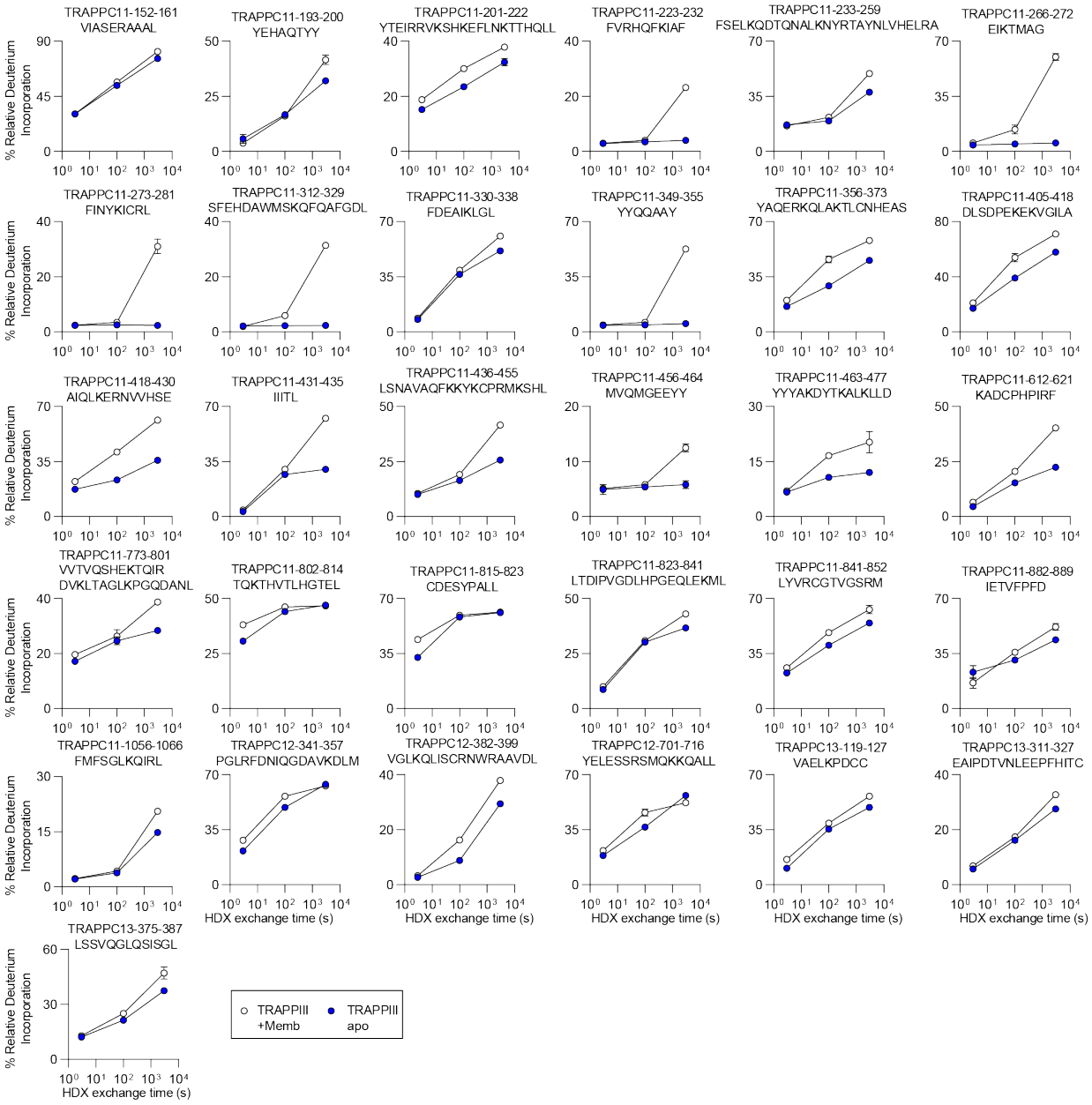

Appendix H. Time course of deuterium incorporation for a selection of peptides covering all regions that showed differences in HDX between TRAPPIII and TRAPPIII-membrane (2/2) (Figure 2-7). Error is shown as standard deviation (n=3).

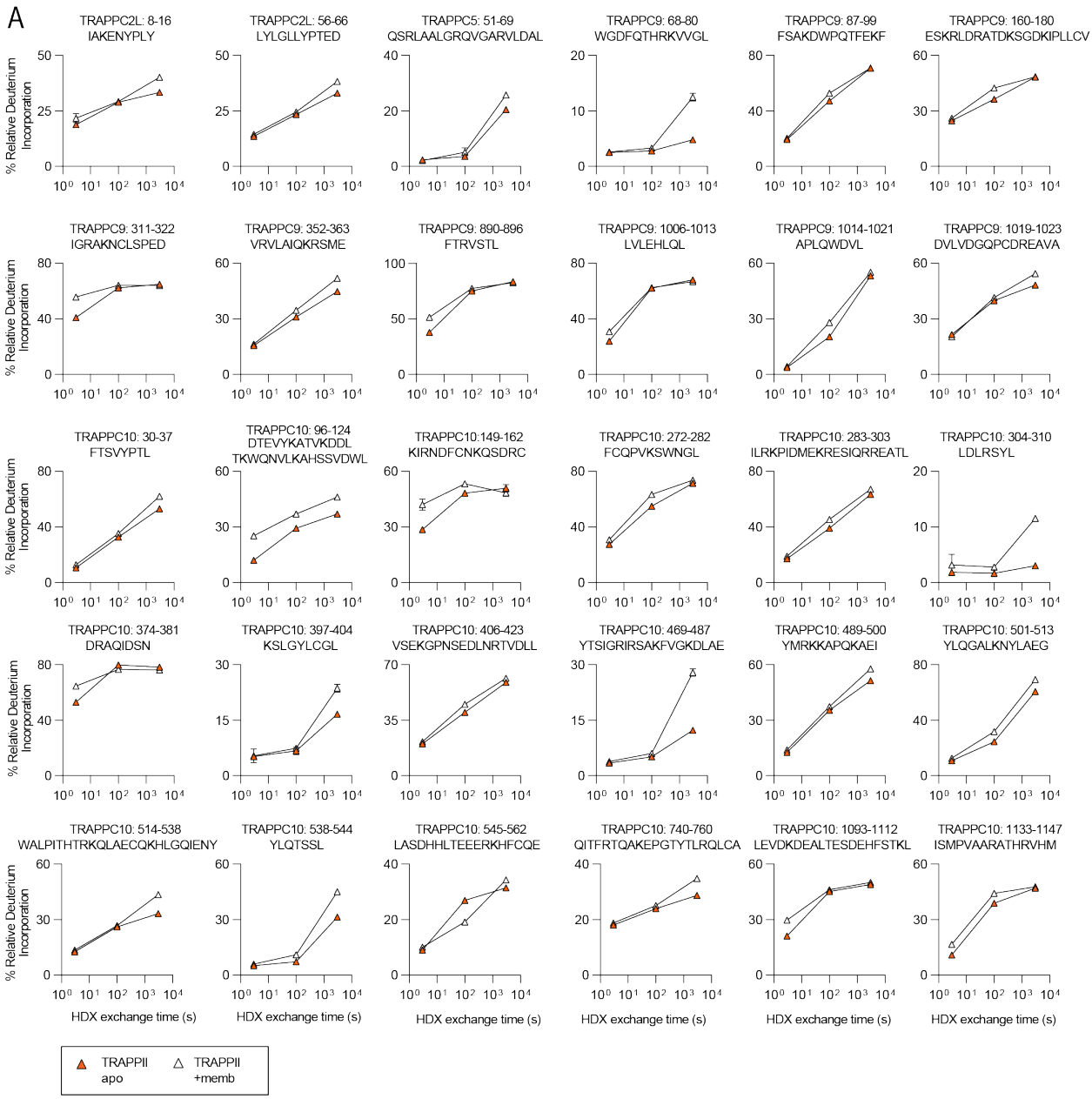

Appendix I. Time course of deuterium incorporation for a selection of peptides covering all regions that showed differences in HDX between TRAPPII and TRAPPII-membrane (Figure 2-8). Error is shown as standard deviation (n=3).

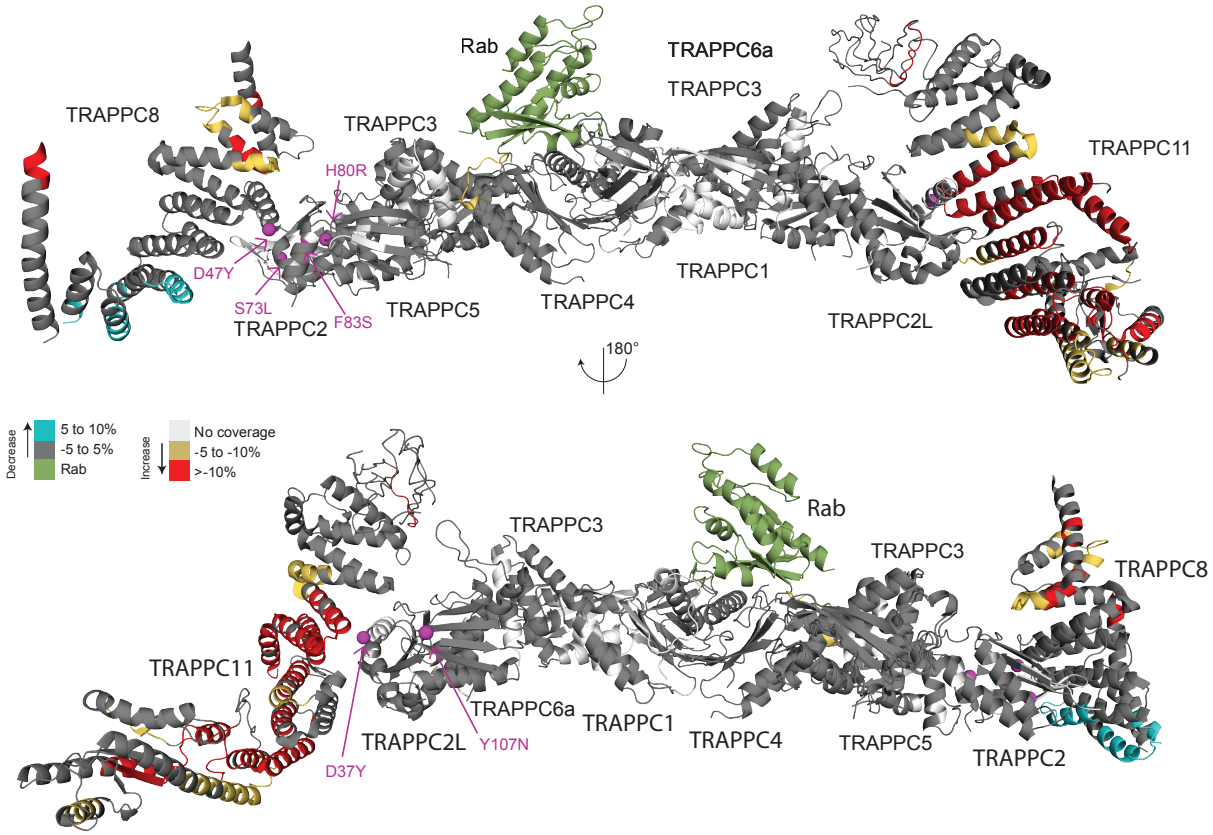

Appendix J. A selection of TRAPP mutations mapped on the structure of TRAPPIII.

Mapped mutations include the TRAPPC2 mutants (D47Y, S73L, H80R and F83S), TRAPPC6a mutant Y107N, and TRAPPC2L mutant D37Y. The HDX data is from the TRAPPIII apo vs Membrane experiment shown in Figure 2-7.

Appendix K. All plasmids used in Chapter 2.

Name	Plasmid	Protein(s)	Sequence(s)	Modifications/Tags	Source
MJ153 [TRAPPIIa]	pBIG1a	TRAPPC1; TRAPPC2L; TRAPPC5; TRAPPC6a; TRAPPC10;	1-145; 1-140; 1-188; 1-173; 1-1259	TRAPPC10 – C-term His Tag (TEV)	[52]
MJ85 [TRAPPIIb]	pBIG1a	TRAPPC3; TRAPPC2; TRAPPC4; TRAPPC9	1-180; 1-140; 1-235; 1-1148	TRAPPC3 – C-term Strep Tag (TEV)	[52]
NH40 [TRAPPIIIa]	pBIG1a	TRAPPC8; TRAPPC11; TRAPPC12; TRAPPC13	1-1435; 1-1147; 300-735; 1-417	TRAPPC12 - C-term Strep Tag (TEV); TRAPPC11 - C-term His Tag (TEV)	This thesis
NH42 [TRAPPIIIb]	pBIG2ab	TRAPPC1; TRAPPC2; TRAPPC2L; TRAPPC3; TRAPPC4; TRAPPC5; TRAPPC6a	1-145; 1-140; 1-140; 1-180; 1-235; 1-188; 1-173;		This thesis
MJ117	pOPTGcH	Rab1a	1-203	N-term GST Tag(TEV); C-term His Tag	[52]
MJ37	pOPTGcH	Rab2a	1-210	N-term GST Tag(TEV); C-term His Tag	[52]
EM11	pOPTGcH	Rab3a	1-217	N-term GST Tag(TEV); C-term His Tag	[52]
MJ36	pOPTGcH	Rab4b	1-210	N-term GST Tag(TEV); C-term His Tag	[52]
DH1	pOPTGcH	Rab5a	1-212	N-term GST Tag(TEV); Q79L mutation	[52]
EM13	pOPTGcH	Rab6a	1-205	N-term GST Tag(TEV); C-term His Tag	[52]
NH20	pOPTGcH	Rab7a	1-204	N-term GST Tag(TEV); C-term His Tag	[52]
MJ40	pOPTGcH	Rab8a	1-203	N-term GST Tag(TEV); C-term His Tag	[52]
EO7	pOPTGcH	Rab11a	1-211	N-term GST Tag(TEV); C-term His Tag	[52]
MJ28	pOPTGcH	Rab11b	1-213	N-term GST Tag(TEV); C-term His Tag	[52]
MJ39	pOPTGcH	Rab12	1-242	N-term GST Tag(TEV); C-term His Tag	[52]
MJ38	pOPTGcH	Rab14	1-212	N-term GST Tag(TEV); C-term His Tag	[52]
EM15	pOPTGcH	Rab18	1-198	N-term GST Tag(TEV); C-term His Tag	[52]
MJ167	pOPTGcH	Rab19	1-214	N-term GST Tag(TEV); C-term His Tag	[52]
MJ27	pOPTGcH	Rab25	1-208	N-term GST Tag(TEV); C-term His Tag	[52]
NH19	pOPTGcH	Rab29	1-201	N-term GST Tag(TEV); C-term His Tag	[52]
NH21	pOPTGcH	Rab32	1-223	N-term GST Tag(TEV); C-term His Tag	[52]
EM17	pOPTGcH	Rab33a	1-234	N-term GST Tag(TEV); C-term His Tag	[52]
Em19	pOPTGcH	Rab35	1-199	N-term GST Tag(TEV); C-term His Tag	[52]
EM23	pOPTGcH	Rab39a	1-214	N-term GST Tag(TEV); C-term His Tag	[52]
EM25	pOPTGcH	Rab43	1-209	N-term GST Tag(TEV); C-term His Tag	[52]
MJ210	pOPTGcH	Rab11A chimera 1	1-209	N-term GST Tag(TEV); C-term His Tag; Rab11 tail swapped with Rab1 tail	This thesis
MJ211	pOPTGcH	Rab1A chimera 1	1-217	N-term GST Tag(TEV); C-term His Tag; Rab1a tail swapped with Rab11a tail	This thesis
MJ201	pOPTGcH	Rab11A chimera 2	1-209	N-term GST Tag(TEV); C-term His Tag; Rab11a tail swapped with Rab1 tail	This thesis
MJ202	pOPTGcH	Rab1A chimera 2	1-217	N-term GST Tag(TEV); C-term His Tag; Rab1a tail swapped with Rab11 tail	This thesis

Appendix L. HDX Statistics for Figure 2-4: TRAPPIII Rab

Data set	TRAPP C1	TRAPP C2	TRAPP C2L	TRAPP C3	TRAPP C4	TRAPP C5
HDX reaction details	%D_2O=82% pH_{read}=7.5 Temp=20ºC	%D_2O=82% pH_{read}=7.5 Temp=20ºC	%D_2O=82% pH_{read}=7.5 Temp=20ºC	%D_2O=82% pH_{read}=7.5 Temp=20ºC	%D_2O=82% pH_{read}=7.5 Temp=20ºC	%D_2O=82% pH_{read}=7.5 Temp=20ºC
HDX time course (s)	3, 30, 300, 3000	3, 30, 300, 3000	3, 30, 300, 3000	3, 30, 300, 3000	3, 30, 300, 3000	3, 30, 300, 3000
HDX controls	N/A	N/A	N/A	N/A	N/A	N/A
Back-exchange	Corrected based on %D_2O	Corrected based on %D_2O	Corrected based on %D_2O	Corrected based on %D_2O	Corrected based on %D_2O	Corrected based on %D_2O
Number of peptides	18	25	22	24	29	23
Sequence coverage	97.2	87.1	90.7	58.3	96.3	87.2
Average peptide /redundancy	Length=11.9 Redundancy= 1.5	Length=13.3 Redundancy= 2.4	Length=11.9 Redundancy=1.9	Length=10.6 Redundancy=1.4	Length=12.2 Redundancy= 1.6	Length=13 Redundancy= 1.6
Replicates	3	3	3	3	3	3
Repeatability	Average StDev=0.9%	Average StDev=0.7%	Average StDev=1.4%	Average StDev=1.1%	Average StDev=1%	Average StDev=1.1%
Significant differences in HDX	>5% and >0.5 Da and unpaired t-test ≤0.01	>5% and >0.5 Da and unpaired t-test ≤0.01	>5% and >0.5 Da and unpaired t-test ≤0.01	>5% and >0.5 Da and unpaired t-test ≤0.01	>5% and >0.5 Da and unpaired t-test ≤0.01	>5% and >0.5 Da and unpaired t-test ≤0.01
Data set	TRAPP C6	TRAPP C8	TRAPP C11	TRAPP C12	TRAPP C13	Rab1a
HDX reaction details	%D_2O=82% pH_{read}=7.5 Temp=20ºC	%D_2O=82% pH_{read}=7.5 Temp=20ºC	%D_2O=82% pH_{read}=7.5 Temp=20ºC	%D_2O=82% pH_{read}=7.5 Temp=20ºC	%D_2O=82% pH_{read}=7.5 Temp=20ºC	%D_2O=82% pH_{read}=7.5 Temp=20ºC
HDX time course (seconds)	3, 30, 300, 3000	3, 30, 300, 3000	3, 30, 300, 3000	3, 30, 300, 3000	3, 30, 300, 3000	3, 30, 300, 3000
HDX controls	N/A	N/A	N/A	N/A	N/A	N/A
Back-exchange	Corrected based on %D_2O	Corrected based on %D_2O	Corrected based on %D_2O	Corrected based on %D_2O	Corrected based on %D_2O	Corrected based on %D_2O
Number of peptides	21	157	126	50	84	41
Sequence coverage	73.4	89	77.2	82.7	95.7	87.3
Average peptide /redundancy	Length=9.2 Redundancy= 1.1	Length=15.1 Redundancy= 1.7	Length=12.4 Redundancy= 1.4	Length= 13.7 Redundancy= 1.6	Length= 11.2 Redundancy= 2.2	Length=14 Redundancy= 2.8
Replicates	3	3	3	3	3	3
Repeatability	Average StDev=1.4%	Average StDev=0.9%	Average StDev=0.9%	Average StDev=0.9%	Average StDev=0.9%	Average StDev=0.9%
Significant differences in HDX	>5% and >0.5 Da and unpaired t-test ≤0.01	>5% and >0.5 Da and unpaired t-test ≤0.01	>5% and >0.5 Da and unpaired t-test ≤0.01	>5% and >0.5 Da and unpaired t-test ≤0.01	>5% and >0.5 Da and unpaired t-test ≤0.01	>5% and >0.5 Da and unpaired t-test ≤0.01

Appendix M. HDX Statistics for Figure 2-5: TRAPPII vs TRAPPIII

Data set	TRAPP C1	TRAPP C2	TRAPP C2L	TRAPP C3	TRAPP C4	TRAPP C5	TRAPP C6
HDX reaction details	%D_2O=78% $pH_{(read)}$=7.5 Temp=4-20ºC	%D_2O=78% $pH_{(read)}$=7.5 Temp=4-20ºC	%D_2O=78% $pH_{(read)}$=7.5 Temp=4-20ºC	%D_2O=78% $pH_{(read)}$=7.5 Temp=4-20ºC	%D_2O=78% $pH_{(read)}$=7.5 Temp=4-20ºC	%D_2O=78% $pH_{(read)}$=7.5 Temp=4-20ºC	%D_2O=78% $pH_{(read)}$=7.5 Temp=4-20ºC
HDX time course (s)	3 at 4 ºC 3, 30, 300, 3000 at 20ºC	3 at 4 ºC 3, 30, 300, 3000 at 20ºC	3 at 4 ºC 3, 30, 300, 3000 at 20ºC	3 at 4 ºC 3, 30, 300, 3000 at 20ºC	3 at 4 ºC 3, 30, 300, 3000 at 20ºC	3 at 4 ºC 3, 30, 300, 3000 at 20ºC	3 at 4 ºC 3, 30, 300, 3000 at 20ºC
HDX controls	N/A	N/A	N/A	N/A	N/A	N/A	N/A
Back-exchange	Corrected based on % D_2O	Corrected based on %D_2O	Corrected based on %D_2O	Corrected based on %D_2O	Corrected based on %D_2O	Corrected based on %D_2O	Corrected based on %D_2O
Number of peptides	22	29	27	27	35	39	25
Sequence coverage	96.6	96.4	94.3	69.4	96.3	88.3	85.5
Average peptide /redundancy	Length=14.5 Redundancy= 2.2	Length= 13.4 Redundancy=2. 8	Length=13.6 Redundancy = 2.6	Length=12 Redundancy = 2.1	Length=12.5 Redundancy = 2.0	Length=13.5 Redundancy = 2.8	Length=12.1 Redundancy = 1.8
Replicates	3	3	3	3	3	3	3
Repeatability	Average StDev=0.6%	Average StDev=0.6%	Average StDev=0.9%	Average StDev=0.8%	Average StDev=0.7%	Average StDev=0.8%	Average StDev=0.7%
Significant differences in HDX	>5% and >0.5 Da and unpaired t-test ≤0.01	>5% and >0.5 Da and unpaired t-test ≤0.01	>5% and >0.5 Da and unpaired t-test ≤0.01	>5% and >0.5 Da and unpaired t-test ≤0.01	>5% and >0.5 Da and unpaired t-test ≤0.01	>5% and >0.5 Da and unpaired t-test ≤0.01	>5% and >0.5 Da and unpaired t-test ≤0.01

Appendix N. HDX Statistics for Figure 2-7 & Figure2-8: Membrane HDX

Data set	TRAPP C1	TRAPP C2	TRAPP C2L	TRAPP C3	TRAPP C4	TRAPP C5	TRAPP C6
HDX reaction details	%D_2O=62% pH_{read}=7.5 Temp=20ºC	%D_2O=62% pH_{read}=7.5 Temp=20ºC	%D_2O=62% pH_{read}=7.5 Temp=20ºC	%D_2O=62% pH_{read}=7.5 Temp=20ºC	%D_2O=62% pH_{read}=7.5 Temp=20ºC	%D_2O=62% pH_{read}=7.5 Temp=20ºC	%D_2O=62% pH_{read}=7.5 Temp=20ºC
HDX time course (s)	3, 100, 3000 at 20ºC	3, 100, 3000 at 20ºC	3, 100, 3000 at 20ºC	3, 100, 3000 at 20ºC	3, 100, 3000 at 20ºC	3, 100, 3000 at 20ºC	3, 100, 3000 at 20ºC
HDX controls	N/A	N/A	N/A	N/A	N/A	N/A	N/A
Back-exchange	Corrected based on %D_2O	Corrected based on %D_2O	Corrected based on %D_2O	Corrected based on %D_2O	Corrected based on %D_2O	Corrected based on %D_2O	Corrected based on %D_2O
Number of peptides	16	26	21	16	29	26	19
Sequence coverage	84.1	88.6	86.4	60.0	91.3	82.4	87.9
Average peptide /redundancy	Length=11.5 Redundancy= 1.3	Length=12.8 Redundancy= 2.4	Length= 12.3 Redundancy= 1.8	Length= 12 Redundancy= 1.1	Length=12.9 Redundancy= 1.7	Length=13.8 Redundancy= 1.9	Length=10.7 Redundancy= 1.2
Replicates	3	3	3	3	3	3	3
Repeatability	Average StDev=0.7%	Average StDev=0.6%	Average StDev=0.9 %	Average StDev=0.6%	Average StDev=0.8 %	Average StDev=0.9 %	Average StDev=1%
Significant differences in HDX	>5% and >0.5 Da and unpaired t-test ≤0.01	>5% and >0.5 Da and unpaired t-test ≤0.01	>5% and >0.5 Da and unpaired t-test ≤0.01	>5% and >0.5 Da and unpaired t-test ≤0.01	>5% and >0.5 Da and unpaired t-test ≤0.01	>5% and >0.5 Da and unpaired t-test ≤0.01	>5% and >0.5 Da and unpaired t-test ≤0.01
Data set	TRAPP C8	TRAPP C9	TRAPP C10	TRAPP C11	TRAPP C12	TRAPP C13	
HDX reaction details	%D_2O=62% pH_{read}=7.5 Temp=20ºC	%D_2O=62% pH_{read}=7.5 Temp=20ºC	%D_2O=62% pH_{read}=7.5 Temp=20ºC	%D_2O=62% pH_{read}=7.5 Temp=20ºC	%D_2O=62% pH_{read}=7.5 Temp=20ºC	%D_2O=62% pH_{read}=7.5 Temp=20ºC	
HDX time course (seconds)	3, 100, 3000 at 20ºC	3, 100, 3000 at 20ºC	3, 100, 3000 at 20ºC	3, 100, 3000 at 20ºC	3, 100, 3000 at 20ºC	3, 100, 3000 at 20ºC	
HDX controls	N/A	N/A	N/A	N/A	N/A	N/A	
Back-exchange	Corrected based on %D_2O	Corrected based on %D_2O	Corrected based on %D_2O	Corrected based on %D_2O	Corrected based on %D_2O	Corrected based on %D_2O	
Number of peptides	142	192	190	132	62	49	
Sequence coverage	82.3	95.9	85	87.3	89.1	78.2	
Average peptide /redundancy	Length=15 Redundancy= 1.5	Length=13 Redundancy= 2.2	Length=13.6 Redundancy= 2.0	Length=12 Redundancy= 1.4	Length=14.4 Redundancy= 2.0	Length=10.8 Redundancy= 1.3	
Replicates	3	3	3	3	3	3	
Repeatability	Average StDev=1%	Average StDev=0.9%	Average StDev=0.8 %	Average StDev=0.9%	Average StDev=0.8 %	Average StDev=1%	
Significant differences in HDX	>5% and >0.5 Da and unpaired t-test ≤0.01	>5% and >0.5 Da and unpaired t-test ≤0.01	>5% and >0.5 Da and unpaired t-test ≤0.01	>5% and >0.5 Da and unpaired t-test ≤0.01	>5% and >0.5 Da and unpaired t-test ≤0.01	>5% and >0.5 Da and unpaired t-test ≤0.01	